A MICROSCOPIC MODEL OF Σ HYPERNUCLEI

by

JOHN ALLISTAIR JOHNSTONE

B.Sc., McMaster University, 1978
M.Sc., McMaster University, 1979

A THESIS SUBMITTED IN PARTIAL FULFILMENT OF

THE REQUIREMENTS FOR THE DEGREE OF

DOCTOR OF PHILOSOPHY

in

THE FACULTY OF GRADUATE STUDIES

(Department of Physics)

We accept this thesis as conforming

to the required standard

THE UNIVERSITY OF BRITISH COLUMBIA

September 1982

In presenting this thesis in partial fulfilment of the requirements for an advanced degree at the University of British Columbia, I agree that the Library shall make it freely available for reference and study. I further agree that permission for extensive copying of this thesis for scholarly purposes may be granted by the head of my department or by his or her representatives. It is understood that copying or publication of this thesis for financial gain shall not be allowed without my written permission.

Department of PHYSICS

The University of British Columbia
1956 Main Mall
Vancouver, Canada
V6T 1Y3

Date OCTOBER 8, 1982

ABSTRACT

A separable potential model is constructed to describe the coupled ΣN-ΛN systems. From this the Σ single particle potential is developed including Pauli effects. The momentum space Schroedinger equation is then solved self-consistently for the complex eigenvalues of 1s and 1p state Σ^0 hypernuclei.

Arising from two quite distinct mechanisms these states are all found to be long lived. In s-states, Pauli suppression of the ΣN→ΛN conversion reduces the widths by as much as 50% from classical estimates in heavy nuclei, and in light nuclei produces widths as small as 1.8 MeV in ${}^{5}_{\Sigma^0}\mathrm{He}$. In p-states, Pauli effects are relatively unimportant and the strong absorption of the potential creates extremely narrow quasi-bound states in the Σ continuum.

TABLE OF CONTENTS

LIST OF TABLES

LIST OF FIGURES

ACKNOWLEDGEMENTS

From among the many colleagues and friends whose help and guidance were so valuable to me in the course of this work, I should like in particular to record my indebtedness to Dr. Tony Thomas for the benefit of his experience and insight, and to Dr. Doug Beder for his interest and constructive comments. Also, I wish especially to thank my wife Leslie for the support and encouragement that was so instrumental in the development of this thesis. To all these people I gladly accord my appreciation and thanks.

AN INTRODUCTION FOR THE NON-SPECIALIST

This short section is intended to introduce the non-specialist to the concepts and terminology used in this work. First, a 'hypernucleus' refers in general to any nucleus in which a nucleon has been replaced by one of the strange baryons Λ, Σ, Ξ, or Ω. As the lightest of these the Λ is unique, in that it is stable in the nucleus. The heavier Σ, Ξ, and Ω hyperons, on the other hand, can decay to a Λ upon interacting with a nucleon, releasing a large amount of energy in the process. This energy release makes the conversion so favourable that the hyperons are expected to be very short-lived in a nucleus, simply because of the large number of nucleons present. Naively, the lifetime wouldn't be expected to be much different from about 10^{-23} seconds, which is roughly the length of time required for the particle to cross the nucleus. More careful analyses which estimate the mean free path of the particle in the nuclear 'gas' do not change this figure appreciably. It has been quite a surprise recently then to find that Σ lives nearly 10 times longer than this figure in the nucleus.

The aim of this work has been to understand this large discrepancy. Some guidance is available from standard

nuclear experience where we know that the interaction of nucleons in a nucleus is not like the interaction of free particles. In particular, the Pauli exclusion principle ensures that no two nucleons can occupy the same quantum state. The result is that no interaction can occur if it will leave a nucleon in a state which is already occupied. This is an important result of early nuclear theory and the main reason why a nucleus can be considered a gas of nucleons which, to a good first approximation, are non-interacting. In fact, one of the earliest triumphs of the Pauli principle was reducing the calculated widths of excited nuclear states from 30-40 MeV to the keV range, in line with experiment. For the Σ one doesn't expect the effects to be as dramatic because the exclusion does not apply to the Σ itself. Nonetheless, the restrictions on the final state N in the $\Sigma N \rightarrow \Lambda N$ reaction can suppress the conversion significantly.

The basic outline of the study has then been to , first, understand and describe the ΣN interaction in free space. We then modify this interaction with the Pauli principle to describe the ΣN interaction in the presence of other nucleons in the nucleus. By summing the interaction of the Σ with each separate nucleon we arrive at an overall description of the Σ-nucleus interaction. It is found by

this procedure that, for a Σ bound in the ground state, Pauli suppresion of the conversion is sufficient to produce a lifetime consistent with the experimental value.

CHAPTER 1 INTRODUCTION AND SUMMARY

Although the field of hypernuclear physics is now relatively old, interest has been renewed in recent years by the observation of long-lived Σ states in the nucleus. Unlike the Λ hyperon, which is stable in nuclear matter, the Σ decays via the strong interaction to a Λ, releasing roughly 80 MeV in the process. For this reason it had long been expected that Σ states would be very broad, e.g. $\Gamma \sim 25$ MeV [1,2], on the basis of semi-classical arguments. Such short-lived states would be extremely difficult to observe even under ideal conditions.

Thus, it was very exciting when in 1979 the Heidelberg-Saclay group reported finding structure in ${}^{9}_{\Sigma^0}$Be with widths less than 8 MeV [3,4], apparently corresponding to unbound p-states. Since this discovery a variety of light Σ hypernuclei have been studied [5,6], and at Brookhaven it has been found that in ${}^{6}_{\Sigma}$Li the level may be as narrow as 3 MeV [5]. Unfortunately the picture is not as clear for s-state hypernuclei, with the only suggestion of narrow states to date being in the ${}^{12}_{\Sigma^0}$C [3], and possibly ${}^{9}_{\Sigma^0}$Be [6] systems.

Historically though it is Λ hypernuclei which have attracted attention. As the lightest of the hyperons the Λ

decays only through the weak interaction and therefore has a relatively long lifetime in the nucleus. In addition, the similarity of the Λ and N masses, and the fact that the ΛN potential is only slightly weaker than that of NN, suggested that in the nucleus the Λ would behave much like a neutron. With strangeness -1 though, the Λ would be distinguishable and therefore make a nearly ideal nuclear probe. The advances in this area and interesting future prospects, such as the study of doubly strange $\Lambda\Lambda$ and Ξ^- hypernuclei formed in (K^-,K^+) reactions, will not be discussed further here but recent reviews are given in, for example, refs.[7,8].

It should be clear though that if one hopes to successfully compare the Y-nucleus (where Y is Σ or Λ) with the N- nucleus interaction it is essential to produce hypernuclear states which have sufficiently simple configurations to allow a unique theoretical interpretation. Ideally one would like the hyperon to simply replace one of the target nucleons, assuming the same state quantum numbers and without disturbing the nuclear core.

Conceptually at least, this is not a difficult problem. A nuclear target is exposed to a beam of low energy kaons and, through the strangeness-exchange reaction $KN \rightarrow \pi Y$, one of the target nucleons is transformed into a hyperon. In a rough approximation the amplitude for this process occurring

in the nucleus is proportional to the product of the elementary two-body amplitude, with a form factor $F(\underline{q})$ which depends on the initial state N, and final state Y wavefunctions as

$$F(\underline{q}) \sim \int d\underline{r}\ \Phi_f^*(\underline{r}) e^{i\underline{q}\cdot\underline{r}} \Phi_i(\underline{r}) \qquad (1)$$

with $\underline{q}$ the momentum transferred to the hyperon, i,f label the state quantum numbers, and the distortion of the K and π wavefunctions has been ignored. For very small values of $\underline{q}$ the exponential is of order unity across the nuclear volume and the overlap integral is therefore maximized for i=f.

In addition $F(\underline{q})$ decreases rapidly with the momentum transferred and, for example, $F(\underline{q}) \sim \exp(-a^2q^2)$ for harmonic oscillator wavefunctions. Experimentally then, for 'recoilless' production (q=0) one would detect the pions scattered in the forward direction and adjust the incident kaon momentum to minimize the momentum transferred to the hyperon. The 'magic' momentum which leaves the Λ at rest in the nucleus is about 500 MeV/c, whereas for Σ it is lower, at 300 MeV/c.

In practice, of course, the situation is not nearly as clean as that outlined above. First of all, the optimum K momentum is not easy to achieve. The kaons decay in flight by the weak interaction with a mean lifetime of $\sim 10^{-8}$

seconds. Consequently the intensity of the beam reaching the target decreases sharply with decreasing momentum. Present experiments typically use a momentum of ~700 MeV/c to partially overcome this intensity problem, but even so 20% of the kaons decay with every meter of flight.

Secondly, this higher momentum creates its own difficulties. For recoilless Λ production, 700 MeV/c is not radically different from the optimum value and the momentum transfer is still fairly low, ~40 MeV/c. For Σ production however the corresponding momentum transfer is 130 MeV/c and, with a value this large, quasifree production competes with the recoilless process. In this case the Σ is kicked into another state and, since there is no Pauli restriction for the Σ in the nucleus, the number of available states is large. The result is that the experimental spectrum degenerates from a sharp recoilless peak into a small bump embedded in a large quasifree background.

Despite these, and many other, complications it is possible to determine the binding energy and width of the Σ states by measuring the momentum of the final state pions. The difference between the π and K energies gives directly the transformation energy $(M_{HY}-M_A)$, where M_{HY} is the mass of the hypernuclear system and M_A is the target mass. The hyperon binding energy is then simply $B_Y=B_N-(M_{HY}-M_A)+(m_Y-m_N)$,

with B_N the binding energy of the nucleon that was replaced, and m_Y, m_N are the obvious masses.

In fig.1 the experimental π energy spectrum of ref. [3] is shown for 720 MeV/c kaons incident on ^{9}Be. The energy scale is given both as a function of the transformation energy and also the Λ,Σ binding energies. Because of the large momentum acceptance of the π spectrometer (600→850 MeV/c) they were able to measure the Λ and Σ hypernuclear spectra simultaneously. In $^9_\Lambda$Be the peak at B_Λ=-6 MeV is attributed to recoilless production on the loosely bound $1p_{3/2}$ neutron, whereas the peak at -17 MeV is a mixture of recoilless strength from the $1p_{3/2}$ and $1s_{1/2}$ neutrons. One can also see the Λ ground state at B_Λ=7 MeV [3].

Just separated from the Λ spectrum by the Σ^o-Λ mass difference is structure which is very similar to that in $^9_\Lambda$Be, and so it is natural to assign these peaks to the $^9_{\Sigma^o}$Be hypernucleus. After correcting for the Σ^o-Λ mass difference they are found to lie systematically ~3 MeV higher in excitation than the Λ peaks, indicating that the Σ-nucleus interaction is slightly weaker than that of Λ-nucleus. More important is that, in p-state at least, the level is surprisingly narrow. In fact the upper limit of 8 MeV for the $^9_{\Sigma^o}$Be level was assesed because the experimental width was

no greater than that of the corresponding peak in $^{9}_{\Lambda}$Be [3]. Conceivably then the Σ state is much longer lived than is implied by the 8 MeV figure.

These findings have sparked a flurry of theoretical activity and a number of mechanisms have now been proposed for suppressing $\Sigma N \rightarrow \Lambda N$ conversion in the nucleus. Gal and Dover [9,10] have emphasized that the conversion proceeds only through the isospin I=1/2 channel, with the implication being that in special cases where the I=3/2 interaction dominates, long-lived states can result. For example, in $^{12}C(K^-,\pi^+)^{12}_{\Sigma^-}Be$ the total isospin (T,T_3) of the initial state is (1/2,-1/2). Conservation of isospin then requires that the Σ^- hypernucleus be a pure (3/2,-3/2) state, and some suppression of the conversion width from nuclear matter estimates is expected.

In very light nuclei this quenching can be substantial, but the drawback to this explanation is that it is operative mainly for the (K^-,π^+) reaction and, therefore, not applicable to either of the original $^{9}_{\Sigma^0}$Be or $^{12}_{\Sigma^0}$C results. The $^{12}_{\Sigma^0}$C hypernucleus is a mixture of isospin 3/2 and 1/2 states and no suppression is expected. Worse, in $^{9}_{\Sigma^0}$Be, which is pure isospin=1, Gal's calculations [2] predict that the p-state should be 20-25% broader than the nuclear matter estimate.

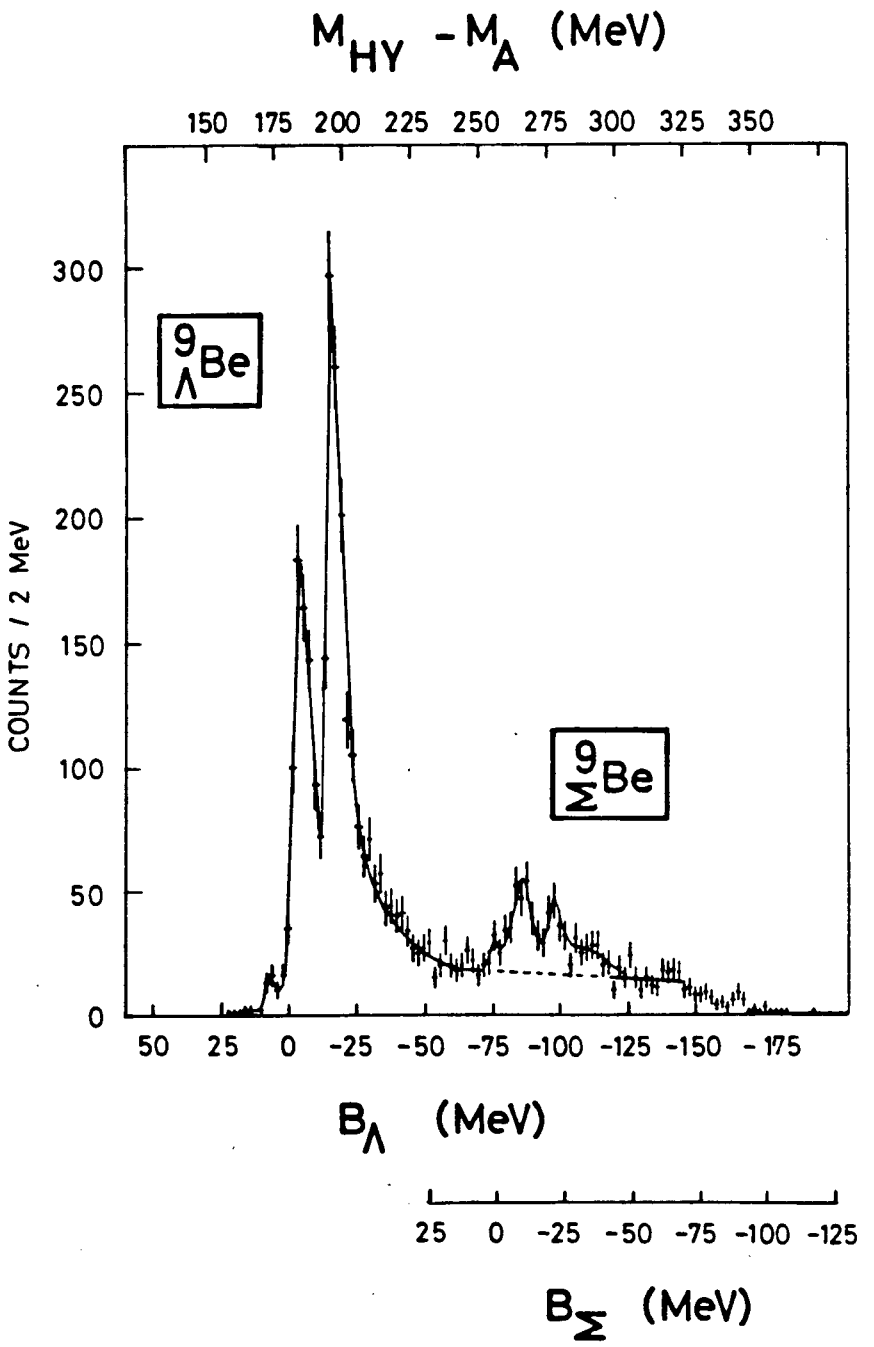

Fig. 1. Spectrum obtained from the (K^-,π^-) reaction on ^{9}Be at a kaon momentum of 720 MeV/c. The π energy spectrum is plotted as the difference between the the target and hypernuclear masses (M_{HY}-M_A). The Σ and Λ binding energy scales are also given. All results are taken from ref.[3].

A particularly intriguing explanation has been proposed by Gal, Toker, and Alexander [11]. Rather than seeking a mechanism to suppress conversion, they have pointed out that in special circumstances strong absorption can produce very narrow bound states embedded in the continuum. Using a phenomenological potential consistent with Σ^- atomic data [12], they demonstrated that the strong absorption could cause an S-matrix pole in the unphysical, third momentum quadrant to cross into the physical, second quadrant and thereby become indistinguishable from an unstable bound state pole.

However, it has been pointed out by Stepien-Rudzka and Wycech [13], that the Σ^- atomic data are sensitive primarily to interactions at the nuclear surface, leaving the interactions in the high density central region almost completely unconstrained. As a result, predictions for hypernuclei based on phenomenological analyses of Σ^- atoms are inconclusive. For the moment then, no more will be said of these unusual states, but they will be discussed again in detail in chapter 4 where they are found to arise in a coupled channels calculation.

All of the above models are mainly applicable to p-levels though. For s-state hypernuclei they generally predict very broad widths in agreement with the classical

estimates [1,2]. One calculation which does predict fairly narrow s-states (and is closest in philosophy to our approach) is the recent work of Stepien-Rudzka and Wycech [13]. Stressing the importance of Pauli blocking in reducing the $\Sigma N \rightarrow \Lambda N$ conversion width, they constructed a simple, local Σ-nucleus potential that was consistent with Σ^- atomic data but which also incorporated exclusion effects for high densities.

Their model indeed produced $\Gamma<10$ MeV s-states in light nuclei but some rather severe approximations used to eliminate the energy dependence and non-localities in the potential made it unclear whether the resulting potential remained consistent with two-body ΣN interactions. In addition, there was no attempt to calculate the lifetime of p-states, where one would expect that Pauli suppression would not be as significant because of the smaller overlap of the Σ wavefunction with the nucleus. It is impossible to decide then if this model can also reproduce the observed p-state widths.

All of the above proposals have some validity for the narrow range of examples they consider. Nonetheless, no attempt has been made to decide whether Σ states are expected to be narrow in general or only in special isolated cases. Our aim is to answer this question by calculating

the Σ single particle potential as accurately as possible, using the elementary ΣN scattering information as input.

A separable potential model is developed in the following chapter to describe the coupled ΣN-ΛN systems. It is argued that a convincing reproduction of the low energy data requires the inclusion of tensor and P-wave interactions. Perhaps more importantly, it is found that the conversion amplitude is strongly energy dependent, suggesting that great care must be exercised in defining the Σ-nucleus potential.

With this reliable description of ΣN scattering as the foundation, the Σ single particle potential is developed in chapter 3. A fairly detailed derivation of the coupled channel G-matrix is presented, with special attention given to the energy variation arising from nucleon binding and centre of mass motion. Pauli exclusion effects are also explicitly introduced since, in s-states at least, this is expected to produce a sizeable suppression of the conversion width. Finally, following from these purely formal developments, a minimum number of physically reasonable approximations are made to reduce the potential to a calculable form.

This careful treatment of the energy dependence of the potential creates its own complications. Chapter 4 is

devoted to a consideration of these technical details, which include the self-consistent solution of the Schroedinger equation, and the interpretation of the complex eigenvalues as poles in the multi-sheet domain of the S-matrix. This latter discussion then leads to the necessity of analytically continuing the Pauli exclusion operator to complex momenta.

With these difficulties resolved, the self-consistent (complex) eigenvalues for the L=0,1 states in light Σ^0 hypernuclei are presented in chapter 5. Remarkably, we find that arising from two quite distinct mechanisms both the s and p states are long lived. In s-state Pauli effects are found to suppress conversion by as much as 50% from the semi-classical estimates. By contrast, in p-state where the exclusion principle is relatively unimportant, the resulting strong absorption can create extremely narrow quasi-bound states embedded in the continuum.

Finally, chapter 6 is quite brief and the findings of the study are simply highlighted. Some possible improvements of the calculation and directions for experiments are also suggested.

CHAPTER 2 TWO-BODY ΣN-ΛN SCATTERING

The foundation of our aim to calculate Σ-hypernuclear states is the description of the underlying ΣN interactions. This description is complicated considerably by the coupling of the ΣN and ΛN channels. In addition, despite the scarcity of ΣN data, there are clear indications that contributions from L>0 partial waves are important. Even at energies as low as 5 MeV the $\Sigma^- p \rightarrow \Sigma^- p$ and $\Sigma^- p \rightarrow \Lambda n$ cross sections show marked forward/backward asymmetries [14,15], indicating the presence of P-waves. It can also be expected that, because of the large ΛN momentum, the $\Sigma^- p(^3S_1) \rightarrow \Lambda n(^3D_1)$ transition is significant.

We remark that the low energies of the ΣN scattering are consistent with non-relativistic kinematics. Clearly 5 MeV of kinetic energy is negligible relative to the ΣN mass of 2135 MeV. Even the ΣN-ΛN mass difference of 80 MeV is small compared to the ΛN mass. So all discussions to follow are in the Schrodinger picture with the energy scale chosen to be zero at the ΣN threshold.

Our program is to fit all of the low-energy ΣN scattering data within a separable potential model and which accounts explicitly for the multi-channel and multi-partial-wave features of the interactions. For spin-zero particles a single-channel potential which is

separable in each partial wave can be defined as

$$V(\underline{k}',\underline{k}) = \sum_{\ell=0}^{\infty} \frac{(2l+1)}{4\pi} V_\ell(k',k) P_\ell(\hat{k}'\cdot\hat{k}) \qquad (2)$$

with $V_\ell(k',k) = v_\ell(k')\lambda v_\ell(k)$

and λ is $-1(+1)$ for attractive (repulsive) interactions. A more convenient notation is to write the potential (operator) V_ℓ in bra-ket form as $V_\ell = |v_\ell\rangle\lambda\langle v_\ell|$, with $|v_\ell\rangle$ defined by $v_\ell(k)$ in momentum space. The more complicated case with coupled channels and particles with spin is discussed later, but for now we mention that there are several advantages to using separable models. It will be shown that in each partial wave the scattering amplitude can be solved algebraically. In addition, separable models can reproduce NN phase shifts over several hundred MeV [16]. The relative simplicity of the model will also allow us to perform sophisticated nuclear calculations with a minimum of purely technical complications.

2.I. The Physical Basis for Separable Interactions

The more important consideration, of course, is whether there is any physical motivation for the separable form. It will be shown that it may be a good approximation to the 'true' potential if the scattering amplitude is dominated by a bound state or resonance. First, we decompose the t-matrix into its spectral representation as

$$t(E) = V + \sum_n V\frac{|\Phi_n><\Phi_n|}{E^+ + B_n}V + \int dE'\, V\frac{|\Psi(E')><\Psi(E')|}{E^+ - E'}V \qquad (3)$$

with V the potential operator (not necessarily separable), $|\Psi(E')>$ is the scattering wavefunction, and where the summation extends over all the (assumed) bound states $|\Phi_n>$ with the $B_n(>0)$ the corresponding binding energies. Clearly for energies E 'near' to $-B_n$, this pole term will dominate in t(E), and the residue is separable.[1]

Conversely, it is straightforward to show that the separable form factor is simply related to the bound state wavefunction (when it exists) [16]. The wavefunction $|\Phi>$ obeys the homogeneous Lipmann-Schwinger equation

$$|\Phi> = -(B+K)^{-1}V|\Phi> \qquad (4)$$

where B (>0) is the binding energy, and K is the kinetic energy operator. If it is <u>assumed</u> that the underlying potential is separable, as in eq.(2), then it follows that

$$\begin{aligned} |\Phi> &= (B+K)^{-1}|v><v|\Phi> \\ \text{or} \quad v(k) &= (B+k^2/2m)\Phi(k)\left[<v|\Phi>\right]^{-1} \end{aligned} \qquad (5)$$

which defines a potential which will reproduce the wavefunction exactly.

---

[1] For degenerate bound states, the residue is modified to become a sum of separable terms [17].

For the case in which t is dominated by resonance poles, rather than bound states, the demonstration is a little more involved but the results will not be surprising. A simple derivation of Lovelace's result [17] is presented here.

Let us define a new potential ν, related to the V in eq.(3) above by the relation

$$\nu(p,q)=e^{-i\delta}V(e^{-i\delta}p,e^{-i\delta}q) \quad , \tag{6}$$

with δ an arbitrary phase parameter. Similarly, a modified t-matrix (τ) is introduced as the solution of the Lipmann-Schwinger equation

$$\tau(p',q';E)=\nu(p',q')+\int dk\ k^2\frac{\nu(p',k)\tau(k,q';E)}{(E^+-k^2/2m)} \tag{7}$$

where p' is related to p by $p'=pe^{-i\delta}$, and similarly $q'=qe^{-i\delta}$.

The integration path can be distorted through the substitution $k\rightarrow ke^{-i\delta}$ ($|\delta|<\pi/2$), which rotates the contour $0\leq k\leq\infty$ about the origin into the fourth quadrant. Of course the distorted contour must not now enclose the pole at $k^2=2mE$. The integrand dies quickly enough for $k\rightarrow\infty$ that when the rotated contour is joined to the real axis at infinity, the integral along the infinite connecting-arc

gives zero contribution. Equation (6) has then become

$$\tau(p',q';E)=\nu(p',q')+e^{-i\delta}\int dk\ k^2\ \frac{\nu(p',e^{-i\delta}k)\tau(e^{-i\delta}k,q';E)}{(e^{2i\delta}E-k^2/2m)} \qquad (8)$$

If eq.(8) is multiplied to the left by $e^{-i\delta}$ it is found, using eq.(6), that this is just the Lipmann-Schwinger equation for t at the new energy $e^{2i\delta}E$, and therefore

$$t(p,q;e^{2i\delta}E)=e^{-i\delta}\tau(e^{-i\delta}p,e^{-i\delta}q;E) \qquad (9)$$

Equation (9) defines the analytic continuation of t to the unphysical energy sheet and clearly, if t has a resonance pole at $e^{2i\delta}E$ then τ has a pole at an energy E. Further, the phase δ can be chosen such that E is a bound state pole of ν so that the contribution of this pole to τ will be separable, in analogy with eq.(3).

'Bound state' is used here in the sense that the poles lie in the second quadrant of the momentum plane and the wavefunction therefore decays exponentially at large distances. However, the pole is not on the imaginary axis and so is unstable and decays exponentially in time as well. This kind of pole will be encountered throughout our discussion of hypernuclei as being the correct bound state description.

It has been shown that if the scattering amplitude is

dominated by bound states and/or resonance poles it is reasonable to expect the separable model to be a good approximation to the t-matrix. This observation will be reassuring later when it is found that the ΣN amplitude is strongly influenced by a pole near the ΣN threshold.

2.II. OBE Predictions of the ΣN-ΛN Interactions

As mentioned earlier, the ΣN cross sections are not well-determined and, therefore, as in all model calculations, we need some reasonable premise for constraining the parameters. The most extensive treatments of ΣN to date are the one-boson-exchange calculations of Nagels et al [18-20] and their results should provide solid guidance for our fit. Their philosophy is that NN data can be described well in an OBE picture and that, with the assistance of SU(3) and SU(6) to fix the relative strengths of coupling constants, the model can be extended consistently to the YN interactions.

All of their calculations include the exchange of nonets of pseudoscalar and vector mesons, and uncorrelated two-pion exchange. Recent works also consider the contributions from a nonet of heavy, scalar mesons. The only phenomenology entering their models is hard-core repulsion, and one of the main differences between models is

the assumptions made regarding the core radii in different channels. These radii, plus F/(F+D) ratios for meson couplings are treated as free parameters for fitting all the ΣN and ΛN data.

The resulting fits are impressive, with a χ^2/data-point less than one for YN in all models. Although in details the model predictions differ, in general conclusions they do not. The conclusions of their best YN fit (model D [19]), which are relevant to our present purposes are summarized below.

(i) isospin 3/2: (a) $^1S_0$: attractive.

(b) $^3S_1$: weak and repulsive.

(ii) isospin 1/2: (a) $^1S_0$: repulsive.

(b) $^3S_1$: attractive, with the elastic Σ^-p cross section dominated by $^3S_1 \rightarrow {}^3S_1$ transitions, and the $\Sigma^-p \rightarrow \Lambda n$ conversion dominated by $^3S_1 \rightarrow {}^3S_1$ and $^3S_1 \rightarrow {}^3D_1$ transitions.

(c) $^3P_1$: attractive, with the forward/backward asymmetry in the cross section due mainly to $^3S_1$-$^3P_1$ interference.

In fact, this model also suggests that the I=3/2 $^1P_1$ interaction is important to the Σ^+p description, but to include this term in our model would require at least one extra parameter and, since our primary concern is the

coupled ΣN-ΛN systems, such an additional freedom does not seem warranted.

These results will be revisited shortly, after specifying our potential model, but for the moment we only remark that our initial suspicion that L>0 ΣN-ΛN interactions are significant is supported by Nagels et al.

2.III. T-Matrix Normalization and ΣN Cross-Sections

Before proceeding to the specific form of the two-body potentials used in this work it is worthwhile to describe the normalizations and resulting ΣN-YN cross-sections.

For two spin-1/2 particles t can be expanded in the basis of the spin spherical harmonics |LSJM> [21], which are the eigenfunctions of the spin, orbital, and total angular momenta (S,L, and J, respectively), and also of the z-component of total J (M). The normalization of the basis states is chosen such that

$$t = \sum_{\substack{JMLL' \\ S'S''}} |L'S''JM\rangle\langle L'S''JM|t|LS'JM\rangle\langle LS'JM| \qquad (10)$$

It has been assumed implicitly of course that the total angular momentum J is a good quantum number in the interaction. The spin and orbital angular momenta need not be conserved separately however. This means that, in

addition to the expected tensor interaction $^3S_1$-$^3D_1$, there are also spin-changing transitions such as $^1P_1$-$^3P_1$, $^1D_1$-$^3D_1$, et cetera. In this work these latter interactions are ignored. P-wave is the lowest angular momentum state in which they occur but, according to the OBE calculations, the $^1P_1$ amplitude is expected to be small in the I=1/2 channel, and the $^3P_1$ small in I=3/2. It is reasonable to conclude that the $^1P_1 \longleftrightarrow {}^3P_1$ transitions are unimportant relative to the elastic I=1/2 $^3P_1$ and I=3/2 $^1P_1$ amplitudes.

To be more specific, let us project out the t-matrix element for scattering from an initial state of momentum $|\underline{k}>$, and spin $|S\nu>$ (with ν the z-projection of S), to a final state $|\underline{k}'>$ and $|S\nu'>$. Then it follows from eq.(10) that

$$<\underline{k}';S\nu'|t|\underline{k};S\nu>=\sum_{\substack{JML\\L'S'}} <\Omega_k';S\nu'|L'S'JM>t^{JS'}_{L'L}(k';k)<LS'JM|S\nu;\Omega_k> \qquad (11)$$

This result becomes a little more familiar if the spin spherical harmonics are expanded in the basis functions $|Lm>|S\nu>$ as, for example

$$\begin{aligned}<\Omega_k';S\nu'|L'S'JM>&= \sum_{m'\nu''} <\Omega_k';S\nu'|L'm'S'\nu''><L'm'S'\nu''|JM>\\ &= \sum_{m'} <L'm'S\nu'|JM>Y^{M'}_{L'}(\Omega_k')\delta_{SS',\nu\nu'}\end{aligned} \qquad (12)$$

where $<LmS\nu|JM>$ is a Clebsch-Gordan coefficient and Y^M_L is a spherical harmonic. The t-matrix element of eq.(11) in this

representation is

$$\langle \underline{k}';S\nu'|t|\underline{k};S\nu\rangle = \sum_{\substack{JMLL'\\ mm'}} \langle LmS\nu|JM\rangle\langle L'm'S\nu'|JM\rangle \; Y_{L'}^{M'}(\Omega')Y_{L}^{M*}(\Omega)t_{L'L}^{JS}(k';k) \tag{13}$$

Independent of the angular momentum decomposition, t may also be expressed in an isospin basis, assuming total I-spin to be conserved. In analogy with the above derivation, for scattering from an initial state of I-spins $|I_2 i_2\rangle|I_1 i_1\rangle$ to a final state $|I_2' i_2'\rangle|I_1' i_1'\rangle$

$$\langle I_1' i_1' I_2' i_2'|t|I_1 i_1 I_2 i_2\rangle = \sum_{Ii} \langle I_1' i_1' I_2' i_2'|Ii\rangle\langle I_1 i_1 I_2 i_2|Ii\rangle \langle Ii|t|Ii\rangle \tag{14}$$

The isospin wavefunctions of the relevant Σ,Λ, N pairs are

$$\begin{aligned}
|\Sigma^- p\rangle &= |1\,-1\rangle|1/2\;\;1/2\rangle = \sqrt{2/3}\;|1/2\rangle + \sqrt{1/3}\;|3/2\rangle \\
|\Sigma^0 n\rangle &= |1\;\;0\rangle|1/2\,-1/2\rangle = -\sqrt{1/3}\;|1/2\rangle + \sqrt{2/3}\;|3/2\rangle \\
|\Sigma^+ p\rangle &= |1\,+1\rangle|1/2\,+1/2\rangle = \;\;|3/2\rangle \\
|\Lambda\; n\rangle &= |0\;\;0\rangle|1/2\,-1/2\rangle = \;\;|1/2\rangle
\end{aligned} \tag{15}$$

With these states, the t-matrix decomposes as

$$\begin{aligned}
\langle\Sigma^- p|t|\Sigma^- p\rangle &= \;\;2/3\;\, t(1/2) + \;1/3\;\, t(3/2) \\
\langle\Lambda\; n|t|\Sigma^- p\rangle &= \sqrt{2/3}\;\, t(1/2) \\
\langle\Sigma^0 n|t|\Sigma^- p\rangle &= -\sqrt{2}\;/3\, t(1/2) + \sqrt{2}\;/3 t(3/2) \\
\langle\Sigma^+ p|t|\Sigma^+ p\rangle &= \;\;t(3/2)\;\,.
\end{aligned} \tag{16}$$

We are in a position now to derive the differential cross-sections for the processes described in eqs.(14). With our δ-function normalization of momentum states, the t-matrix has the same definition as that used by Goldberger and Watson [22]. Their result for the cross-section describing scattering from an initial state $|\alpha\rangle$ of spin S and z-projection ν, to a final state $|\beta\rangle$ of spin S and z-projection ν' is

$$d\sigma_{\alpha\beta}(S\nu';S\nu)=\left(\frac{2\pi}{v_\alpha}\right)^4\delta^0(E_\beta-E_\alpha)\delta^3(\underline{k}_\beta+\underline{p}_\beta)\,|t_{\alpha\beta}(S\nu';S\nu)|^2 d\underline{k}_\beta d\underline{p}_\beta \quad (17)$$

where v_α is the incident flux $=|\underline{k}_\alpha|/m_\alpha$, and $\underline{k}_\beta,\underline{p}_\beta$ are the final state momenta. The δ functions allow us to integrate immediately over $\underline{p}_\beta$ and the magnitude of $\underline{k}_\beta$, with the result

$$d\sigma_{\alpha\beta}(S\nu';S\nu)=(2\pi)^4\frac{k_\beta}{k_\alpha}m_\alpha m_\beta\,|t_{\alpha\beta}(S\nu';S\nu)|^2 d\Omega_\beta \quad (18)$$

Experimentally, only the unpolarized cross-sections have been measured . Since the incident beam comprises a random mixture of spins, and orientations, eq.(18) should be summed over all S and averaged over ν - that is, we sum over ν and divide by the total possible spin projections $(2S_\Sigma+1)(2S_N+1)$. We should also sum over ν' since in the final state all orientations are detected. The unpolarized cross-section is then

$$d\bar{\sigma}_{\alpha\beta}=(2\pi)^4\frac{k_\beta}{k_\alpha}m_\alpha m_\beta(1/4)\sum_{S\nu\nu'}|t_{\alpha\beta}(\underline{k}_\beta,S\nu';\underline{k}_\alpha,S\nu)|^2d\Omega_\beta \quad (19)$$

If the scattering amplitude $f_{\alpha\beta}$ is defined in terms of the t-matrix by

$$f_{\alpha\beta}=-4\pi^2\sqrt{\frac{k_\beta}{k_\alpha}m_\alpha m_\beta}\;t_{\alpha\beta} \quad (20)$$

then the familiar relation $d\sigma_{\alpha\beta}=|f_{\alpha\beta}|^2d\Omega$ results.

The summation over ν,ν' can be performed to simplify eq.(19). For the moment we concentrate on just the $|t|^2$ term, which is

$$|t(\underline{k}',S\nu';\underline{k},S\nu)|^2=\sum_{\substack{JJ'L'L''L'''\\ \text{all } m}}\langle LmS\nu|JM\rangle\langle L'm'S\nu'|JM\rangle\langle L''m''S\nu|J'M'\rangle \langle L'''m'''S\nu'|J'M'\rangle Y_{L'}^{M'}(\Omega')Y_{L'''}^{M'''*}(\Omega') \quad (21)$$
$$Y_{L''}^{M''}(\Omega)Y_{L}^{M*}(\Omega)t_{L'L}^{JS}(k';k)t_{L'''L''}^{J'S*}(k';k)$$

Specializing to the case where the z-axis is the incident direction, $m=m''=0$, $M=M'=\nu$, and $m'=m'''=\nu-\nu'$, eq. (21) simplifies considerably since the spherical harmonics become

$$Y_{L'}^{M'}(\Omega')Y_{L'''}^{M'''*}(\Omega')=(-)^{\nu-\nu'}\sum_{l}\langle L'0L'''0|l0\rangle\langle L'\nu-\nu'L'''\nu'-\nu|l0\rangle \hat{L}'\hat{L}'''\,P_l(\underline{k}\cdot\underline{k}') \quad (22)$$

with $Y_{L}^{0}(\Omega)Y_{L''}^{0}(\Omega)=\hat{L}\hat{L}''/4\pi$, and $\hat{L}\equiv(2L+1)^{1/2}$.

It can be shown that the summation in eq.(21) plus the sum over ν,ν' just gives a product of Wigner 6J symbols

(appendix I), and the cross section takes the convenient form

$$d\bar{\sigma}_{\alpha\beta}=\pi^2(k_\beta/k_\alpha m_\beta m_\alpha)(1/4)\sum_{all\ J,L,S}\hat{L}\hat{L}'\hat{L}''\hat{L}'''\hat{1}^2\hat{J}^2\hat{J}^{2\prime}\ P_1(\hat{\underline{k}}'\cdot\hat{\underline{k}}) \qquad (23)$$
$$\begin{pmatrix} L & L'' & 1\\ 0 & 0 & 0\end{pmatrix}\begin{pmatrix} L' & L''' & 1\\ 0 & 0 & 0\end{pmatrix}\begin{Bmatrix} L'' & J' & S\\ 1 & L' & J\end{Bmatrix}\begin{Bmatrix} J' & L'' & S\\ 1 & J & L\end{Bmatrix} t^{JS}_{L'L}\, t^{J'S*}_{L'''L''}$$

In our case, where no spin transitions are allowed the above separates into singlet, and triplet cross-sections.

2.IV. The Coupled-Channel, Separable ΣN-ΛN Potentials

We assume that the channel-coupling potentials are all rank-one separable. That is, the potential operator coupling any two channels (α,β) $V_{\alpha\beta}$ can be written as $|v_\alpha\rangle\lambda^{\alpha\beta}\langle v_\beta|$, in our earlier notation. For N coupled channels, the transition operator describing scattering from the channel $|\alpha\rangle$ to the channel $|\beta\rangle$ (where α,β refer to the set of all quantum numbers for the state, i.e. L,S,J,I, plus a channel label), is in general

$$t_{\beta\alpha} = |v_\beta\rangle\lambda^{\beta\alpha}\langle v_\alpha| + |v_\beta\rangle\sum_{\gamma=1}^{N}\lambda^{\beta\gamma}\langle v_\gamma|G_o^\gamma\, t_{\gamma\alpha}\ , \qquad (24)$$

where $\lambda^{\beta\alpha}=-1(+1)$ for attractive (repulsive) interactions, and G_o^γ is the γ-channel Green's function, defined by

$$G_o^\gamma(E) = \left(E + \Sigma m_\gamma - (m_\Sigma + m_N) - K^2/2\mu_\gamma + i\varepsilon\right)^{-1}\ , \qquad (25)$$

with Σm_γ the sum of the masses of the particles in that

channel, and μ_γ their reduced mass. Following the procedure of Londergan et al. [23], we impose the restriction that all constants λ are the same sign within any set of coupled channels. In this case the solution has the particularly simple form (appendix II)

$$t_{\beta\alpha} = \frac{|v_\beta\rangle \lambda^{\beta\alpha} \langle v_\alpha|}{1 - \sum_{\gamma=1}^{N} \lambda^{\gamma\gamma} \langle v_\gamma | G_o^\gamma | v_\gamma\rangle} \quad , \tag{26}$$

where the summation extends over the diagonal elements of all coupled channels.

The form factors are chosen to have the behaviour[2]

$$\begin{aligned} \langle p|v_\gamma\rangle &= \bar{v}_\gamma(\beta_o^2 + p^2)^{-1} \quad \text{for } \ell = 0 \ , \\ &= \bar{v}_\gamma p \beta_1^{-1}(\beta_1^2+p^2)^{-1} \quad \text{for } \ell = 1 \ , \\ &= \bar{v}_\gamma p^2(\beta_2^2+p^2)^{-2} \quad \text{for } \ell = 2 \ , \end{aligned} \tag{27}$$

where the β_ℓ are the inverse ranges, and $\bar{v}_\gamma$ the strengths of the interactions. With the normalization of the t-matrix given by eq.(10), the overlap integrals $\langle v|G_o|v\rangle$ in eq.(28) are found to be

$$\int_o^\infty \frac{d\kappa \kappa^2 v_\gamma^2(\kappa^2)}{E+\Delta m-\kappa^2/2\mu_\gamma+i\varepsilon} = \frac{-\pi\mu_\gamma\bar{v}_\gamma^2}{(\beta^2+\kappa_\gamma^2)^2}\left[1/2\beta\left(\beta^2-\kappa_\gamma^2\right) + i\kappa_\gamma\right], \quad \ell=0 \ ,$$

---

[2] This choice of momentum dependence ensures that the phase shift $\delta_\ell \sim p^{2\ell+1}$ for $p \to 0$.

$$= \frac{-\pi\mu_\gamma \bar{v}_\gamma^2}{\beta^2(\beta^2+\kappa_\gamma^2)^2}\left[\beta/2\left(\beta^2+3\kappa_\gamma^2\right)+i\kappa_\gamma^3\right], \ell=1, \qquad (28)$$

$$= \frac{-\pi\mu_\gamma \bar{v}_\gamma^2}{(\beta^2+\kappa_\gamma^2)^4}\left[1/16\beta\left(\beta^6+5\beta^4\kappa_\gamma^2+15\beta^2\kappa_\gamma^4-5\kappa_\gamma^6\right)+i\kappa_\gamma^5\right], \ell=2,$$

2.V. Coulomb Modifications to the Two-Body T-Matrix

So far no mention has been made of the Coulomb interaction and yet its inclusion is clearly important to a complete description of $\Sigma^{\pm}p$ scattering. It will soon become apparent that another calculational advantage of separable potentials is that it is still possible to solve for the strong interaction amplitude in closed form even in the presence of the Coulomb potential [24,25].

In analogy with eq.(13), the partial-wave expansion of the scattering amplitude is

$$f(\underline{k}',S\nu';\underline{k},S\nu)=4\pi\sum_{JMLL'S}\langle LmS\nu|JM\rangle\langle L'm'S\nu'|JM\rangle Y_{L'}^{M'*}(\Omega_k')Y_L^M(\Omega_k)\, f_{L'L}^{JS}(k;k') \qquad (29)$$

with $$f_{L'L}^{JS}(k;k') = [\exp(2i\Delta_{L'L}^{JS})-\delta_{L'L}]/2ik \qquad (30)$$

where $\Delta_{L'L}^{JS}$ is the phase shift in that channel. If the underlying potential is the sum of the Coulomb and a short-range interaction then it is profitable to write Δ as the sum of the pure Coulomb phase shift σ_L and a

Coulomb-modified strong phase shift ${}^{C}\delta^{JS}_{L'L}$. The partial amplitude can then be rearranged to read

$$f^{JS}_{L'L}(k';k)=\delta_{L'L}(e^{2i\sigma_L}-1)/2ik+e^{2i\sigma_L}(e^{2i^{C}\delta^{JS}_{L'L}}-\delta_{L'L})/2ik \qquad (31)$$

The first term is just the l-th partial-wave Coulomb amplitude $f^{C}_{L}(k;k')$ (apart from the Kronecker delta), and the second term is the perturbed strong amplitude ${}^{C}f^{JS}_{L'L}(k';k)$. The summation over all angular momenta variables for the Coulomb amplitude can be calculated in eq.(29) using the orthogonality of the Clebsch-Gordan coefficients with the result [22]

$$f^{C}(\Theta)=\sum_{l=0}^{\infty}(2l+1)f^{C}_{l}(k;k')P_{l}(\hat{\underline{k}}\cdot\hat{\underline{k}}') \qquad (32)$$

$$=-\frac{\eta}{2k\sin^2(\Theta/2)}\exp[2i\sigma_0-i\eta\ln(\sin^2(\Theta/2))]$$

and $\eta=\alpha m/k$, $\sigma_0=\frac{\Gamma(1+i\eta)}{\Gamma(1-i\eta)}$, $\sigma_l=\sigma_0+\sum_{s}^{l}\tan^{-1}(\eta/s)$

Two remarks can be made about this result. First, it should be realized that when forming $|f|^2$ to calculate the cross-section, an overall factor of $\exp(2i\sigma_0)$ disappears since it is common to both f^{C}_{L} and ${}^{C}f^{JS}_{L'L}$ in all partial waves. Second, the phase ${}^{C}\delta^{JS}_{L'L}$ is not the same as it would be without the Coulomb interaction present. In this work we assume

that the two are the same, and it is the error introduced by this approximation we now wish to investigate.

At this point we consider the example in which there are two strongly coupled channels with the Coulomb potential present in only one of these, as in $\Sigma^- p - \Lambda n$ (I=1/2) for example. The results can be easily generalized to the multi-channel situation, or specialized to a single-channel case. The derivation which we follow is an extension of the single-channel result of Haeringen and Wageningen [24].

The total t-matrix T for Coulomb plus short-range potentials is the solution of the Lipmann-Schwinger equation

$$T(E) = (V_C + V_S) + (V_C + V_S) G^0(E) T(E) \tag{33}$$

where V,T, and G^0 are the matrices

$$\begin{aligned} V_S &= \begin{pmatrix} v_{11} & v_{12} \\ v_{21} & v_{22} \end{pmatrix}, \quad V_C = \begin{pmatrix} v_C & 0 \\ 0 & 0 \end{pmatrix} \\ T &= \begin{pmatrix} t_{11} & t_{12} \\ t_{21} & t_{22} \end{pmatrix}, \quad G^0 = \begin{pmatrix} G_{11} & 0 \\ 0 & G_{22} \end{pmatrix} \end{aligned} \tag{34}$$

with v_{ij}, v_C the strong, and Coulomb potentials, and G_{ii} the free two-body propagator $(E_{ii} - H_0)^{-1}$. A pure Coulomb t-matrix t_C can be defined as the solution of

$$t_C \equiv \begin{pmatrix} t^C_{11} & 0 \\ 0 & 0 \end{pmatrix} = V_C + V_C G^0 \begin{pmatrix} t^C_{11} & 0 \\ 0 & 0 \end{pmatrix} \tag{35}$$

and the total t-matrix written as the sum of t_C and a Coulomb-modified strong amplitude t_S^C. After a little algebra it follows that t_S^C is expressable as[3]

$$t_S^C(E)=[1+t_C(E)G^0(E)]\tilde{t}_S^C(E)[1+G^0(E)t_C(E)] \tag{36}$$

where $\tilde{t}_S^C(E)$ is the solution of

$$\tilde{t}_S^C(E)=V_S+V_SG^C(E)\tilde{t}_S^C(E) \tag{37}$$

and G^C is a Coulomb propagator matrix, defined as

$$G^C \equiv G^0+G^0t_CG^0=\begin{pmatrix} G_{11}^C & 0 \\ 0 & G \end{pmatrix} \tag{38}$$

with $$G_{11}^C=(E_{11}^+-H_0-V_C)^{-1}$$

The only difference between $\tilde{t}_S^C(E)$ and the purely strong t-matrix [eq.(24)] is the replacement of the free propagator G^0 by one appropriate for interactions in the presence of the Coulomb potential. If the v_{ij} are all rank-one separable $|v_i\rangle\lambda^{ij}\langle v_j|$ with all λ^{ij} equal to λ, then $\tilde{t}_S^C(E)$ can be obtained algebraically:

$$\tilde{t}_S^C(E)=\frac{|V\rangle\lambda\langle V|}{(1-\lambda\langle V|G^C(E)|V\rangle)} \equiv |V\rangle D^C(E)\langle V| \tag{39}$$

where $|V\rangle$ is the column matrix of $|v_i\rangle$. From eq.(36), Coulomb modified form factors may also be defined as

---

[3] The angular momentum projections of the operators in eqs.(36) and (37) obey the same equations.

$$|V_C(E)\rangle = (1+t_C(E)G^0(E))|V\rangle$$
$$= \begin{pmatrix} (1+t_{11}(E)G_{11}(E))|v_1\rangle \\ |v_2\rangle \end{pmatrix} \qquad (40)$$

In the notation of eq.(39) the t-matrix becomes

$$t_S^C(E) = |V_C(E)\rangle D^C(E) \langle V_C(E)| \qquad (41)$$

To compare the phase shift predictions of eq.(41) with the corresponding results where the Coulomb potential has been turned off we specialize considerably to the case of single-channel scattering with rank-one Yamaguchi form factors $(\beta^2+p^2)^{-1}$.

The solution of $D^C(E)$ in eq.(39) involves some non-trivial integration, leading to the hypergeometric functions. However, to lowest order in the fine-structure constant α, Haeringen [25] has shown that the Coulomb modified scattering length and effective range are

$$\frac{1}{a_S^c} = \frac{e^{-\delta\nu}}{a_S} - 2\beta\nu(\gamma+\ln(4\nu)) + O(\nu^2)$$
$$\frac{r_S^c}{2} = \frac{r_S}{2} e^{-\delta\nu} + 2\nu/\beta(1+2/(3\beta a_S)) + O(\nu^2) \qquad (42)$$

where $\nu=\alpha m/\beta$, γ is Euler's constant (0.5772...), and a_S, r_S are the corresponding values with no Coulomb interaction.

$$\frac{1}{a_S} = -\beta(\beta^3/(\lambda\pi m v_o^2)+1/2)$$

$$\frac{r_s}{2} = (4/\beta a_s + 3)/2\beta \tag{43}$$

and v_o^2 is the strength of the interaction.

At low energies the phase shifts are related to the effective range expansions by

$$k\cot\delta_s = 1/a_s + r_s k^2/2 + O(k^4) \quad : \text{No Coulomb} \tag{44}$$

$$\frac{2\pi\eta}{e^{2\pi\eta}-1}\, k\cot\delta_s^c + 2k\eta h(\eta) = 1/a_s^c + r_s^c k^2/2 + O(k^4) \quad : \text{Coulomb} \tag{45}$$

with $$h(\eta) = -\gamma + \ln\eta + \eta^2 \sum_{l=1}^{\infty} [l(l^2+\eta^2)]^{-1}$$

and since all the ΣN data exists for energies less than 8 MeV and ν=.0185, this approximation should be adequate for our purposes.

Anticipating the results of this comparison of the phase shifts, the Σ^+p scattering parameters of section 2.VI. will be used. These values are β=1.053 fm^{-1}, and in $^1S_0$ a_s=4.338 fm, r_s=3.681 fm, (a_s^c=3.380 fm, r_s^c=3.493 fm), and in $^3S_1$ a_s=-.358 fm, r_s=-7.232 fm, (a_s^c=-.399 fm, r_s^c=-6.766 fm).

The phase shifts in I=3/2 $^1S_0$, and $^3S_1$ corresponding to the two expansions eqs.(42) and (43) are given in table I for energies less than 10 MeV. In the energy region of the ΣN data ($\sim$3<E<$\sim$7 MeV), the Coulomb modifications to the

E (MeV)	$^1S_0$		$^3S_1$	
	δ_s°	$\delta_s^{c\circ}$	δ_s°	$\delta_s^{c\circ}$
1.0	30.4	22.2	-3.26	-2.44
2.0	35.1	29.8	-4.45	-3.75
3.0	36.8	34.1	-5.27	-4.85
4.0	37.4	35.1	-5.90	-5.54
5.0	37.5	35.5	-6.40	-5.98
6.0	37.2	35.8	-6.80	-6.33
7.0	36.9	35.7	-7.13	-6.68
8.0	36.5	35.6	-7.41	-6.97
9.0	36.0	35.3	-7.65	-7.23
10.0	35.5	35.0	-7.85	-7.46

Table I. Comparison of the Coulomb-corrected phase-shifts δ_s^c with the purely strong phase δ_s in Σ^+p scattering

strong phases may be neglected, to the extent that the correction is less than 5% of δ_S and yet the errors in the data typically exceed 20%. In $\Sigma^- p$ interactions the influence is expected to be even smaller since the Coulomb potential is not present in the coupled ΛN channel and the propagator is unmodified.

2.VI. Results of the Fit to the ΣN Data

With the t-matrix completely defined for ΣN scattering our problem now is to minimize the number of parameters in the model without sacrificing any of its essential features. The difficulty is especially clear since, regardless of the chronic shortage of ΣN data, it was decided earlier that the description of the I=1/2 channel required P and D waves to be included.

Consequently we are obliged to make some rather severe assumptions about the interactions to arrive at a unique fit. First, the range β^{-1} is arbitrarily chosen to be the same in all channels. Clearly, in a more realistic calculation the ΛN potential is expected to be of shorter range than the ΣN interaction. For example, the longest range contribution to the ΣN potential is generated by one-pion exchange, whereas in the elastic ΛN interaction two pions must be exchanged. On the other hand, each π in

$\Lambda N \rightarrow \Lambda N$ scattering is emitted with roughly 80 MeV of energy corresponding to the Σ-Λ mass difference. To some extent this compensates for the shorter range of the two π process.

Second, in S state the $^1S_0$ strengths are related to $^3S_1$ in each isospin channel by the weighting $|\underline{\sigma}_\Sigma \cdot \underline{\sigma}_N|$ with the signs the same as $(\underline{t}_\Sigma \cdot \underline{t}_N)(\underline{\sigma}_\Sigma \cdot \underline{\sigma}_N)$, in agreement with the OBE calculation. We also include the I=1/2 ^3P_J waves assuming the potential strengths to be attractive, and equal in all total J states. Finally, an attractive $^3D_1$ interaction is included in the ΛN channel, but is ignored in ΣN because of the large kinematic suppression of D-waves at low energies.

Assuming the I=1/2 strengths to be the same in both ΣN and ΛN channels, this gives a total of five free parameters; a single range β^{-1}, and one strength parameter in each of the I=1/2 $^3S_1$, ^3P_J, $^3D_1$, and I=3/2 $^3S_1$ channels.

The five parameters of the model were adjusted to fit all the existing ΣN data, which comprises:

(i) elastic $\Sigma^- p, \Sigma^+ p$ differential, and total cross sections [15],

(ii) conversion $\Sigma^- p \rightarrow \Lambda n$ differential, and total cross sections [14], and the

(iii) charge-exchange $\Sigma^- p \rightarrow \Sigma^0 n$ total cross section [14].

Because of the small angular region explored by the experiments, the total cross sections quoted in those works are the differential cross sections integrated over the small angular interval and then multiplied by a factor appropriate for an isotropic distribution. That is,

$$\sigma_{\Sigma N} = \frac{4\pi}{\cos\theta_{MAX} - \cos\theta_{MIN}} \int_{\cos\theta_{MIN}}^{\cos\theta_{MAX}} \frac{d\sigma(\theta)}{d\Omega} \, d\cos\theta \, . \qquad (46)$$

Since with this definition the total cross sections contain Coulomb amplitudes, and neglect possible P-wave contributions in extrapolating to all angles, we have decided to follow the experimental procedure in comparing calculated cross sections with the data.

The results of our fit are shown in figs. 2 and 3 and it is found that, despite the heavy constraints placed on the parameters, the fit is over-determined, with a χ^2/data-point of 0.75 for the 45 points, indicating that the errors in the data have been over-estimated. The best-fit coupling strengths are listed in table II, and in table III the scattering lengths and effective ranges in the elastic Σ^-p channel are given. Also, the phase shifts (δ), and absorption coefficients (η) for elastic Σ^-p scattering in the separate LSJI channels are shown in figs. 4.

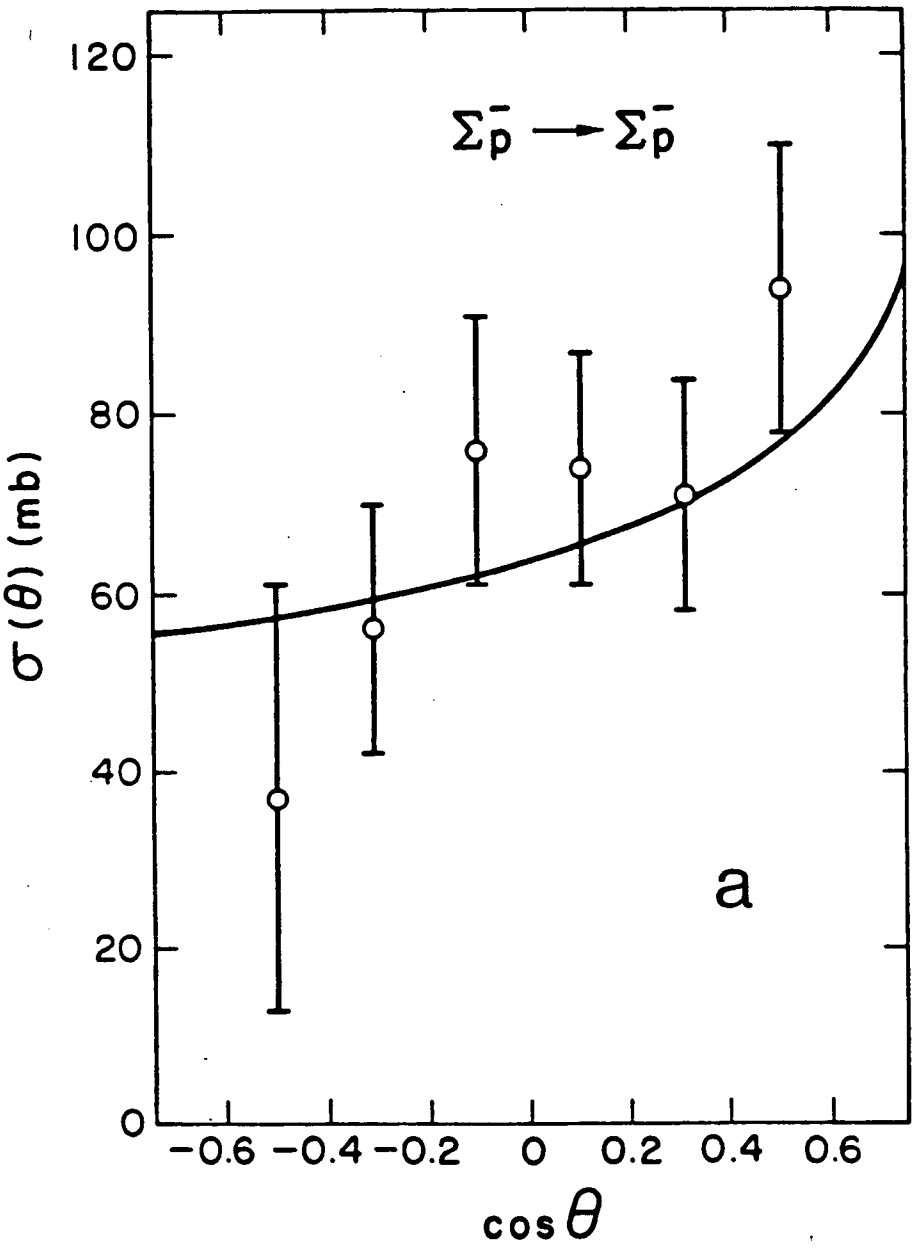

Fig. 2. The ΣN differential cross-sections at 160 MeV/c momentum. a) Elastic $\Sigma^- p$ reaction, b) $\Sigma^- p \rightarrow \Lambda n$ conversion, and c) elastic $\Sigma^+ p$ reaction.

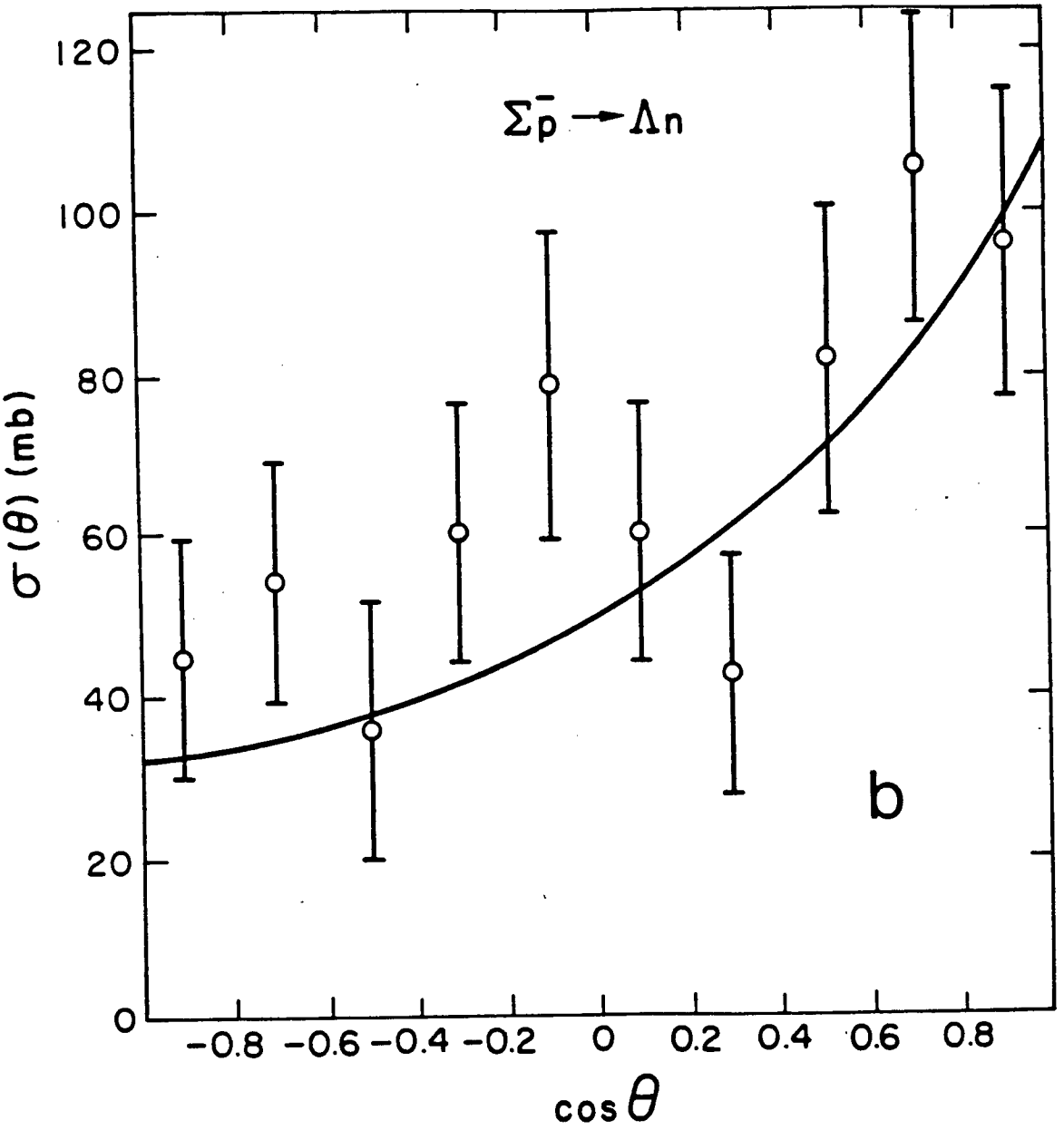
$\Sigma^- p \rightarrow \Lambda n$
b
$\sigma(\theta)$ (mb)
$\cos\theta$
120
100
80
60
40
20
0
-0.8
-0.6
-0.4
-0.2
0
0.2
0.4
0.6
0.8

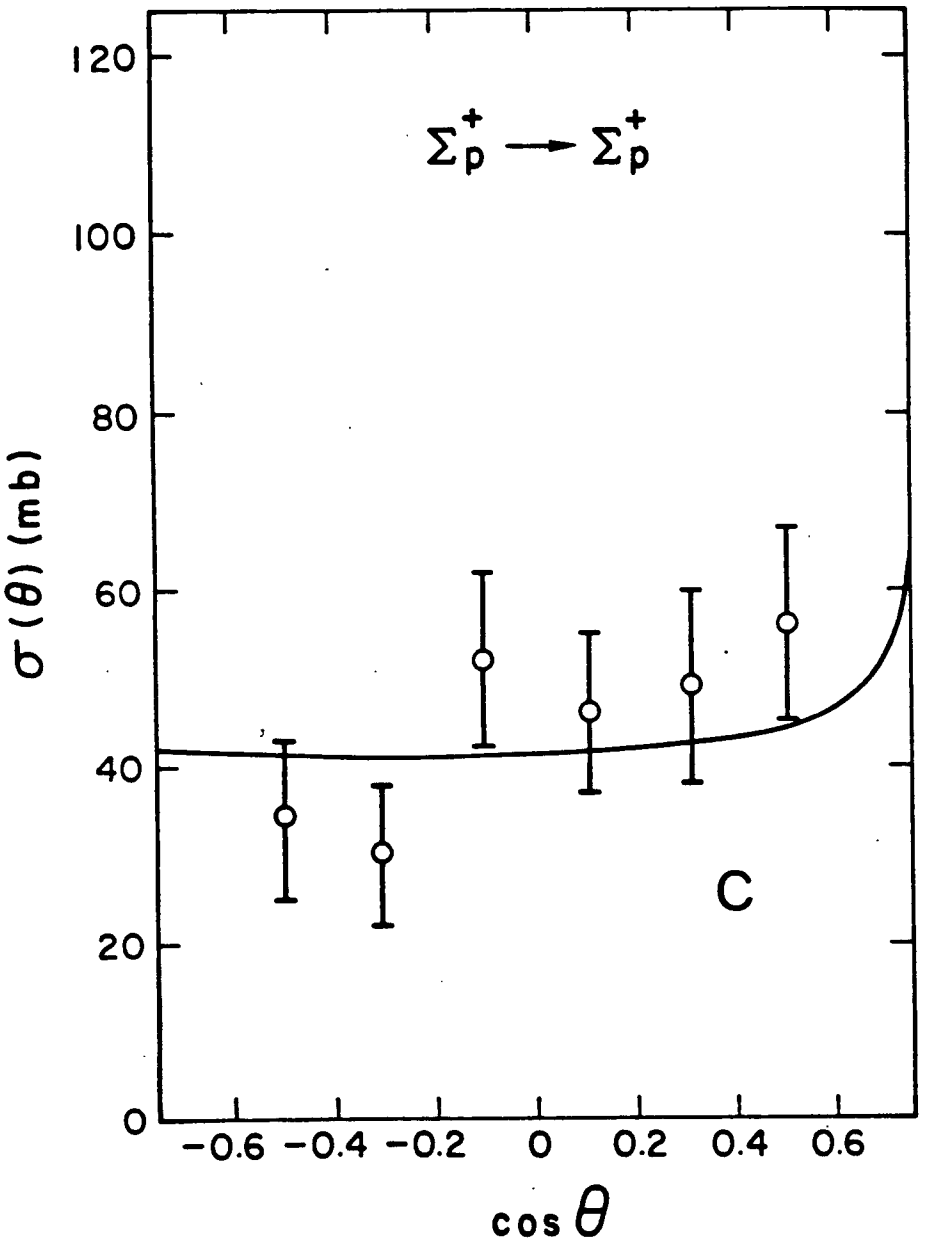
$\Sigma_p^+ \rightarrow \Sigma_p^+$
120
100
80
60
40
20
0
$\sigma(\theta)$ (mb)
−0.6 −0.4 −0.2 0 0.2 0.4 0.6
cos θ
C

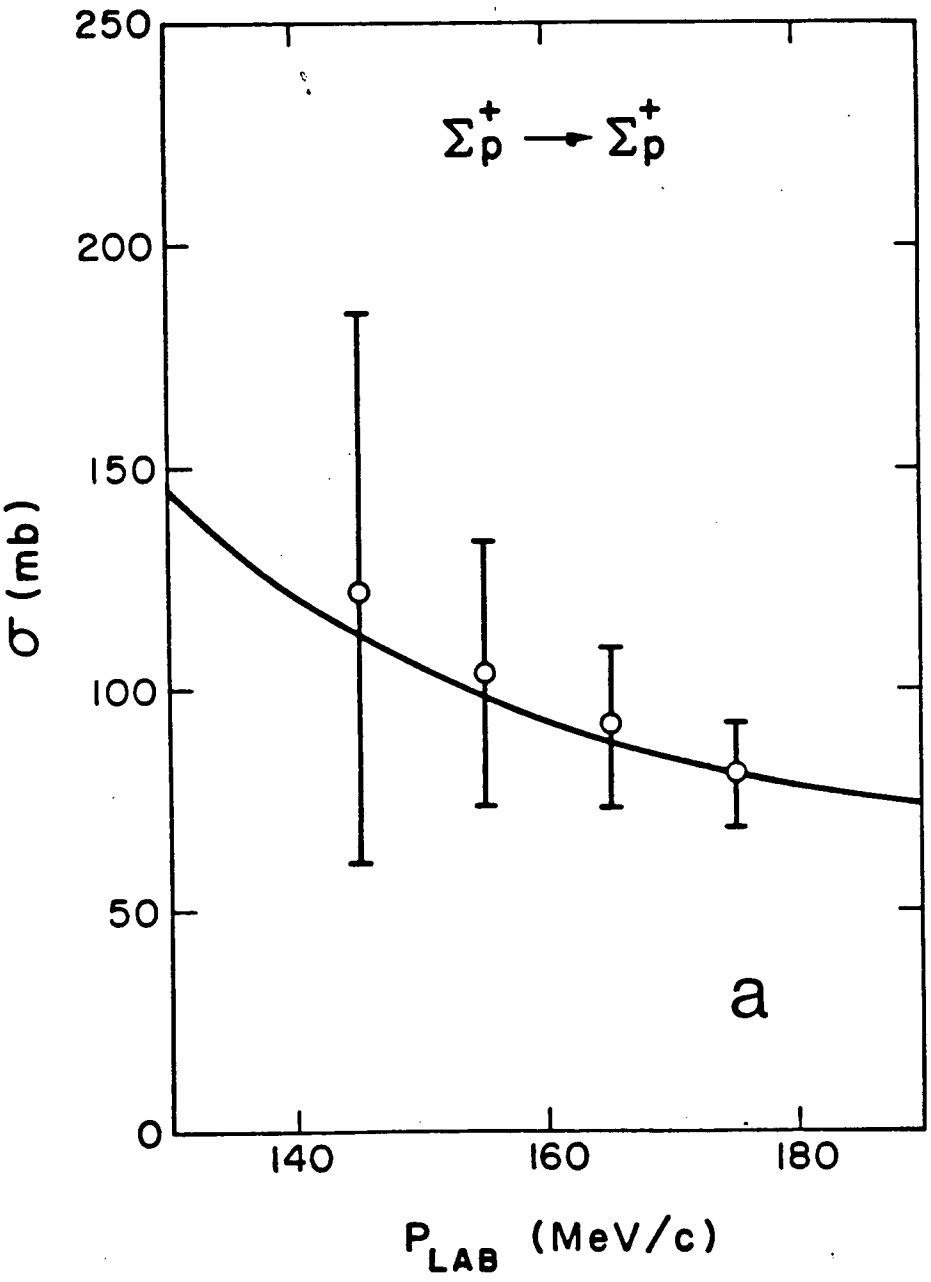

Fig. 3. The low energy ΣN total cross sections. a) Elastic $\Sigma^+ p$ reaction, b) $\Sigma^- p \rightarrow \Lambda n$ conversion, c) elastic $\Sigma^- p$ reaction, and d) $\Sigma^- p \rightarrow \Sigma^0 n$ charge-exchange.

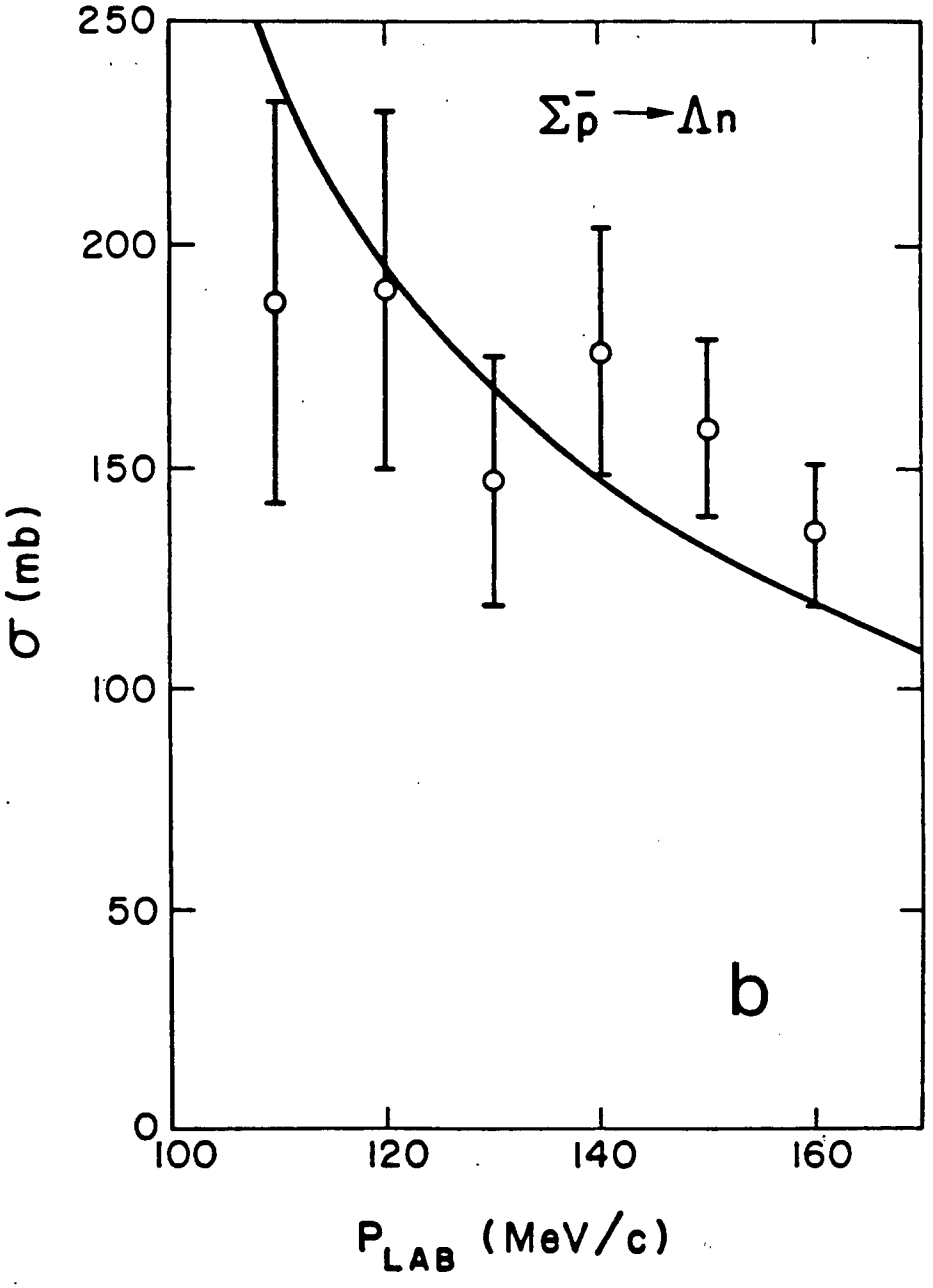
250
200
150
100
50
0
σ (mb)
$\Sigma^- p \rightarrow \Lambda n$
b
100
120
140
160
P_{LAB} (MeV/c)

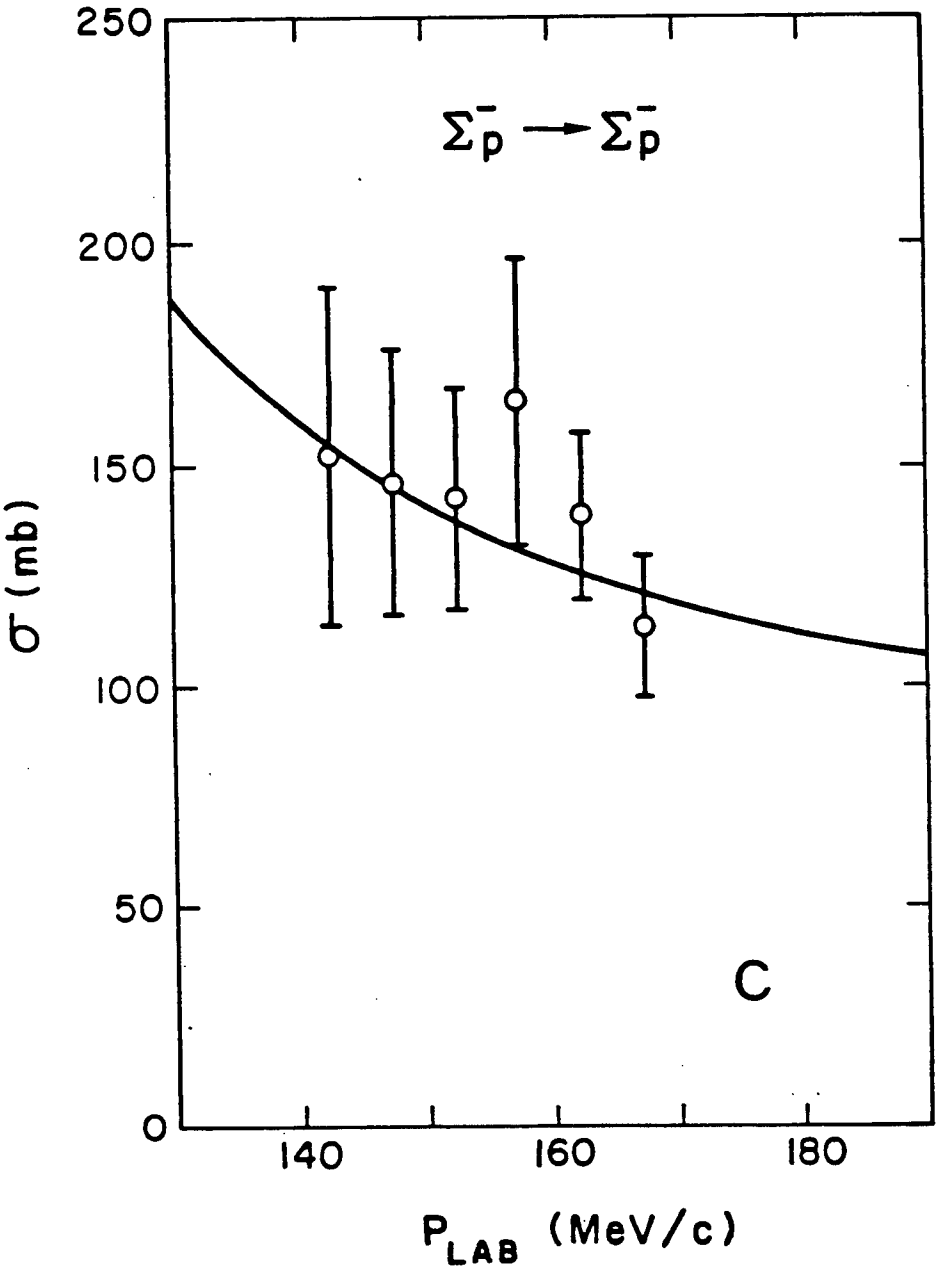
250
200
150
100
50
0
σ (mb)
$\Sigma^- p \rightarrow \Sigma^- p$
C
140
160
180
P_{LAB} (MeV/c)

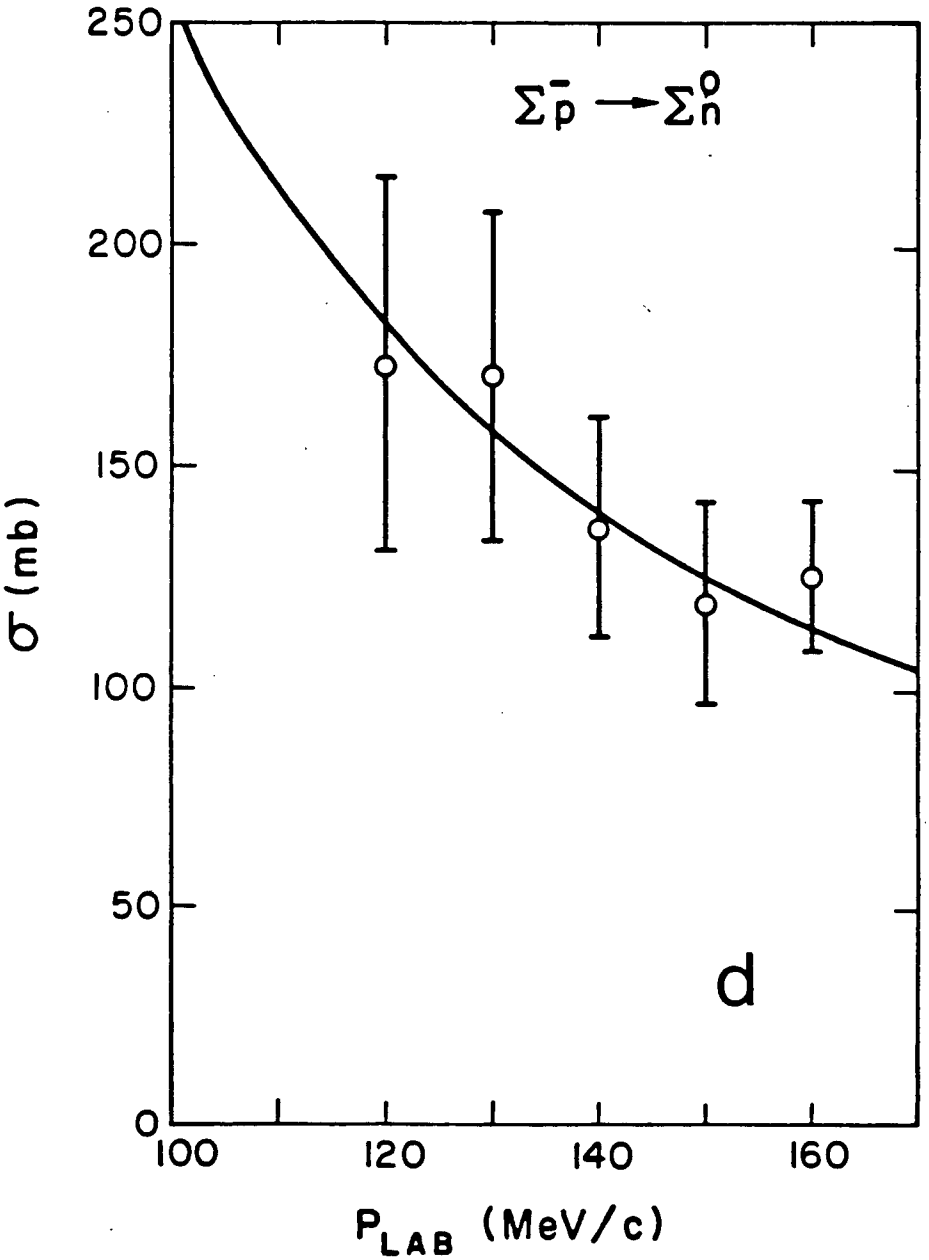
250
200
150
100
50
0
σ (mb)
$\Sigma^- p \rightarrow \Sigma^0 n$
d
100
120
140
160
P_{LAB} (MeV/c)

	I = 1/2				I = 3/2	
	$^1S_0$	$^3S_1$	^3P_J	$^3D_1$	$^1S_0$	$^3S_1$
$^1S_0$	164.46	0	0	0	-38.314	0
$^3S_1$	0	-54.822	0	-37.581	0	12.771
^3P_J	0	0	-14.357	0		
$^3D_1$	0	-37.581	0	-25.762		

Table II. Best-fit coupling strengths $\overline{v}_\beta \lambda^{\beta\alpha} \overline{v}_\alpha$ (MeV/fm). Strengths are identical for ΣN and ΛN channels, except for $^3D_1$ which is ignored for ΣN. $\beta = 1.0563$ fm^{-1} in all channels.

	I = 1/2		I = 3/2	
	a	r	a	r
	fm		fm	
$^1S_0$	-1.448 + i0.374	0.515 - i0.595	4.338	3.682
$^3S_1$	1.027 + i4.757	3.010 - i0.717	-0.358	-7.232
^3P_J	1.045 + i0.461			

Table III. Scattering lengths a and effective ranges r in the elastic $\Sigma^- p$ channel.

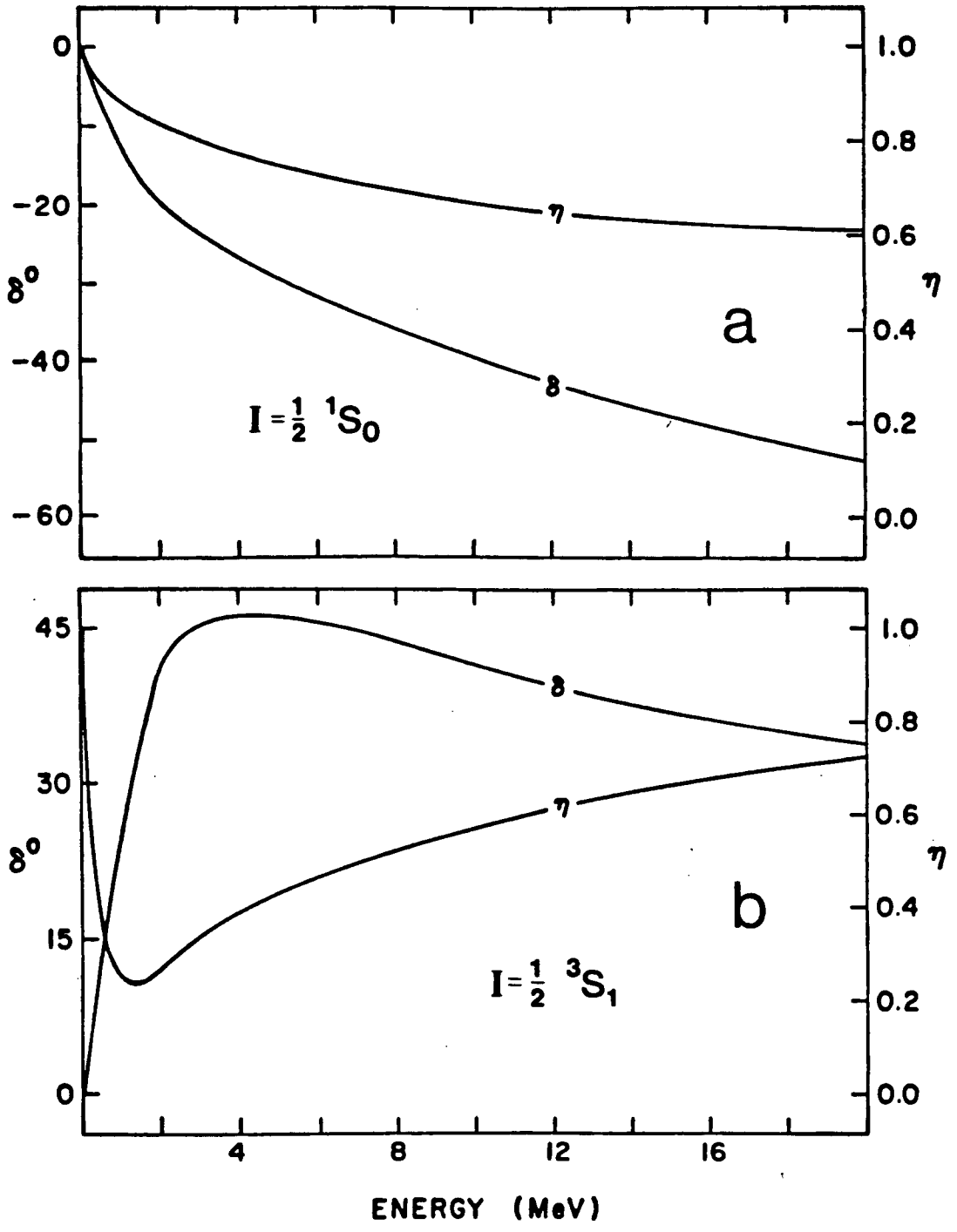

Fig. 4 . Phase shift δ and absorption coefficients η for ΣN→ΣN scattering. a) $^1S_0$ I=1/2, b) $^3S_1$ I=1/2, c) ^3P_J I=1/2, and d) $^1S_0$, $^3S_1$ I=3/2.

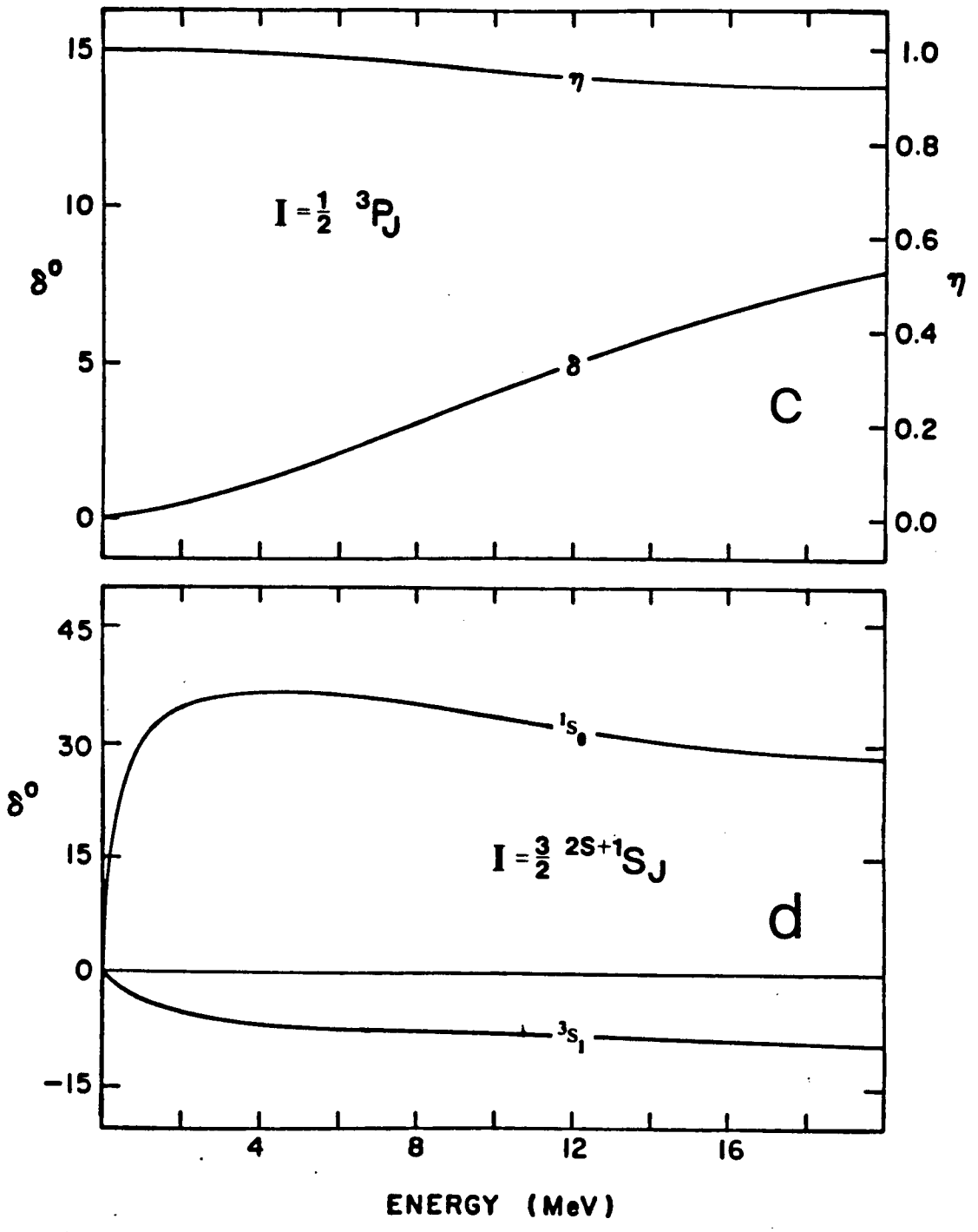
15
10
5
0
δ°
1.0
0.8
0.6
0.4
0.2
0.0
η
η
δ
I = 1/2 ³P_J
c
45
30
15
0
−15
δ°
¹S₀
³S₁
I = 3/2 ²S+¹S_J
d
4
8
12
16
ENERGY (MeV)

Considering the poor quality of ΣN data it is clear that the fits obtained will not be sensitive to even large changes in the parameters. However, there is an accurately known datum, free of P-wave contributions, that is sensitive to the ratio of $^3S_1$ to $^1S_0$ amplitudes. This is the capture ratio at rest,

$$R = \sum_{S=0}^{1} \frac{(2s+1)}{4} \frac{\sigma_{2s+1}(\Sigma^- p \to \Sigma^0 n)}{\sigma_{2s+1}(\Sigma^- p \to \Lambda n) + \sigma_{2s+1}(\Sigma^- p \to \Sigma^0 n)} , \qquad (47)$$

where 2S+1=1,3 for singlet, triplet respectively. The calculated value of R is 0.485, in excellent agreement with the measured value of 0.47±0.01 [ref. 18, and references given therein]. With some confidence we can look at the predictions of the model in more detail.

Most importantly it is found that the inclusion of the I=1/2 P and D-wave terms is essential to the description of ΣN→ΛN conversion. The P-waves comprise less than 2% of the elastic Σ^-p cross section at 160 MeV/c lab momentum, but yield nearly 16% of the conversion cross section. The I=1/2 $^3S_1 \to {}^3D_1$ transition is even more important, contributing 25% of the conversion cross section. In agreement with Nagels et al., we find that the I=1/2 $^3S_1 \to {}^3S_1$ amplitude dominates the Σ^-p reactions and is responsible for 75% of the elastic cross section and over 50% of the conversion reaction.

The I=1/2 $^3S_1$ amplitude is of particular interest. In

the reaction $K^-d \rightarrow \pi^-\Lambda p$ a strong enhancement of the Λp invariant mass distribution has been established near the Σ^+n threshold [26]. It has often been suggested that this enhancement cannot be explained by threshold effects alone and that the cusp arises from either a nearby resonance pole or an unstable ΣN bound state in the $^3S_1$ channel [27].[1]

The status of this pole has been addressed in several model calculations. The OBE calculations of Nagels et al. do not support a bound state, but their results are fairly sensitive to the parameters in this respect. In some of their models no resonances are found [18,20] while others predict a resonance above the Σ^+n threshold on the unphysical energy sheet [19]. Toker et al [28] have studied the $K^-d \rightarrow \pi^-\Lambda p$ reaction in a Faddeev calculation. Using only S-wave separable interactions,[2] they found that the data could be reproduced with or without a ΣN bound state but that the best reproduction of the shoulder in the Λp distribution favoured a resonance pole rather than a bound state. This model (A) placed the pole on the second Riemann

---

[1] This state occurs in the SU(3) $\{\overline{10}\}$ representation of the dibaryon system, another member of which is the deuteron. At least according to exact SU(3) symmetry, one therefore expects a pole in this ΣN amplitude.

[2] Toker et al reproduced the ΣN total cross sections using only the $I=1/2$ $^3S_1$ interaction which probably results in an over-sensitivity to the pole position.

sheet at a momentum of $k=0.162-i0.163\ fm^{-1}$.

The results of our work support model A of Toker et al, producing a pole above the Σ^-p threshold at $k=0.163-i0.082\ fm^{-1}$. The close proximity of this pole to the physical sheet creates very strong energy dependence in the scattering amplitude near threshold. This is demonstrated in fig. 5 where, with zero coupling to the $^3D_1$ ΛN channel, the variation of the off-shell amplitude $-\pi mt(k'=k=0;E)$ near threshold is shown for different values of the $^3S_1$ coupling strength.

This strong energy dependence of the (dominant) $^3S_1$ amplitude will be of particular importance to our study of hypernuclear states. Clearly the large enhancement of the $\Sigma^-p\rightarrow\Lambda n$ conversion near threshold will tend to decrease the lifetime of the Σ-hyperon in the nuclear medium.

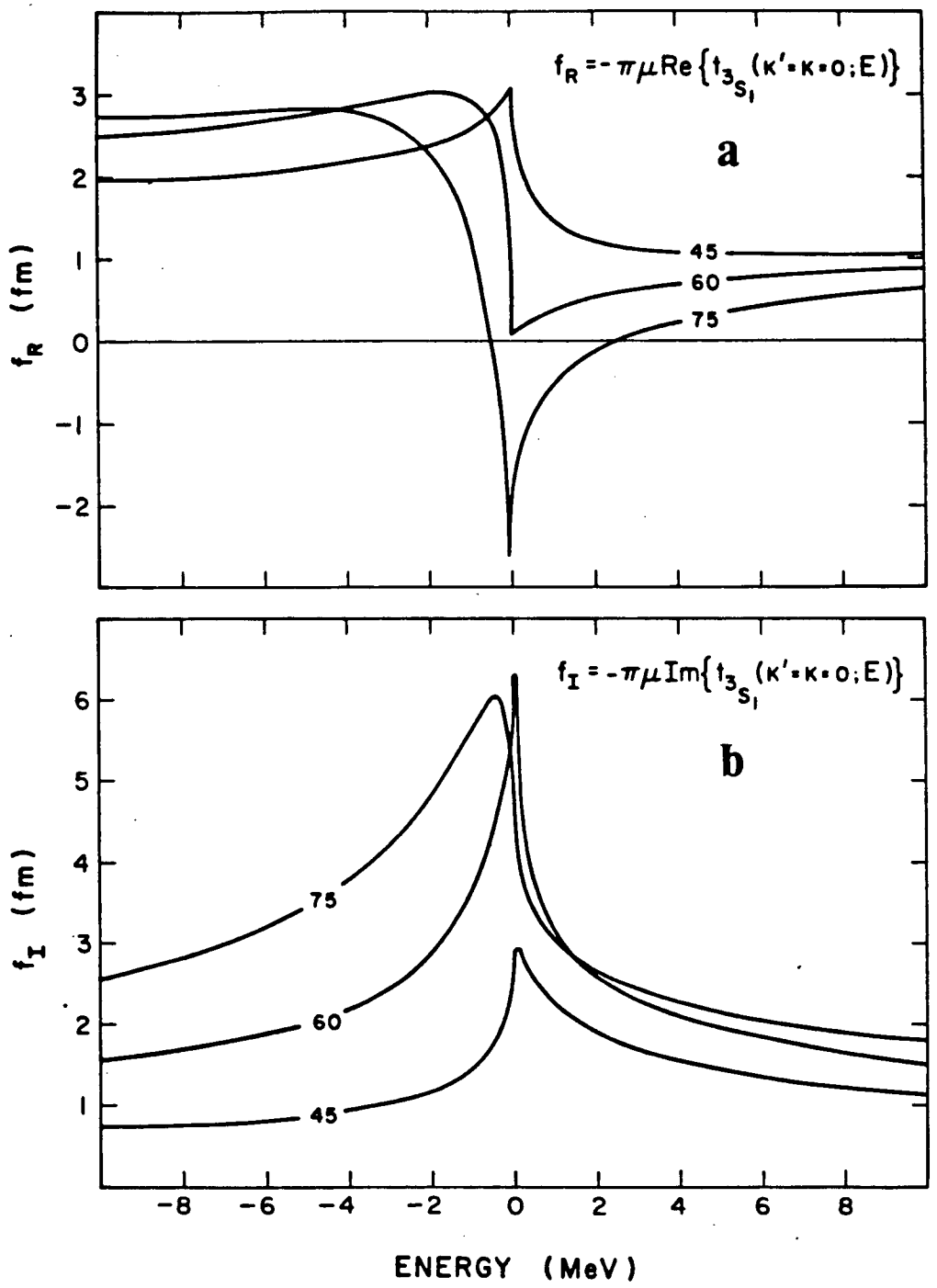

Fig. 5. The energy dependence of the off-shell I=1/2 $^3S_1$ amplitude near the ΣN threshold for different $^3S_1$ coupling strengths as shown (in units of MeV/fm). a) The real component of the amplitude f_R, and b) the imaginary component f_I.

CHAPTER 3 THE Σ-NUCLEUS POTENTIAL

Very little is known about the nature of the Σ-nucleus interaction, and one of the few indications we do have comes from Batty's analysis of Σ^- atoms [12]. In that work the atomic energy shifts were reproduced with a phenomenological potential of the factored ($t\rho$) form

$$V_\Sigma(r) = -\frac{4\pi}{2\mu_{\Sigma A}}\left(1+\frac{m_\Sigma}{m_N}\right) A\,\bar{a}_B\rho(r)\ , \qquad (48)$$

with the medium-corrected ΣN scattering length $\bar{a}_B$ treated as a (complex) parameter. As pointed out by many authors though [1,9], the value of $\bar{a}_B$ consistent with the atomic data leads to predictions for the widths of hypernuclear levels which are very broad. (For example, in s-state $^{12}_{\Sigma^0}C$, calculations using eq.(48) give $\Gamma\sim22$ MeV [9]). Further, this effective scattering length bears little resemblance to the free value, differing by as much as an order of magnitude from some ΣN analyses. (e.g. 0.19i fm as compared with the 1.22i fm of the present work).

3.I. The Need for Many-Body Effects

It is clear from the above results that nuclear many-body effects must play a critical role in the connection between free ΣN, atomic ΣN, and nuclear ΣN interaction descriptions. Amongst these effects, Pauli

blocking of the final state nucleon in ΣN-ΛN conversion and the binding of the nucleons are expected to be most significant.

In the atomic situation, the Σ is bound with essentially zero energy in a Coulomb orbital of high angular momentum and, therefore, absorption occurs primarily on the loosely bound valence nucleons at the nuclear surface. This is a region of low density and correspondingly low Fermi momentum (within a local density approximation). For example, in ^{32}S the 4f orbital is the lowest level reached by the Σ^- [12], and absorption occurs mainly in a region of ~1/5 the central density [29]. The local Fermi momentum is therefore ~60% of the central value, or ~150 MeV/c. Since the momentum of the final state N in ΣN→ΛN decay is roughly twice this value Pauli exclusion should not have too large an effect on the absorptive strength of the potential in this circumstance.

A Σ bound in the ground state of a hypernucleus, on the other hand, is confined almost exclusively to the nuclear interior and absorption occurs mainly on the deeply bound s-state nucleons. In this high density central region both nucleon binding and Pauli effects make important modifications to Σ absorption.

To appreciate the size of correction that nucleon

binding may introduce, consider a Σ bound with (say) 5 MeV which is absorbed on an s-state nucleon bound with 35 MeV. The total energy of the pair is -40 MeV and upon decay the ΛN pair emerges with +40 MeV. Phase space considerations alone require that the amplitude for this conversion be reduced by ~30% relative to the atomic case where the ΣN pair have roughly zero energy.

In addition, for the ΣN decaying at rest the final state nucleon emerges with 285 MeV/c momentum which is comparable to the Fermi momentum at the central density. This implies that a large proportion of decays are forbidden because the final state nucleon is produced with sub-sea momentum. (i.e. The naive picture presented above predicts ~50% suppression for k_F=285 MeV/c).

These simple estimates have been essentially confirmed by Dabrowski and Rozynek [30]. Using an OBE potential of the Nijmegan group [19] in Brueckner reaction matrix theory, they demonstrated that in nuclear matter Pauli exclusion suppressed ΣN decay by 50% from classical estimates.

On the basis of these arguments Pauli blocking and nucleon binding are essential features in understanding the lifetimes of Σ states and a complete microscopic description of the hypernucleus must take them into account.

3.II. The Σ Single-Particle Potential

We turn to the problem of constructing the Σ-nucleus potential with special attention to many-body effects. The coupled equations describing the Σ + A-nucleon system (assuming only pair-wise interactions) are

$$\begin{aligned}
&\Big(K_\Sigma + \sum_i K_i + \sum_i v^i_{\Sigma\Sigma} + \frac{1}{2}\sum_{i\neq j} u_{ij} - E\Big)|\Psi(1\ldots A;\Sigma)\rangle = -\sum_i v^i_{\Sigma\Lambda}|\Psi(1\ldots A;\Lambda)\rangle, \\
&\Big(K_\Lambda + \sum_i K_i + \sum_i v^i_{\Lambda\Lambda} + \frac{1}{2}\sum_{i\neq j} u_{ij} - (E+\Delta m_{\Sigma\Lambda})\Big)|\Psi(1\ldots A;\Lambda)\rangle \qquad (49) \\
&\qquad\qquad = -\sum_i v^i_{\Lambda\Sigma}|\Psi(1\ldots A;\Sigma)\rangle.
\end{aligned}$$

The K_i are single-particle kinetic energy operators, $v_{YY'}$ and u_{ij} are two-body YN and NN potentials, the Ψ are the Y + A -nucleon wavefunctions, and $\Delta m_{\Sigma\Lambda}$ is the Σ-Λ mass difference.

The diverse schemes for approximating solutions to many-body equations like (49) form the foundation of the whole field of nuclear structure physics. These techniques stem from the observation that, as a good first approximation, the nucleus comprises particles which move independently - each bound in an average potential generated by all the other particles. The success of the independent-particle model in predicting many features of nuclei suggests that the most important corrections are due to two-body correlations.

Specifically, we need to extract the interaction of a single YN pair from each of the (A+1)-body equations (49). The sum over YN potentials in each channel can be written in terms of the Σ + nucleon pair, Λ + nucleon pair, single particle, and residual interactions as

$$\sum_i \left(v^i_{\Sigma\Sigma} |\Psi(\Sigma)> + v^i_{\Sigma\Lambda} |\Psi(\Lambda)> \right) = v^A_{\Sigma\Sigma} |\Psi(\Sigma)> + v^A_{\Sigma\Lambda} |\Psi(\Lambda)> + V_\Sigma |\Psi(\Sigma)> + \left[\sum_{i\neq A} \left(v^i_{\Sigma\Sigma} |\Psi(\Sigma)> + v^i_{\Sigma\Lambda} |\Psi(\Lambda)> \right) - V_\Sigma |\Psi(\Sigma)> \right],$$

$$\sum_i \left(v^i_{\Lambda\Lambda} |\Psi(\Lambda)> + v^i_{\Lambda\Sigma} |\Psi(\Sigma)> \right) = v^A_{\Lambda\Lambda} |\Psi(\Lambda)> + v^A_{\Lambda\Sigma} |\Psi(\Sigma)> + V_\Lambda |\Psi(\Lambda)> + \left[\sum_{i\neq A} \left(v^i_{\Lambda\Lambda} |\Psi(\Lambda)> + v^i_{\Lambda\Sigma} |\Psi(\Sigma)> \right) - V_\Lambda |\Psi(\Lambda)> \right]. \quad (50)$$

The V_Y are the hyperon single-particle potentials and the aim is to define them such that the contribution from the residual interactions (the terms in square brackets) is minimized. In other words, we wish to find the V_Σ that gives the best possible estimate of the Σ energy in an effective one-body Hamiltonian.

Similarly for nucleon A we may write

$$\frac{1}{2} \sum_{i\neq j} u_{ij} = \frac{1}{2} \sum_{i\neq j\neq A} u_{ij} + U_A + \left(\sum_{j\neq A} u_{Aj} - U_A \right). \quad (51)$$

and U_A is the nucleon single-particle potential. Neglecting

the residual interactions, the hyperon single-particle potential operators are defined formally using eq.(49) as

$$V_\Sigma|\Psi(\Sigma)\rangle = \sum_{i\neq A}\left(v^i_{\Sigma\Sigma}+v^i_{\Sigma\Lambda}\,\frac{1}{(E+\Delta m_{\Sigma\Lambda}-K_\Lambda-\sum_i K_i-U_A-1/2\sum_{i\neq j\neq A}u_{ij}-V_\Lambda-v_{\Lambda\Lambda})}\times\right.$$
$$\left.\times\sum_j v^j_{\Lambda\Sigma}\right)|\Psi(\Sigma)\rangle\ ,$$
$$V_\Lambda|\Psi(\Lambda)\rangle = \sum_{i\neq A}\left(v^i_{\Lambda\Lambda}+v^i_{\Lambda\Sigma}\,\frac{1}{(E-K_\Sigma-\sum_i K_i-U_A-1/2\sum_{i\neq j\neq A}u_{ij}-V_\Sigma-v_{\Sigma\Sigma})}\times\right. \qquad (52)$$
$$\left.\times\sum_j v^j_{\Sigma\Lambda}\right)|\Psi(\Lambda)\rangle\ ,$$

and where, for economy of space, in the equations (50)-(52) the (A+1)-body wavefunctions $|\Psi(1\ldots A;Y)\rangle$ have been abbreviated to $|\Psi(Y)\rangle$. Because residual interactions have been dropped in the propagators of eqs.(52), matrix elements of V_Y taken between independent-particle states will restrict the sum over j to the one term j=i.

The (A+1)-body equations themselves now become

$$\left(K_\Sigma+K_A+K_{A-i}+v^A_{\Sigma\Sigma}+V_\Sigma+U_A+\frac{1}{2}\sum_{i\neq j\neq A}u_{ij}-E\right)|\Psi(\Sigma)\rangle = -v^A_{\Sigma\Lambda}|\Psi(\Lambda)\rangle\ , \qquad (53)$$
$$\left(K_\Lambda+K_A+K_{A-i}+v^A_{\Lambda\Lambda}+V_\Lambda+U_A+\frac{1}{2}\sum_{i\neq j\neq A}u_{ij}-(E+\Delta m_{\Sigma\Lambda})\right)|\Psi(\Lambda)\rangle = -v^A_{\Lambda\Sigma}|\Psi(\Sigma)\rangle\ .$$

The ΣK_i has been divided explicitly into the nucleon-A and (A-1)-core kinetic energy operators to emphasize the three-body nature of the interaction. That the equations

(53) are indeed three-body equations, and that the recoil of the core is necessary in guaranteeing elastic unitarity has been stressed by many authors [31,32].

The ΣA pair can now be isolated from eq.(53). Defining the YA pair wavefunctions $|\Psi_{\sigma\alpha}(\Sigma A)\rangle$, and $|\Psi_{\lambda\alpha}(\Lambda A)\rangle$ as the overlap integrals $\langle\Phi(A-1)|\Psi(\Sigma)\rangle$ and $\langle\Phi(A-1)|\Psi(\Lambda)\rangle$, with $\langle\Phi(A-1)|$ the (A-1)-core wavefunction, eqs.(53) are multiplied to the left by $\langle\Phi(A-1)|$. Further, separating K_{A-1} into centre-of-mass and internal components, it is found that, since only the average of $K^{INT}_{A-1}+1/2\Sigma u_{ij}$ is needed, this internal Hamiltonian can be replaced by $E-E_{\sigma\alpha}$, where $E_{\sigma\alpha}$ is the ΣA pair energy. Finally, writing the Y and nucleon kinetic energy operators in relative, and centre-of-mass terms they can be combined with the core kinetic energy to give

$$K_Y+K_A+K^{CM}_{A-1} = K_{YA} + P^2/2\mu_Y \ ,$$

with (54)

$$\mu_Y = m_{A-1}(m_N+m_Y)/(m_A+m_Y) \ ,$$

and where P is the YA pair total momentum as measured in the Y-nucleus rest frame.

Assembling all of the above results we arrive at the coupled YA pair equations in relative co-ordinates

$$\left(K_{\Sigma A}+P^2/2\mu_\Sigma+v_{\Sigma\Sigma}+V_\Sigma+U_A-E_{\sigma\alpha}\right)|\psi_{\sigma\alpha}(\Sigma A)> = -v_{\Sigma\Lambda}|\psi_{\lambda\alpha}(\Lambda A)> \ , \tag{55}$$

$$\left(K_{\Lambda A}+P^2/2\mu_\Lambda+v_{\Lambda\Lambda}+V_\Lambda+U_A-(E_{\sigma\alpha}+\Delta m_{\Sigma\Lambda})\right)|\psi_{\lambda\alpha}(\Lambda A)> = -v_{\Lambda\Sigma}|\psi_{\sigma\alpha}(\Sigma A)> \ .$$

As pointed out earlier, Pauli exclusion is expected to play an important role in the Σ lifetime. These effects can be included explicitly by modifying the two-body potentials $v_{\gamma\gamma'}$ to the form $Q_\alpha v_{\gamma\gamma'}$, where Q_α is a projection operator for hyperon and nucleon states defined as

$$Q_\alpha \equiv \underline{1}_\gamma \otimes \left(|\alpha><\alpha| + \sum_{\gamma>K_F} |\gamma><\gamma|\right) \ . \tag{56}$$

Here the $|x>$ are independent-particle states for the nucleons, and the second term in eq.(56) projects only onto those states unoccupied in the nuclear ground state. The presence of the operator $\underline{1}$ for projection on hyperon states just reflects the fact that no Pauli restrictions apply to the hyperon in the nucleus.

If the potential V_Σ has been chosen by a variational procedure to yield the best single-particle energies ϵ, then the difference between $E_{\sigma\alpha}|\psi_{\sigma\alpha}> - <\sigma\alpha|v_{\Sigma\Sigma}|\psi_{\sigma\alpha}>|\sigma\alpha> - <\sigma\alpha|v_{\Sigma\Lambda}|\psi_{\lambda\alpha}>|\sigma\alpha>$ and $(\epsilon_\sigma+\epsilon_\alpha)|\psi_{\sigma\alpha}>$ is a second order correction, and therefore eq.(55) becomes

$$\left(K_{\Sigma A}+P^2/2\mu_\Sigma+Qv_{\Sigma\Sigma}+V_\Sigma+U_A-(\varepsilon_\sigma+\varepsilon_\alpha)\right)|\psi_{\sigma\alpha}(\Sigma A)> = -Qv_{\Sigma\Lambda}|\psi_{\lambda\alpha}(\Lambda A)> ,$$
$$\left(K_{\Lambda A}+P^2/2\mu_\Lambda+Qv_{\Lambda\Lambda}+V_\Lambda+U_A-(\varepsilon_\sigma+\varepsilon_\alpha+\Delta m_{\Sigma\Lambda})\right)|\psi_{\lambda\alpha}(\Lambda A)> = -Qv_{\Lambda\Sigma}|\psi_{\sigma\alpha}(\Sigma A)> , \quad (57)$$

where Q projects only onto unfilled levels in the ground state. In this form it is convenient to eliminate the ΛA wavefunction from eq.(57) to give the ΣA pair equation

$$(K_{\Sigma A}+P^2/2\mu_\Sigma+Qv_{\Sigma A}+V_\Sigma+U_A)|\psi_{\sigma\alpha}(\Sigma A)> = (\varepsilon_\sigma+\varepsilon_\alpha)|\psi_{\sigma\alpha}(\Sigma A)> , \quad (58)$$

with the effective ΣA complex potential $v_{\Sigma A}$ defined as

$$v_{\Sigma A} \equiv v_{\Sigma\Sigma} + v_{\Sigma\Lambda}\frac{1}{(\varepsilon_\sigma+\varepsilon_\alpha+\Delta m_{\Sigma\Lambda}-K_{\Lambda A}-P^2/2\mu_\Lambda-U_A-V_\Lambda-Qv_{\Lambda\Lambda})}Qv_{\Lambda\Sigma} . \quad (59)$$

Asymptotically $|\Psi_{\sigma\alpha}>$ must reduce to the model wavefunctions $|\sigma\alpha>$ as $v_{\Sigma A}\to 0$. Therefore, $|\Psi_{\sigma\alpha}>$ is the solution of the integral relation

$$|\psi_{\sigma\alpha}(\Sigma A)> = |\sigma\alpha> + \frac{1}{(\varepsilon_\sigma+\varepsilon_\alpha-K_{\Sigma A}-P^2/2\mu_\Sigma-V_\Sigma-U_A)}Qv_{\Sigma A}|\psi_{\sigma\alpha}(\Sigma A)>. \quad (60)$$

If we now introduce the Brueckner reaction matrix τ_α which has the property that $\tau_\alpha|\sigma\alpha> = v_{\Sigma A}|\Psi_{\sigma\alpha}>$ then, using eq.(60), τ_α is

$$\tau_\alpha = v_{\Sigma A} + v_{\Sigma A}(\varepsilon_\sigma+\varepsilon_\alpha-K_{\Sigma A}-P^2/2\mu_\Sigma-V_\Sigma-U_A)^{-1}Q\tau_\alpha . \quad (61)$$

Here τ_α is the effective ΣN interaction, in the sense that τ_α acting on the model wavefunctions is equivalent to $v_{\Sigma A}$

acting on the pair wavefunction.

At this point we are in a position to define the Σ single-particle potential. Since $v_{\Sigma A}$ is independent of particle labels the Σ-nucleus Schroedinger equation can be written as

$$(K_{\Sigma A}+H_N+Av_{\Sigma A})|\Psi(\Sigma)> = E\ |\Psi(\Sigma)> \ , \tag{62}$$

where $K_{\Sigma A}$ is the Σ-nucleus kinetic energy operator in relative co-ordinates and H_N is the internal nuclear Hamiltonian. Provided only the ground state expectation value of eq.(62) is needed, $E-H_N$ can be replaced by ϵ_σ. Multiplying eq.(62) to the left by the ground state nuclear wavefunction <0| produces the Σ single particle equation

$$\begin{aligned}\epsilon|\sigma> &= K_{\Sigma A}|\sigma> + A\Sigma_\alpha <\alpha|v_{\Sigma A}|\Psi_{\sigma\alpha}> \\ &= (K_{\Sigma A}+A\Sigma_\alpha <\alpha|\tau_\alpha|\alpha>)|\sigma>\end{aligned} \tag{63}$$

Therefore, the single-particle potential is clearly

$$V_\Sigma|\sigma> = A\Sigma_\alpha <\alpha|\tau_\alpha|\alpha\sigma> \tag{64}$$

Specifically, introducing the Σ states $|\underset{\sim}{k}>, |\underset{\sim}{k}'>$ the total Σ potential is

$$<\underset{\sim}{k}'|V_\Sigma|\underset{\sim}{k}> = \sum_\alpha \int d\underset{\sim}{p}\ \phi^*_\alpha(\underset{\sim}{p}-\underset{\sim}{q})<\underset{\sim}{k}',\ \underset{\sim}{p}-\underset{\sim}{q}|\tau_\alpha(\omega)|\underset{\sim}{k},\underset{\sim}{p}>\ \phi_\alpha(\underset{\sim}{p}) \ , \tag{65}$$

where q is the three-momentum transfer, Φ_α is the nucleon single-particle wavefunction, and ω is the complicated energy variable defined by eq.(61).

Until now the development of V_Σ has been purely formal and so it is worthwhile to consider what V_Σ means at the microscopic level. First of all, let us expand the integral equation (61) for τ in the Born series

$$\langle\sigma\alpha|\tau|\sigma\alpha\rangle=\langle\sigma\alpha|v_{\Sigma A}|\sigma\alpha\rangle+\sum_{\sigma'\alpha'}\langle\sigma\alpha|v_{\Sigma A}\frac{|\sigma'\alpha'\rangle\ Q\ \langle\sigma'\alpha'|}{(\epsilon_\sigma+\epsilon_\alpha-\epsilon'_\sigma-\epsilon'_\alpha)}v_{\Sigma A}|\sigma\alpha\rangle \qquad (66)$$

$$+\sum_{\substack{\sigma'\alpha'\\ \sigma''\alpha''}}\langle\sigma\alpha|v_{\Sigma A}\frac{|\sigma'\alpha'\rangle\ Q\ \langle\sigma'\alpha'|}{(\epsilon_\sigma+\epsilon_\alpha-\epsilon'_\sigma-\epsilon'_\alpha)}v_{\Sigma A}\frac{|\sigma''\alpha''\rangle\ Q\ \langle\sigma''\alpha''|}{(\epsilon_\sigma+\epsilon_\alpha-\epsilon''_\sigma-\epsilon''_\alpha)}v_{\Sigma A}|\sigma\alpha\rangle+\ldots$$

where, as usual, the Q operators restrict the summations over $|\alpha'\rangle$, $|\alpha''\rangle$ to nucleon states above the Fermi sea. In addition to this infinite series, the definition of $v_{\Sigma A}$ in eq.(59) shows that each term $\langle\sigma\alpha|v_{\Sigma A}|\sigma\alpha\rangle$ implicitly comprises all possible ΛN intermediate states and so can also be expanded in a infinite series. If we simplify the notation of the propagator G of eq.(59) to the form

$$G = (\epsilon_\sigma+\Delta m_{\Sigma\Lambda}+\epsilon_\alpha-H_0-Qv_{\Lambda\Lambda})^{-1} \qquad (67)$$

then $G = G^0+G^0Qv_{\Lambda\Lambda}G$, and $G^0 = (\epsilon_\sigma+\Delta m_{\Sigma\Lambda}+\epsilon_\alpha-H_0)^{-1}$

with $H_0= K_{\Lambda A}+P^2/2m+U_A+V_\Lambda$.

The effective potential $v_{\Sigma A}$ is equivalent to the series

$$\langle\sigma\alpha|v_{\Sigma A}|\sigma\alpha\rangle = \langle\sigma\alpha|v_{\Sigma\Sigma}|\sigma\alpha\rangle+\sum_{\lambda'\alpha'}\langle\sigma\alpha|v_{\Sigma\Lambda}\frac{|\sigma\alpha'\rangle\ Q\ \langle\sigma\alpha'|}{(\epsilon_\sigma+\epsilon_\alpha-\epsilon'_\lambda-\epsilon'_\alpha)}v_{\Lambda\Sigma}|\sigma\alpha\rangle \qquad (68)$$

$$+\sum_{\substack{\lambda'\alpha'\\ \lambda''\alpha''}} \langle\sigma\alpha|v_{\Sigma\Lambda}\frac{|\lambda'\alpha'\rangle\ Q\ \langle\lambda'\alpha'|}{(\epsilon_\sigma+\epsilon_\alpha-\epsilon_\lambda'-\epsilon_\alpha')}v_{\Lambda\Lambda}\frac{|\lambda''\alpha''\rangle\ Q\ \langle\lambda''\alpha''|}{(\epsilon_\sigma+\epsilon_\alpha-\epsilon_\lambda''-\epsilon_\alpha'')}v_{\Lambda\Sigma}|\sigma\alpha\rangle+\ldots$$

This series for τ is shown graphically below. As is standard in Goldstone diagrams, arrows pointing into a vertex are states occupied before the interaction, and arrows pointing away are states occupied afterwards.

$\langle\sigma\alpha|\tau|\sigma\alpha\rangle =$ 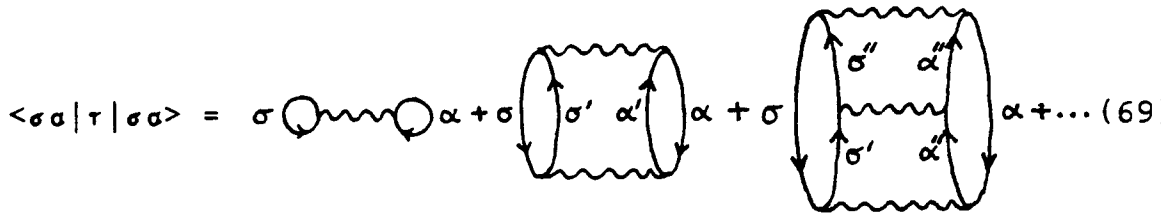

(69)

and <u>each</u> wiggly line of the form σ'/σ ~ α'/α represents the infinite series $\langle\sigma'\alpha'|v_{\Sigma\Lambda}|\sigma\alpha\rangle$:

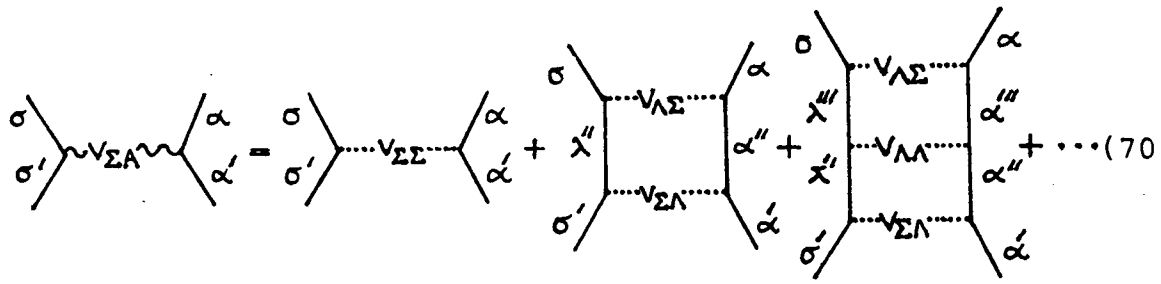

(70)

A sum over all intermediate states is to be understood in these diagrams.

So we find that using this definition of the potential V_Σ to calculate the Σ binding energy is equivalent to summing the contributions fromm all possible diagrams which involve only two particles. In other words, higher order

corrections to the Σ energy must involve at least three body clusters .

In practice V_Σ is difficult to evaluate, particularly since ω also depends on V_Σ. The best approach is the Brueckner-Hartree iterative method in which τ is calculated initially using a reasonable spectrum of single-particle energies and the single-particle potentials in ω are set equal to zero. V_Σ is then determined by eq.(65) and a new value for the Σ energy is fixed by the Σ-nucleus Schroedinger equation. This cycle is repeated until a self-consistent solution is achieved.

A remark worth making at this point is that a complete, self-consistent solution would also include optimization of the nucleon single particle states since the contribution of the ΣN potential to U_A perturbs the nuclear density. Fortunately, this influence can be safely ignored since first, it is an O(1/A) correction and, second, it is known experimentally that the Σ is only weakly bound (if at all) so that the ΣN potential must be weak relative to NN interactions.

3.III. Approximations in the Single-Particle Potential

In the present work we shall not demand a fully self-consistent solution. We wish is to approximate eq.(65)

to a more manageable form while retaining its most important features. Essentially our aim is to apply the Brueckner-Hartree method only to first order. That is, the single-particle potentials entering τ will be set equal to zero and then the momentum-space Schrodinger equation solved self-consistently for the Σ binding energy. Higher-order corrections to V_Σ would involve the Σ and N potentials but in this work the primary interest is the lifetime of the hypernuclear levels and, therefore, with the energy available in asymptotic states. The energy dependence defined above should be appropriate for this purpose.

In partial compensation for this ambiguity in the energy dependence we invoke closure approximation to replace the nucleon energies ϵ_α by an average value -B which is treated as a parameter in practice. Our final simplification is to replace τ_α by its spin-, and isospin-averaged value $\bar{\tau}$, which is exact to O(1/A). The expression for the Σ^0 single-particle potential is then

$$V_\Sigma(\underset{\sim}{k}',\underset{\sim}{k};E_\Sigma) = \int d\underset{\sim}{p}\ \bar{\tau}(\underset{\sim}{\kappa}',\underset{\sim}{\kappa};\omega) \sum_\alpha \phi_\alpha^*(\underset{\sim}{p}-\underset{\sim}{q})\phi_\alpha(\underset{\sim}{p}) \ , \qquad (71)$$

where $\underset{\sim}{k},\underset{\sim}{k}'$ are the initial and final state Σ-nucleus relative momenta; $\underset{\sim}{\kappa}$, $\underset{\sim}{\kappa}'$ are the initial and final state ΣN momenta in the ΣN rest frame, and ω is the three-body energy

$$\omega = \varepsilon_\Sigma - B - (\underset{\sim}{k}+\underset{\sim}{p})^2/2\mu_\Sigma \ . \qquad (72)$$

Despite our simplifications, the many-body effects embedded in τ still make the integrand of eq.(71) a very complicated function. It can be seen from the integral relation (61) that τ resembles the free ΣN t-matrix except that the free propagator has been replaced by one appropriate for a Σ interacting with a bound nucleon. This analogy can be pushed farther. If partial-wave mixing in τ is ignored (which is equivalent to using the angle-averaged Pauli operator [33,34]) it can be shown that to describe scattering from the state $|\alpha>$ to $|\beta>$, τ satisfies

$$\begin{aligned} \tau_{\beta\alpha}(\omega) &= |v_\beta>\lambda^{\beta\alpha}\Big(1 - \sum_\gamma \lambda^{\gamma\gamma}<v_\gamma|Q^0G_\gamma(\omega)|v_\gamma>\Big)^{-1}<v_\alpha| \ , \\ &\equiv |v_\beta>D_{\beta\alpha}(\omega)<v_\alpha| \ , \end{aligned} \tag{73}$$

where Q^0 is the angle-averaged Pauli operator (to be discussed fully in sect. 3.IV.), the $|v_\gamma>$ are the form factors of the separable potentials of chapter 2, and the summation over γ includes all coupled channels.

The main difficulty presented in integrating eq.(71) is the angular dependence of the energy variable ω, since all other factors normally have a closed, analytic form. A number of approximation schemes have been devised to circumvent this difficulty. In the simplest, fully factored form τ is removed from the integrand and evaluated at some

'average' value of the nucleon momentum. A much better approach is to leave τ within the integral but replace all angles in τ by their average value [32]. Although the latter is much better than the former, the angular dependence is still treated only approximately. The obvious successes of such models in describing scattering situations may be attributable to incident energies which are large in comparison with nucleon energies, and a τ which is a slowly varying function of energy.

A priori, neither of the above features can be expected to hold true in Σ hypernuclei. The Σ and N energies are comparable in the hypernucleus. Perhaps more importantly, all separable potential predictions of ΣN scattering lead to strong energy dependence in the (dominant) $^3S_1$ I=1/2 channel near threshold [c.f. section 2.VI.,and also ref. 28].

Consequently, we make no further approximations in evaluating eq.(71). That is, we evaluate the full, three-dimensional integral exactly.

The potential (71) can be put in a more convenient form for angular integration by changing variables from the nucleon momentum $\underline{p}$ to the ΣN total momentum $\underline{P}=\underline{k}+\underline{p}$. In this way ω becomes a scalar function of $\underline{P}$ and all angular dependence resides in the simpler τ form factors and nuclear wavefunction. With this substitution V_Σ becomes

$$V_\Sigma(\underset{\sim}{k}',\underset{\sim}{k};E_\Sigma) = \int d\underset{\sim}{P}\ \bar{\tau}\left(\underset{\sim}{k}'-\varepsilon\underset{\sim}{P},\underset{\sim}{k}-\varepsilon\underset{\sim}{P};\omega(P^2)\right) F(\underset{\sim}{P}-\underset{\sim}{k}';\underset{\sim}{P}-\underset{\sim}{k}) \ , \tag{74}$$

and $\varepsilon \equiv m_\Sigma/(m_\Sigma+m_N)$, and $F(\underset{\sim}{P}-\underset{\sim}{k}';\underset{\sim}{P}-\underset{\sim}{k}) \equiv \sum_\alpha \phi^*_\alpha(\underset{\sim}{P}-\underset{\sim}{k}')\phi_\alpha(\underset{\sim}{P}-\underset{\sim}{k})$.

With harmonic oscillator single-particle nucleon wavefunctions F may be expanded in partial waves as

$$\begin{aligned} F(\underset{\sim}{P}-\underset{\sim}{k}';\underset{\sim}{P}-\underset{\sim}{k}) &= f_o\left(1+a^2\nu\left(P^2-\underset{\sim}{P}\cdot(\underset{\sim}{k}+\underset{\sim}{k}')+\underset{\sim}{k}\cdot\underset{\sim}{k}'\right)\right)e^{-a^2\left(P^2+\frac{1}{2}(k^2+k'^2)-\underset{\sim}{P}\cdot(\underset{\sim}{k}+\underset{\sim}{k}')\right)} \ , \\ &= f_o\ e^{-a^2\left(P^2+\frac{1}{2}(k^2+k'^2)\right)} \sum_{\ell\ell'} (2\ell+1)(2\ell'+1)\left(\rho^o_{\ell\ell'}+\rho^1_{\ell\ell'}\hat{k}\cdot\hat{k}'\right) \\ &\quad P_\ell(\hat{P}\cdot\hat{k})P_{\ell'}(\hat{P}\cdot\hat{k}') \ , \end{aligned} \tag{75}$$

with $f_o=4a^3/\pi^{3/2}$, $\nu=(A-4)/6$, and a^2 chosen to fit the r.m.s. matter radius [35]. This result follows by expanding the exponentials separately in partial waves and using the recursion relations for Legendre polynomials. The functions $\rho^o_{\ell\ell'}$ and $\rho^1_{\ell\ell'}$ are given by

$$\begin{aligned} \rho^o_{\ell\ell'} &= \left(1-\nu(\ell+\ell')+a^2\nu P^2\right) i_\ell(x)\, i_{\ell'}(x') - \nu\left(x\, i_{\ell+1}(x)\, i_{\ell'}(x') + x'\, i_\ell(x)\, i_{\ell'+1}(x')\right), \\ \rho^1_{\ell\ell'} &= a^2\nu k k'\, i_\ell(x)\, i_{\ell'}(x') \ , \end{aligned} \tag{76}$$

with $x=a^2Pk$, $x'=a^2Pk'$, and the i_ℓ are modified spherical bessel functions.

Similarly, the two-body τ can be expanded as a function of the three angles $\hat{k}\cdot\hat{k}'$, $\hat{P}\cdot\hat{k}$, and $\hat{P}\cdot\hat{k}'$. The normalization of τ is chosen to be the same as was used for the two-body t-matrix. The spin-, and isospin-averaged τ is then

$$\bar{\tau}(\kappa',\kappa;\omega) = 1/4\pi \sum_{ILSJ} \frac{(2J+1)(2I+1)}{24} \tau^{I}_{LSJ}(\kappa',\kappa;\omega) P_L(\hat{\kappa}\cdot\hat{\kappa}') \ , \tag{77}$$

with $$\tau^{I}_{LSJ}(\kappa',\kappa;\omega) = v_L(\kappa') D^{I}_{LSJ}(\omega) v_L(\kappa) \kappa^L \kappa'^L \ .$$

In our case the v_L are the Yamaguchi form factors in both S and P waves.

Note that eq.(77) defines the expansion of $\bar{\tau}$ in the ΣN centre-of-mass whereas the integral (74) requires $\bar{\tau}$ in the Σ-nucleus frame. Using $\underline{\kappa} = \underline{k} - \epsilon \underline{P}$, and $\underline{\kappa}' = \underline{k}' - \epsilon \underline{P}$ it has been shown [36,37] that the general relation connecting spherical harmonics in the two frames is

$$\kappa^L \kappa'^L P_L(\hat{\kappa}\cdot\hat{\kappa}') = (4\pi)^2 \sum_{\substack{a\alpha \\ b\beta}} \sum_{m} \left(\binom{2L+1}{2a} \binom{2L+1}{2b} \frac{1}{(2a+1)(2b+1)} \right)^{\frac{1}{2}} (-\epsilon P)^{a+b} k^{L-a} k'^{L-b}$$
$$\binom{a\ L-a\ L}{\alpha\ m-\alpha-m} \binom{b\ L-b\ L}{\beta\ m-\beta-m} Y^{\alpha}_{a}(\hat{P}) Y^{\beta *}_{b}(\hat{P}) Y^{m-\alpha}_{L-a}(\hat{k}) Y^{m-\beta *}_{L-b}(\hat{k}') \ . \tag{78}$$

The two-body form factors expand as

$$v(\kappa) = \left(\beta^2 + (\underline{k} - \epsilon \underline{P})^2\right)^{-1} = \frac{1}{2\epsilon P k} \sum_{n} (2n+1) Q_n \left(\frac{\beta^2 + k^2 + \epsilon^2 P^2}{2\epsilon P k} \right) P_n(\hat{P}\cdot\hat{k}),$$
$$\equiv \sum_{n} v_n(k;P) P_n(\hat{k}\cdot\hat{P}) \ , \tag{79}$$

where the Q_n are Legendre polynomials of the second kind.

With equations (75)-(79) inserted into eq.(74) the

angular integrals can be performed. This is a fairly straightforward, but lengthy, exercise producing the general result (appendix III)

$$V_\Sigma(\underset{\sim}{k}',\underset{\sim}{k};E_\Sigma) = 1/4\pi \sum (2\ell+1)V_\ell(k',k;E_\Sigma)P_\ell(\hat{k}\cdot\hat{k}') \ ,$$

where

$$V_\ell(k',k;E_\Sigma) = 4\pi f_o e^{-a^2/2(k^2+k'^2)} \int dp p^2 e^{-a^2p^2} \sum_{\ell'=0}^{1} \sum_{\ell''\ell'''} (2\ell''+1)(2\ell'''+1)$$

$$\rho^{\ell'}_{\ell''\ell'''} \sum_{ILSJ} \frac{(2J+1)}{4} \frac{(2I+1)}{6} D^I_{LSJ}(\omega) \sum_{ab}^{L} (-\varepsilon P)^{a+b} \ k^{L-a} \ k'^{L-b}$$

$$\sum_{nm} v_n(k:P) v_m(k':P) \left(\frac{(2L)!}{(2a)!(2(L-a))!} \frac{(2L)!}{(2b)!(2(L-b))!} \right)^{1/2} (2L+1)$$

$$\sum_{L'L''L'''L^{iv}} (2L'+1)(2L''+1)(2L'''+1)(2L^{iv}+1) \begin{pmatrix} \ell & \ell' & L' \\ 0 & 0 & 0 \end{pmatrix}^2 \begin{pmatrix} n & \ell'' & L'' \\ 0 & 0 & 0 \end{pmatrix}^2$$

$$\begin{pmatrix} m & \ell''' & L''' \\ 0 & 0 & 0 \end{pmatrix}^2 \begin{pmatrix} L' & L'' & L-a \\ 0 & 0 & 0 \end{pmatrix} \begin{pmatrix} L' & L''' & L-b \\ 0 & 0 & 0 \end{pmatrix} \begin{pmatrix} b & L'' & L^{iv} \\ 0 & 0 & 0 \end{pmatrix} \begin{pmatrix} a & L''' & L^{iv} \\ 0 & 0 & 0 \end{pmatrix}$$

$$\begin{Bmatrix} L-a & L' & L'' \\ L & L-b & b \\ a & L''' & L^{iv} \end{Bmatrix} . \qquad (80)$$

This is not a very convenient-looking expression, but with only S and P waves included in $\bar{\tau}$ it simplifies considerably. Then at least two of the entries in the 9J symbol are always zero, thereby reducing it to a 3J.

The advantage of the above form is that we have found it possible to reduce the Brueckner potential to an exact one-dimensional integral without relying on untested

approximations affecting the energy dependence.

3.IV. The Pauli Exclusion Principle

So far the Pauli principle has only been introduced formally into the ΣN interactions via the operator equation (61). It has been repeatedly stressed though that Pauli effects will be a major factor influencing the lifetime of Σ states, and so in this section a closer look will be taken at the Q operator.

As defined by eq.(56), Q projects only onto unoccupied nucleon levels in the nuclear ground state, and thereby excludes the propagation of the intermediate state nucleon through filled states. The formal similarity of the Lipmann-Schwinger equations for $\tau(\omega)$ and the free t-matrix $t(\omega)$ can be exploited to write the exact relation

$$\tau(\omega)=t(\omega)-t(\omega)\tilde{Q}G_0(\omega)\tau(\omega) \qquad (81)$$

where the matrices in eq.(81) couple the ΣN and ΛN channels (but have not been expanded in partial waves). $G_0(\omega)$ is the propagator in the nuclear medium, with the energy dependence ω defined by eq.(72). The operator $\tilde{Q}=1-Q$ projects onto occupied levels in the ground state.

Since τ is embedded in the three-body space of the Σ,N, and (A-1) spectator core, matrix elements are taken between

states $|\underline{k},\underline{P}>$ and $|\underline{k}',\underline{P}>$, with $\underline{k}$ the ΣN pair relative momentum, and $\underline{P}$ the core momentum relative to the pair. That $\underline{P}$ must be the same in initial and final states is simply a reflection of the fact that the core is non-interacting. Similarly, the other operators have the matrix elements

$$<\underline{k}',\underline{P}|t(\omega)|\underline{k},\underline{P}> = \delta(\underline{P}-\underline{P}')<\underline{k}'|t[\omega,P^2]|\underline{k}> \qquad (82)$$

$$<\underline{k}',\underline{P}|\tilde{Q}G_0(\omega)|\underline{k},\underline{P}>=\delta(\underline{P}-\underline{P}')\delta(\underline{k}-\underline{k}')\tilde{Q}(\underline{k},\underline{P})G_0[\omega,P^2]$$

The notation used above is intended to emphasize that t and G_0 depend on $\underline{P}$ only through the magnitude P^2, whereas $\tilde{Q}(\underline{k},\underline{P})$ depends on the angle $\hat{k}\cdot\hat{P}$ as well. For example, in nuclear matter the operator $\tilde{Q}$ is

$$\tilde{Q}(\underline{k},\underline{P}) = 1 \quad \text{for } |\underline{k}-\eta\underline{P}| < k_{FERMI} \qquad (83)$$
$$= 0 \quad \text{otherwise}$$

with $\eta=m_N/(m_N+m_\Sigma)$, and $\eta\underline{P}-\underline{k}$ is the momentum of the intermediate state nucleon.

The difficulties of incorporating the Pauli principle exactly become apparent in the integral relation

$$<\underline{k}',\underline{P}|\tau|\underline{k},\underline{P}>=<\underline{k}'|t|\underline{k}>-\int d\underline{p}\ <\underline{k}'|t|\underline{p}>G_0(\omega)\tilde{Q}(\underline{p},\underline{P}) \qquad (84)$$
$$<\underline{p},\underline{P}|\tau|\underline{k},\underline{P}>$$

If $\tilde{Q}$ was angle-independent then eq.(84) could be expanded in

partial waves with $\hat{k}\cdot\hat{k}'$ the only angle. However with $\tilde{Q}$ given by eq.(82), $\tau(\omega)$ clearly depends not only on $\hat{k}\cdot\hat{k}'$ but also on the orientation of the relative momenta with respect to $\underline{P}$. It is then impossible to expand eq.(83) in partial waves of definite angular momentum.

It has already been seen in the partial wave expansion of the Σ single-particle potential that partial wave mixing of the ΣN interaction arises just from the three-body kinematics. Now it is apparent that mixing also arises from the complete description of the Pauli exclusion process. In practice this latter complication can be overcome by using the angle-averaged value of $\tilde{Q}$. That is, $\tilde{Q}$ is expanded in partial waves and only the l=0 term is retained. For the nuclear matter $\tilde{Q}$ of eq.(82) this expansion is

$$\tilde{Q}(\underline{k},\underline{P}) = \sum_{\ell=0}^{\infty} \tilde{Q}_\ell(k;P)P_\ell(\hat{k}\cdot\hat{P}) \tag{85}$$

with the coefficients

$$\begin{aligned} \tilde{Q}_\ell(k;P) &= \delta_{0\ell} \quad \text{for} \quad k+\eta P < k_F \\ &= 0 \quad \text{for} \quad |k-\eta P| > k_F \\ &= \tfrac{1}{2}[P_{\ell-1}(x_0)-P_{\ell+1}(x_0)] \quad \text{otherwise} \end{aligned} \tag{86}$$

and $x_0=(k^2+\eta^2P^2-k_F^2)/2\eta Pk$. The P_ℓ are Legendre polynomials.

Replacing $\tilde{Q}(\underline{k},\underline{P})$ by $\tilde{Q}_0(k;P)$ certainly simplifies τ considerably, but it must still be decided whether the

approximation is likely to be a good one. It can be seen immediately that for $|x_0|>1$, $\tilde{Q}_0$ is the entire operator $\tilde{Q}$. In the region $|x_0|<1$ the $\tilde{Q}_\ell$ on the average are all smaller than $\tilde{Q}_0$ with the maximum values attained by the $l=0\rightarrow 3$ coefficients being 1,.75,.48,and .35. Of course for $l>0$ the magnitude of $P_\ell(\hat{k}\cdot\hat{P})$ is less than one everywhere except at the end points. In addition, the oscillatory nature of the Legendre polynomials causes some cancellation in higher partial waves.

These considerations are encouraging but we can be more precise. The operator $\tilde{Q}$ can be split into the sum of the angle-independent term $\tilde{Q}_0$, and the angle-dependent terms, denoted by $\tilde{q}_\ell(\underline{k},\underline{P})=\sum_{\ell>0}\tilde{Q}_\ell(k;P)P_\ell(\hat{k}\cdot\hat{P})$. It then follows that τ is the solution of the integral equation

$$\tau(\omega) = \tau^0(\omega)-\tau^0(\omega)\tilde{q}_\ell G_0(\omega)\tau(\omega) \qquad (87)$$

where $\tau^0(\omega)$ is the solution that is independent of $\hat{k}\cdot\hat{P}$, satisfying

$$\tau^0(\omega) = t(\omega)-t(\omega)\tilde{Q}_0 G_0(\omega)\tau^0(\omega) \qquad (88)$$

It is sufficient for our purposes here to assume that the particles are spinless so that $\tau^0(\underline{k}',\underline{k})$ can be expanded in partial waves of the orbital angular momentum as

$$\tau^0(\underline{k}',\underline{k}) = \sum_{\ell=0}^{\infty} \frac{(2l+1)}{4\pi} \tau_\ell^0(k';k) P_\ell(\hat{k}\cdot\hat{k}') \qquad (89)$$

We estimate the most important correction to the approximation $\tau=\tau^0$ by iterating eq.(86) once to form

$$\tau(\underline{k}',\underline{k};\underline{P}) \backsim \tau^0(\underline{k}',\underline{k}) - \sum_{\ell\ell'\ell''} \frac{(2\ell+1)(2\ell''+1)}{(4\pi)^2} \int dp p^2 \tau_\ell^0(k';p) \qquad (90)$$
$$\tilde{Q}_{\ell'}(p;P) G_0(\omega) \tau_{\ell''}^0(p;k) \int d\Omega_k'' P_\ell(\hat{k}\cdot\hat{p})$$
$$P_{\ell'}(\hat{p}\cdot\hat{P}) P_{\ell''}(\hat{p}\cdot\hat{k})$$

Considering only the $l'=1$ term, it is found that

$$\tau(\underline{k}',\underline{k};\underline{P}) \backsim \tau^0(\underline{k}',\underline{k}) - \frac{1}{4\pi} \int dp p^2 \tilde{Q}_1(p;P) G_0(\omega) \qquad (91)$$
$$[\tau_0^0(k';p)\tau_1^0(p,k)\hat{k}\cdot\hat{P} + \tau_1^0(k',p)\tau_0^0(p,k)\hat{k}\cdot\hat{P}]$$

This is an important result. For small momenta $\underline{k},\underline{k}'$ the s-wave interactions dominate, and yet the lowest order correction to τ^0 involves the p-wave τ_1^0 terms (in addition to the p-wave $\tilde{Q}_1$ term of course). It is reasonable then to expect that this correction is suppressed at low momenta and therefore to a good approximation

$$\tau(\underline{k}',\underline{k};\underline{P}) \simeq \tau^0(\underline{k}',\underline{k}) \qquad (92)$$

The angle-averaged Pauli operator Q_0 $(=1-\tilde{Q}_0)$ will be discussed again in section 4.II where we extend its definition to encompass complex momenta.

CHAPTER 4 TECHNICAL DETAILS AND NUMERICAL METHODS

With the development in the last chapter of a reliable description of the Σ single-particle potential we can consider the search for Σ^0 bound states and resonances.

These states appear as poles in the elastic S- or T-matrix and it is worthwhile to consider their movements in the ΣN channel as the inelastic ΛN coupling is introduced. First we will briefly describe the structure of the Riemann surface.

4.I. Bound States and Resonance Poles

For two coupled channels there are two square-root branch cuts along the positive energy axis starting at the ΣN and ΛN thresholds. On crossing one of these cuts the imaginary component of the corresponding channel momentum changes sign, and another crossing returns it to its original value. As a result there are four sheets to the surface and it is convenient to label them by

$$\begin{aligned} &\text{sheet 1} : \mathrm{Imp}_\Lambda > 0 \; ; \; \mathrm{Imp}_\Sigma > 0 \\ &\text{sheet 2} : \mathrm{Imp}_\Lambda < 0 \; ; \; \mathrm{Imp}_\Sigma > 0 \\ &\text{sheet 3} : \mathrm{Imp}_\Lambda < 0 \; ; \; \mathrm{Imp}_\Sigma < 0 \\ &\text{sheet 4} : \mathrm{Imp}_\Lambda > 0 \; ; \; \mathrm{Imp}_\Sigma < 0 \end{aligned} \qquad (93)$$

Crossing the energy axis above the Σ threshold changes the sign of both Imp_Σ and Imp_Λ and, therefore, sheets 1 and 3 are connected. Similarly, for energies between the two thresholds just Imp_Λ changes sign and so sheets 2 and 4 are connected.

In a simple, one-channel interaction bound state poles are located on the positive, imaginary momentum axis, and the reflection property $S(k)=S^*(-k^*)$ ensures that resonance poles are symmetric about this axis [on the unphysical ($Imk<0$) sheet]. In addition, because of the unitarity condition $S(k)S(-k)=1$, a pole of S at k on the unphysical sheet is accompanied by a zero of S at -k on the physical sheet.

In the elastic scattering situation the third quadrant pole is too far from the physical region to influence the cross section. The fourth quadrant pole on the other hand can lie very close to the physical momentum axis and is then responsible for the characteristic resonant bump in the scattering amplitude.

With the introduction of coupling to an inelastic channel the unitarity conditions in each partial wave are modified to [21] $S_\ell^{ij}(p_\Lambda,p_\Sigma)=S_\ell^{ij*}(-p_\Lambda^*,-p_\Sigma^*)$, and $\sum_n S^{in}S^{jn}=\delta_{ij}$, with the superscripts i,j referring to either Σ or Λ

channels and the summation includes both channels. The solution of these equations can be written quite generally as

$$S_\ell(E) = 1+2iP^{\ell+1/2}[A_\ell(E)-iP^{2\ell+1}]^{-1}P^{\ell+1/2} \qquad (94)$$

with $P^n_{ij}=p^n_i\delta_{ij}$. $A_\ell(E)$ is a real, symmetric matrix which depends on the channel energies E_i, but not the momenta p_i.

The poles of S_ℓ occur as zeros of the determinant

$$|A_\ell(E)-iP^{2\ell+1}|=0=(a_{\Sigma\Sigma}-ip_\Sigma^{2\ell+1})(a_{\Lambda\Lambda}-ip_\Lambda^{2\ell+1})-(a_{\Sigma\Lambda})^2 \qquad (95)$$

Specializing to an S-wave interaction, the solution for the pole in the ΣN channel is

$$p_\Sigma = -ia_{\Sigma\Sigma}+\frac{a^2_{\Lambda\Sigma}}{(a^2_{\Lambda\Lambda}+p^2_\Lambda)}(ia_{\Lambda\Lambda}-p_\Lambda) \qquad (96)$$

Assuming that the coupling is small, we find that the effect of the open channel is to shift a bound state pole ($a_{\Sigma\Sigma}<0$) into the second quadrant of the p_Σ plane (on sheet 2). The small real component of p_Σ produces the absorptive width of the state. Similarly, a virtual state pole ($a_{\Sigma\Sigma}>0$) is also shifted to the left in the momentum plane with the pole on sheet 4.

Following the same arguments as above for P-wave interactions, with $a_{\Sigma\Sigma}>0$ and no inelastic coupling, it is simple to show that resonance poles occur at $p_\Sigma=a_{\Sigma\Sigma}^{1/3}e^{7\pi i/6}$,

and $a_{\Sigma\Sigma}^{1/3} e^{11\pi i/6}$ on the unphysical sheet. As the channel coupling is gradually increased from zero the fourth quadrant pole moves away from the real axis causing the resonant width to increase with increasing absorption, as expected. The third quadrant pole however, shifts closer to the negative real axis. This pole still does not affect the cross-section but, as indicated earlier, it is accompanied by a zero of the S-matrix approaching the positive real axis from the physical sheet. The presence of the nearby zero is manifested by a large reduction in the magnitude of the S-matrix at this energy. In other words, for $|S| \sim 0$ all the incoming waves are in the Σ channel and all outgoing waves are in the Λ channel. The positions and movements of all these singularities are shown in fig. 6.

There is a particularly interesting limit of the above cases. If the channel coupling is sufficiently strong, it is possible for the third quadrant pole (either resonant or virtual state) to cross from sheet 4 into the physical region of sheet 2. We then have the unique situation that the strong absorption of the potential is responsible for creating a quasi-bound state. In fact, it can be seen from eq.(96) that if the coupling is so strong that the diagonal elements may be neglected by comparison, there is always a solution with both p_Σ and p_Λ purely imaginary. In this (rather unrealistic) limit a bound state appears below both thresholds.

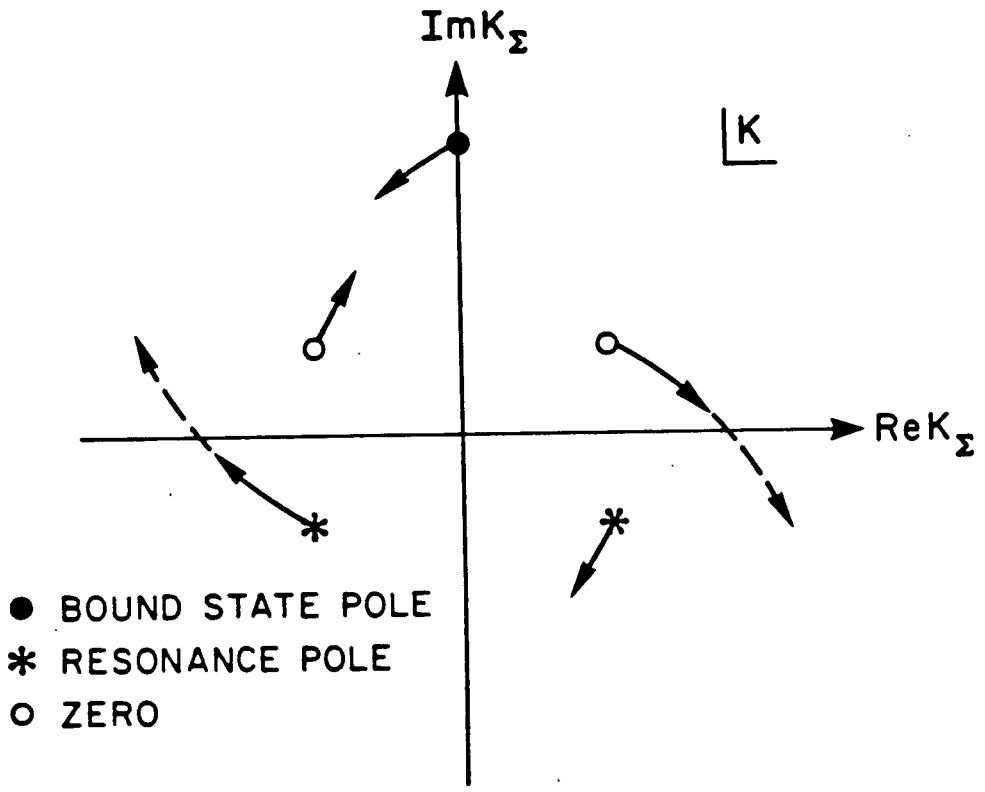

Fig. 6. Movement of the S-matrix singularities in the ΣN momentum plane as coupling to the ΛN channel is increased from zero. For strong coupling the pole in the third quadrant can move into the physical region to become a bound state.

In the present study these extremely deep bound states do not occur. What is of particular importance to us is that, for moderate strength coupling, in principle the pole can lie arbitrarily close to the real axis. It is possible then for the state to have a vanishingly small width, despite the fact that the effective Σ-nucleus potential is strongly absorptive.

We have labelled this situation a bound state although it is recognized to be an unusual one. The Σ wavefunction for this energy (on the physical sheet) decays exponentially at large distances and the scattering phase shift has the characteristic bound state signature $\delta(0)-\delta(\infty)=\pi$. Conversely, the real component of the 'binding' energy is positive; embedded in the Σ continuum states. We also stress again that the pole responsible for this state is not the usual bound state one, but rather has moved from a normally inaccessible region of the unphysical energy sheet.

The observation that a strongly absorptive potential can lead to narrow states is not new. Their existence was first realized by Fonda and Newton [38,21], and recently Gal et al [11] have considered this as the possible explanation in Σ hypernuclei. They found that with their one-channel phenomenological model narrow p-states arose naturally from this mechanism. It should be noted though that their

potential predicts very broad s-states (e.g. $\Gamma \sim 23$ MeV in $^{12}_{\Sigma^0}C$) because of the strong absorption.

4.II. Analytic Continuation of the Pauli Operator

In the last section it was noted that at a Σ bound state the corresponding ΛN channel energy was perturbed into the lower half of the momentum plane. Because we search for the self-consistent eigenvalues $E = \epsilon - i\Gamma/2$ of the Schroedinger equation, $\tau(\omega)$ [eq. (73)] must be evaluated at complex energies. This leads to difficulties in evaluating the overlap integrals $\langle v|Q^0G|v\rangle$ appearing in $\tau(\omega)$.

The problem is best clarified by an example. Consider the case in which the ΛN energy $k_\gamma^2/2m$ is real and positive. The overlap integrals then have the general form

$$\int dk k^2 \frac{v^2(k^2)Q^0(k,P)}{k_\gamma^2 - k^2 + i\epsilon} = P\int dk\ k^2 v^2(k^2) \frac{Q^0(k,P)}{k_\gamma^2 - k^2} - i\pi \int dk k^2 \delta(k_\gamma^2 - k^2) v^2(k^2) Q^0(k,P) \tag{97}$$

where 'P' denotes principal value integration, and the second (pole) term is simply

$$-i\pi \frac{k_\gamma}{2} v^2(k_\gamma^2) Q^0(k_\gamma, P) \tag{98}$$

Provided k_γ is chosen to be real and positive then $Q^0(k_\gamma, P)$ is well-defined. If, however, k_γ is taken to be on the unphysical (negative) momentum axis, then Q^0 has no clear

interpretation with the definition used in sect. 3.IV.

It is realized then that the correct evaluation of the τ overlap integrals requires the analytic continuation of the Pauli operator Q^o to the second sheet. This is not a trivial problem since in the usual Fermi gas approximation Q^o is only a piece-wise continuous function of nucleon momentum. This point was not considered in the model of Stepien-Rudzka and Wycech [13] because they made no attempt to compute the Σ-nucleus potential self-consistently.

In nuclear matter approximation Q is defined by the zero temperature limit of the Fermi-Dirac distribution:

$$Q \equiv 1 - |0><0| = 1 - \lim_{\theta\to\infty}\left(1+\exp\left[\theta\left(\kappa_N^2-\kappa_F^2\right)\right]\right)^{-1}, \qquad (99)$$

where k_N, k_F are the nucleon, and Fermi momenta. Eventually the limit of an infinite θ will be taken but for now a finite value allows Q to be defined for complex momenta.

If partial-wave mixing in τ via Q is ignored then only the angle-averaged value of Q is required. With k_γ,P the relative, and total ΛN momenta this means

$$Q^o(\kappa_\gamma;P:\kappa_F) \equiv 1/2\int d(\hat{P}\cdot\hat{\kappa}_\gamma)\,Q(|\underline{\kappa}_\gamma-\eta\underline{P}|)\,, \qquad (100)$$

$$= 1 - \lim_{\theta\to\infty} 1/4\eta P\kappa_\gamma\theta\ \ell n\left\{\frac{1+\exp\left[\theta\left(\kappa_F^2-(\kappa_\gamma-\eta P)^2\right)\right]}{1+\exp\left[\theta\left(\kappa_F^2-(\kappa_\gamma+\eta P)^2\right)\right]}\right\},$$

with $\eta=m_N/(m_N+m_\Lambda)$. In the limit that $\Theta\to\infty$ it is found that for complex momentum $k_\gamma=k+i\gamma$ Q^0 behaves as

$$\begin{aligned} Q^0(\kappa_\gamma;P:\kappa_F) &= 0 && \text{for } (\kappa+\eta P)^2,(\kappa-\eta P)^2 < \kappa_F^2+\gamma^2 , \\ &= 1 && \text{for } (\kappa+\eta P)^2,(\kappa-\eta P)^2 > \kappa_F^2+\gamma^2 , \\ &= \frac{\kappa_F^2-(\kappa_\gamma-\eta P)^2}{4\eta P\kappa_\gamma} && \text{for } (\kappa+\eta P)^2 < \kappa_F^2+\gamma^2 < (\kappa-\eta P)^2 , \\ &= \frac{(\kappa_\gamma+\eta P)^2-\kappa_F^2}{4\eta P\kappa_\gamma} && \text{for } (\kappa+\eta P)^2 > \kappa_F^2+\gamma^2 > (\kappa-\eta P)^2 . \end{aligned} \tag{101}$$

In the limit that $\gamma\to 0$ the above result of course reduces to the previous definition of the angle-averaged Pauli operator.

With this simple description of Q^0 for complex momentum it is straightforward to evaluate the overlap integrals. The contour of integration is distorted from the real axis to enclose the pole in the lower half-plane at k_γ so that in the ΛN channel, for complex k_γ^2 the required integral is

$$\oint dk k^2 \frac{v^2(k^2)}{(k_\gamma^2-k^2)} Q^0(k,P) = \int_0^\infty dk k^2 v^2 \frac{(k^2)Q^0}{(k_\gamma^2-k^2)}(k,P) - i\pi k_\gamma v^2(k_\gamma^2)Q^0(k_\gamma,P) \tag{102}$$

With this technical detail clarified we can consider solving for the Σ states.

4.III. The Σ-Nucleus T-Matrix

The Σ^0 single-particle potential has been completely defined now and it remains to determine the (complex) eigenvalues ϵ_σ. By this point it has probably become apparent that the intention is to find these values by searching for poles in the Σ-nucleus S-, or T-matrix.

In the extreme single-particle model there is no difficulty in defining the transition amplitude. The Σ obeys the effective one-body Schroedinger equation

$$(K+V_\Sigma)|\sigma\rangle = \epsilon_\sigma|\sigma\rangle \qquad (103)$$

where V_Σ is the operator $\langle 0|A\bar{\tau}|0\rangle$, and $|0\rangle$ is the nuclear ground state wavefunction. By definition of the single particle model, the nucleus remains in the ground state throughout the interaction, and the T-matrix is simply

$$T = A\langle 0|\bar{\tau}|0\rangle + A\langle 0|\bar{\tau}|0\rangle(\epsilon_\sigma - K)^{-1}T \qquad (104)$$

While this result seems almost obvious, it can not possibly be correct. For example, in the limit that there is only one nucleon V_Σ reduces to the free ΣN t-matrix t, and T of course should reduce to the identity T=t. According to eq.(104) though we are left with the series

$$T = t + t\sum_{n>0}(G_0 t)^n \quad \text{for } A=1 \qquad (105)$$

The difficulty is apparent. Since t is, by definition, the sum of all ΣN potential ladder graphs, the terms with n>0 describe processes already included in t. The problem can be corrected if it is pictured that for the first scattering event the Σ can interact with any of the A nucleons. The second event must be with a different nucleon though so that there are only A-1 choices, and similarly, only A-1 choices in all higher order terms. Replacing $A\bar{\tau}$ by $(A-1)\bar{\tau}$ in the second term of eq.(104) ensures the correct counting to all orders in the Born series.

To put this another way, let us use Goldstone diagrams again for simplicity. The reaction matrix $\bar{\tau}$ is represented by a solid line ⊢——⊣, and the potential $v_{\Sigma A}$ by a wiggly line ⊢∿∿⊣. We are saying that, while it is quite correct to include the diagram in eq.(106) below [or eq.(69)] in the theory, second order (or higher) diagrams such as eq.(107) should not be included since they represent processes already included in $\bar{\tau}$. That is, we should count

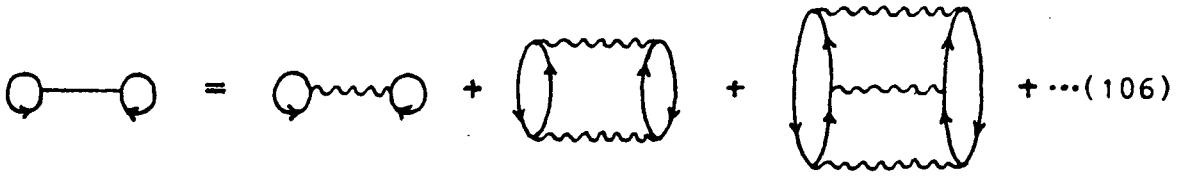

(106)

but not

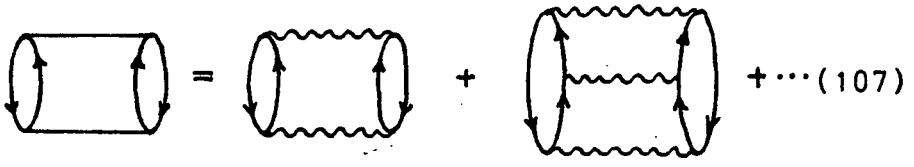

(107)

This should emphasize that $\bar{\tau}$ is to be considered the effective interaction only in the sense given by the discussion following equation (61).

Although replacing A by (A-1) produces the right result, it is not very satisfactory to include physical behaviour in such an ad hoc manner. Within the extreme single-particle model this is the best we can do, and to have correct counting inherent in the theory requires a more careful treatment of the (A+1)-body equation. The Σ-nucleus Schroedinger equation again is

$$(K+H_N+V_\Sigma)|\Psi(\Sigma)> = E|\Psi(\Sigma)> \qquad (108)$$

where V_Σ is now the operator $Av_{\Sigma A}$ [c.f. eq.(103)], and H_N is the nuclear Hamiltonian. It follows that the T-matrix is

$$T = Av_{\Sigma A} + Av_{\Sigma A}\,(E-H_N-K)^{-1}T \qquad (109)$$

with

$$Av_{\Sigma A} = A[1+\bar{\tau}(E-H_N-K)^{-1}]^{-1}\bar{\tau} \qquad (110)$$

Substituting eq.(110) into (109), we find that T satisfies the many-body equation

$$T = A\bar{\tau}+(A-1)\bar{\tau}(E-H_N-K)^{-1}T \qquad (111)$$

The double-counting problem in higher order terms has been eliminated, but not without exacting its price. Since we have elected to work in the (A+1)-body Hilbert space the

intermediate scattering states in eq.(111) must include nuclear excitations. The contribution of these states to T can be isolated by writing eq.(111) as the pair of coupled equations

$$T' = \bar{\tau}' + \bar{\tau}' |0\rangle \frac{1}{(\epsilon_\sigma - K)} \langle 0| T' \tag{112}$$

and

$$\bar{\tau}' = (A-1) \left\{ \bar{\tau} + \bar{\tau} |n\rangle \frac{1}{(\epsilon_\sigma - \epsilon_n - K)} \langle n| \bar{\tau}' \right\} \tag{113}$$

where $|n\rangle$ is an excited state, and ϵ_n the corresponding excitation energy. T' is related to the physical amplitude T by $T = AT'/(A-1)$. (Of course if we are only interested in poles of T, the normalization constant $A/(A-1)$ is irrelevant).

The contribution from excited states in eq.(113) is expected to be $O(1/A)$ relative to the first term. This is because ground state transitions $\langle 0|\Sigma\bar{\tau}|0\rangle$ involve all the nucleons, whereas in $\langle n|\Sigma\bar{\tau}|0\rangle$ only the one nucleon that is excited contributes. In the spirit of the single-particle model these transitions are neglected and T' reduces to our earlier result

$$\langle 0|T'|0\rangle = (A-1)\langle 0| \left\{ \bar{\tau} + \bar{\tau}|0\rangle \frac{1}{(\epsilon_\sigma - K)} \langle 0|T' \right\} |0\rangle \tag{114}$$

or, with explicit Σ plane-wave initial and final states

$$T'(\underline{k}', \underline{k}, \epsilon) = V'(\underline{k}', \underline{k}, \epsilon) + \int d\underline{p}\; V'(\underline{k}', \underline{p}, \epsilon) \frac{T'(\underline{p}, \underline{k}, \epsilon)}{(\epsilon - p^2/2m)} \tag{115}$$

where $V' = (A-1)\langle 0|\bar{T}|0\rangle = (A-1)V_\Sigma/A$, and the ground state label has been suppressed.

With the same normalization for T' as used elsewhere in this work, eq.(115) decomposes into partial waves as

$$T'_\ell(k';k:\epsilon) = V'_\ell(k';k:\epsilon) + \int dp\ p^2 V'_\ell(k';p:\epsilon)\frac{T'_\ell(p;k:\epsilon)}{(\epsilon - p^2/2m)} \quad (116)$$

4.IV. Numerical Solution of the T-Matrix

Before searching for poles of the T-matrix we need to be able to solve the integral equation (116) for any (in general, complex) value of ϵ. Unlike the true scattering situation, the energies will usually be located off the real axis in the complex k-plane and therefore there is no singularity in the propagator along the contour of integration.

We use the standard technique of approximating the integral equation by a system of linear equations. That is, the continuous variable of integration p is replaced by a set of N (Gauss) quadrature points p_m, and corresponding weights w_m. In matrix form eq.(116) is

$$T(p_i,p_j;\epsilon) = V(p_i,p_j;\epsilon) + \sum_{m=1}^{N} K(p_i,p_m;\epsilon)T(p_m,p_j;\epsilon) \quad (117)$$

with $$K(p_i,p_m;\epsilon)=w_m p_m^2 V(p_i,p_m;\epsilon)/(\epsilon-p_m^2/2m) \qquad (118)$$

The subscript 1 and superscript ' have been dropped but this should not cause confusion. The solution for T_{ij} is

$$T(p_i,p_j;\epsilon)= \frac{1}{|K'|}\sum_{m=1}^{N} C_{mi}V(p_m,p_j;\epsilon) \qquad (119)$$

where C_{mi} is the mith co-factor of $|K'|$, and $|K'|$ has elements

$$K'_{ij}=\delta_{ij}-K(p_i,p_j;\epsilon) \qquad (120)$$

While this method of solution is perfectly adequate for bound states where the real component of ϵ is less than zero, for resonance poles it becomes inaccurate. If there is a pole at an energy $\epsilon=\omega+i\gamma$ with $\omega>0$, then for small γ this pole approaches the real axis, causing strong energy dependence in the integrand of eq.(116). Either a large number of points is required to achieve accuracy, or the integration technique must be modified.

One such modification is based on the well-known result that in the limit $\eta\rightarrow 0$

$$(\epsilon+i\eta-H_0)^{-1}= \frac{P}{(\epsilon-H_0)}-i\pi\delta(\epsilon-H_0) \qquad (121)$$

with P denoting principal value integration. If the energy

ϵ is allowed to become complex the two integrals above behave as

$$P\int \frac{dp}{(\omega+i\gamma-p^2/2m)} = 0 \quad \text{for } \gamma=0 \qquad (122)$$

$$= -i\pi \frac{m}{k_\epsilon} \quad \text{otherwise, and } k_\epsilon^2/2m=\omega+i\gamma$$

$$-i\pi\int dp\,\delta(\omega+i\gamma-p^2/2m) = -i\pi\frac{m}{k_o} \quad \text{for } \gamma=0, \text{ and } k_o^2/2m=\omega$$

$$= 0 \quad \text{otherwise}$$

Returning to the integral equation, it is found to be equivalent to

$$T(k',k)=V(k',k)+ P\int dp\, \frac{[p^2V(k',p)T(p,k)-k_o^2V(k',k_o)T(k_o,k)]}{(\omega+i\gamma-p^2/2m)}$$

$$-i\pi\frac{k_o^2}{k_\epsilon}mV(k',k_o)T(k_o,k) \qquad (123)$$

With $\omega<0$ we set $k_o=0$ and this reduces to our earlier result. For $\omega>0$ and $\gamma=0$ the second term in the integrand exactly cancels the contribution from the δ function. With $\gamma=0$ the principal value integration of the second term is zero, and eq.(123) then represents a true scattering situation. The advantage of this now technique is that the integrand is a smooth function of energy near the pole, and the principal value 'P' can be removed.

If we are only interested in the energy dependence of the T-matrix then a little algebra shows that with a new potential defined as

$$u_{ij}=V_{ij}-V_{io}V_{oj}\frac{I}{(1+V_{oo}I)} \qquad (124)$$

with $V_{io} = V(p_i,k_o;\epsilon)$, and $I = 2mk_o^2[\sum_{m=1}^{N}\frac{w_m}{(k_\epsilon^2-p_m^2)} + \frac{i\pi}{2k_\epsilon}]$

the solution for $T(p_i,p_j;\epsilon)$ is still given by eqs.(118)-(120) but with u_{ij} substituted everywhere for V_{ij}.

Once the values T_{ij} have been determined, the on-shell, and half off-shell values T_{oo}, and T_{oj} are calculated to be

$$T_{oj}=u_{oj}+\sum_{m}^{N}\frac{w_m p_m^2 u_{om}T_{mj}}{(\omega+i\gamma-p^2/2m)} \quad ; \quad T_{jo}=T_{oj} \qquad (125)$$

$$\text{and} \quad T_{oo}=u_{oo}+\sum_{m}^{N}\frac{w_m p_m^2 u_{om}T_{mo}}{(\omega+i\gamma-p^2/2m)}$$

The solution T_{ij} as given by eq.(119) shows clearly that a pole in T at an energy ϵ is equivalent to a zero of the Fredholm determinant $|K'|$ at ϵ. In principle these zeros are simple to find via a Newton Raphson algorithm. With an initial value ϵ_o, the first iteration produces a value ϵ_1

$$\epsilon \simeq \epsilon_1=\epsilon_o-|K'(\epsilon_o)|/\partial_\epsilon|K'(\epsilon_o)| \qquad (126)$$

Of course in general the derivative of $|K'|$ will need to be calculated numerically as well.

Usually the initial value of ϵ is not a crucial factor in the iteration since it is found that any value of ϵ_0 with the correct sign and of the same order of magnitude as the root ϵ will lead to convergence. However with a complicated expression for $V(\epsilon)$, as is the case here, the time required to calculate $|K'(\epsilon)|$ also becomes an important consideration.

To evaluate $|K'(\epsilon)|$, $V(k',k;\epsilon)$ must be calculated at $N(N+1)/2$ momentum points for each value of ϵ. The first derivative of the determinant therefore requires V to be recalculated at (at least) an additional $N(N+1)/2$ points. With a poor initial value of ϵ_0 the number of iterations required for convergence may be large.

In the event that the potential is energy independent or only a slowly-varying function of energy, this does not pose any difficulty. To calculate the derivative of $|K'(\epsilon)|$ one can assume that all energy dependence arises from the propagators, which certainly will reduce the computing time. However it has been found that the potential used in this work is too strongly energy dependent for this technique to converge.

It is possible to improve on the starting value ϵ_0 by using the Born series for T [21]. In the immediate region of the pole the Born expansion is divergent, but this fact can be used to advantage. Writing the T-matrix as the series

$$T = \sum_{n=0}^{\infty} V(G_0V)^n \tag{127}$$

then in the regions where the series converges, the convergence test claims that

$$\lim_{n\to\infty}\left|\frac{V(G_0V)^{n+1}}{V(G_0V)^n}\right| \leq 1 \tag{128}$$

with the equality holding only at the pole itself. The simplest approximation to this result is obviously

$$\left|\frac{VG_0V}{V}\right| \approx 1 \tag{129}$$

and while this may seem to be a very crude approximation, it is exact for a coupled-channel separable model.

To calculate $T(0,0;\epsilon)$ to second Born approximation requires V at (N+1) points. (There is no point in calculating T to third Born approximation because V will be needed at another N(N+1)/2 points). Again using a Newton-Raphson algorithm, N/2 iterations to the root ϵ_0 of eq.(129) can be performed in the time required to calculate $|K'(\epsilon)|$ and its derivative once. With this value of ϵ_0 as the

starting point we enter the exact iterative solution to the root ϵ. For the potential used in this work it has been found that ϵ_0 was always within 50% of the true value.

So far we have assumed implicitly that the pole is on the physical energy sheet. The Newton Raphson algorithm will fail if the root is located on the lower half of the k-plane because $|K'(\epsilon)|$ is invariant under a sign change of the momentum. One approach that would normally overcome this problem is to analytically continue T by rotating or distorting the contour of integration to enclose the pole on the second sheet. This is not possible with our potential because the harmonic oscillator wavefunctions behave pathologically away from the real axis.

A different approach is needed and we can now use the symmetries of the S-matrix to our advantage. As discussed in sect. 4.I., a pole of S at -k on the second sheet is accompanied by a zero of S at k on the physical sheet. Finding the position of a zero is then equivalent to finding a pole. Also as discussed earlier, the only resonant pole in S which may be of interest is the normally inaccessible one in the third quadrant. The S-matrix can not be solved at complex momenta for the same reason that the integration contour can not be rotated, so instead an approximation method is needed for continuing S off the real axis.

The S-matrix is related to the phase shifts by

$$S_\ell = \frac{k^{2\ell+1}\cot\delta_\ell + ik^{2\ell+1}}{k^{2\ell+1}\cot\delta_\ell - ik^{2\ell+1}} \qquad (130)$$

and the condition $S(k)S(-k)=1$ restricts $k^{2\ell+1}\cot\delta_\ell$ to being an even function of k. Therefore it can be approximated at low energies by the Taylor series

$$k^{2\ell+1}\cot\delta_\ell \approx 1/a + rk^2/2 + O(k^4) \qquad (131)$$

which of course is just the effective range expansion.

There are several choices as to how to proceed. The obvious approach is to determine the first few coefficients in the expansion by calculating δ_ℓ at several energies and substituting this series directly into eq.(130). Our aim though is to extrapolate S_ℓ reliably to complex energies which would require a fairly large number of terms for accuracy. On the other hand, high-order polynomial approximations are infamous for their instability.

A better method is to construct an [L/M] Pade approximant of the effective range expansion. This is defined as the ratio of two polynomials of orders L,M that exactly reproduces the first L+M+1 terms in the Taylor series. The greatest advantage of the Pade approximant is that, since it contains poles, it is well suited for

reproducing the analytic structure of the function.

This latter approach is the usual Pade technique. However the step of determining the coefficients of the effective range expansion seems redundant. Instead an [L,M] approximant can be constructed that reproduces $k^{2\ell+1}\cot\delta_\ell$ exactly, and not just the Taylor series, at L+M+1 points.

Precisely this problem has been examined at length by Hartt [39] and he has found that the best reproduction of the singularities in S is given by the choice L=M+1.[1]

The Pade approximant is defined as

$$\frac{P_L}{Q_{L-1}} = \frac{\sum_0^L a_{2m} k^{2m}}{\sum_0^{L-1} a_{2m+1} k^{2m}} \quad , \quad a_0 = 1 \tag{132}$$

and the (complex) coefficients are determined by solving the set of linear equations

$$P_L(k_i^2) = k_i^{2\ell+1}\cot\delta_\ell^i \, Q_{L-1}(k_i^2) \quad , \quad i = 1,2,\ldots 2L \tag{133}$$

The convergence and analytic continuation properties of Pade approximants have been discussed by many authours (for example, ref.40), but the only convincing argument for their

---

[1] This would not be true in special cases, such as the separable potential, for which the expansion to k^4 is exact.

use is if they work. Although this infringes on the topic of chapter 5, the bound state predictions for a few s-state hypernuclei are reported in table IV. The exact results listed are those calculated using the Newton-Raphson method discussed earlier.

The agreement between the two methods is very good and the Pade solution converges quickly to the root. As expected, the best result is obtained for the pole nearest to the real energy axis. In p-state, where this method will be used, the zeros are close to the physical axis, and so we have reason for confidence.

	$\Sigma^0\,{}^{9}Be$	$\Sigma^0\,{}^{12}C$	$\Sigma^0\,{}^{16}O$
EXACT	-.202 + .255i	-.300 + .450i	-.306 + .576i
[2/1]	-.208 + .251i	-.286 + .470i	-.352 + .623i
[3/2]	-.204 + .253i	-.296 + .460i	-.338 + .602i
[4/3]	-.202 + .255i	-.299 + .451i	-.313 + .582i

Table IV. Positions of the bound s-state pole in the momentum plane predicted by [L/M] Pade approximants compared with the exact (Newton-Raphson) solution. Units are in fm^{-1}.

CHAPTER 5 RESULTS IN LIGHT Σ^0 HYPERNUCLEI

A great deal of care has been taken to construct the Σ^0 single-particle potential consistently with the two-body ΣN interactions. Before proceeding to the calculation of bound states we should also check the consistency of the model with the Σ^- atomic data.

5.I. Σ^- Atoms

Although no attempt is made to fit the model to the data, a comparison with Batty's phenomenological result can be made in some appropriate limit. In Σ^- atoms the Σ is bound with essentially zero energy and consequently the potentials should be comparable for very small momenta. At zero momentum transfer the volume integral of the model potential is proportional to Batty's value $\bar{a}_B$, with the theoretical value given by the expression

$$\bar{a}_{th} = -\pi \frac{\eta}{\mu_{\Sigma A}} \int d\underset{\sim}{p}\, F(p,p) \sum_{ILSJ} \frac{(2J+1)}{4} \frac{(2I+1)}{6} \tau^I_{LSJ}(\omega)$$

and

$$\tau^I_{LSJ}(\omega) = \frac{(\epsilon P)^{2L}}{(\beta^2+\epsilon^2 P^2)^2} D^I_{LSJ}\,(-B-P^2/2\mu) \quad . \tag{134}$$

Notice that even at zero incident momentum (in the Σ-nucleus frame) $\bar{a}_{th}$ receives contributions from L=1 and higher ΣN partial waves.

For $^{13}_{\Sigma^0}C$ $\bar{a}_{th}$ has been examined in some detail. With the nucleon binding parameter B chosen (rather arbitrarily) to be 10 MeV and a Fermi momentum of 260 MeV/c it is found that $\bar{a}_{th}$=.346+i.197 fm in comparison with $\bar{a}_B$=(.35±.04)+i(.19±.03) fm. The agreement of these results is relatively insensitive to the choice of parameters, as shown in detail in fig. 7, where the elliptical region defines the values allowed from Batty's analysis. With a Fermi momentum of 260 MeV/c and any value of 0<B<20 MeV $\bar{a}_{th}$ is consistent with $\bar{a}_B$. Conversely, with B=10 MeV any k_F in the range 250<k_F<275 MeV/c is consistent (i.e. an average nuclear density of ~75-100% of nuclear matter).

In addition, with the central values of B=10 MeV, and k_F=260 MeV/c the Σ^0-^{12}C scattering lengths are similar in the two models. Batty's potential gives -2.94+i1.20 fm, as compared with the -3.41+i1.44 fm of our model.

Although these agreements are suggestive, they require further investigation for definite interpretation. It is not clear that either the volume integral or the scattering length is the relevant quantity for comparison. This is particularly ambiguous since Batty's potential is local, whereas ours is highly non-local. In addition, the Fermi momenta used above are probably larger than are appropriate for L>3 atoms.

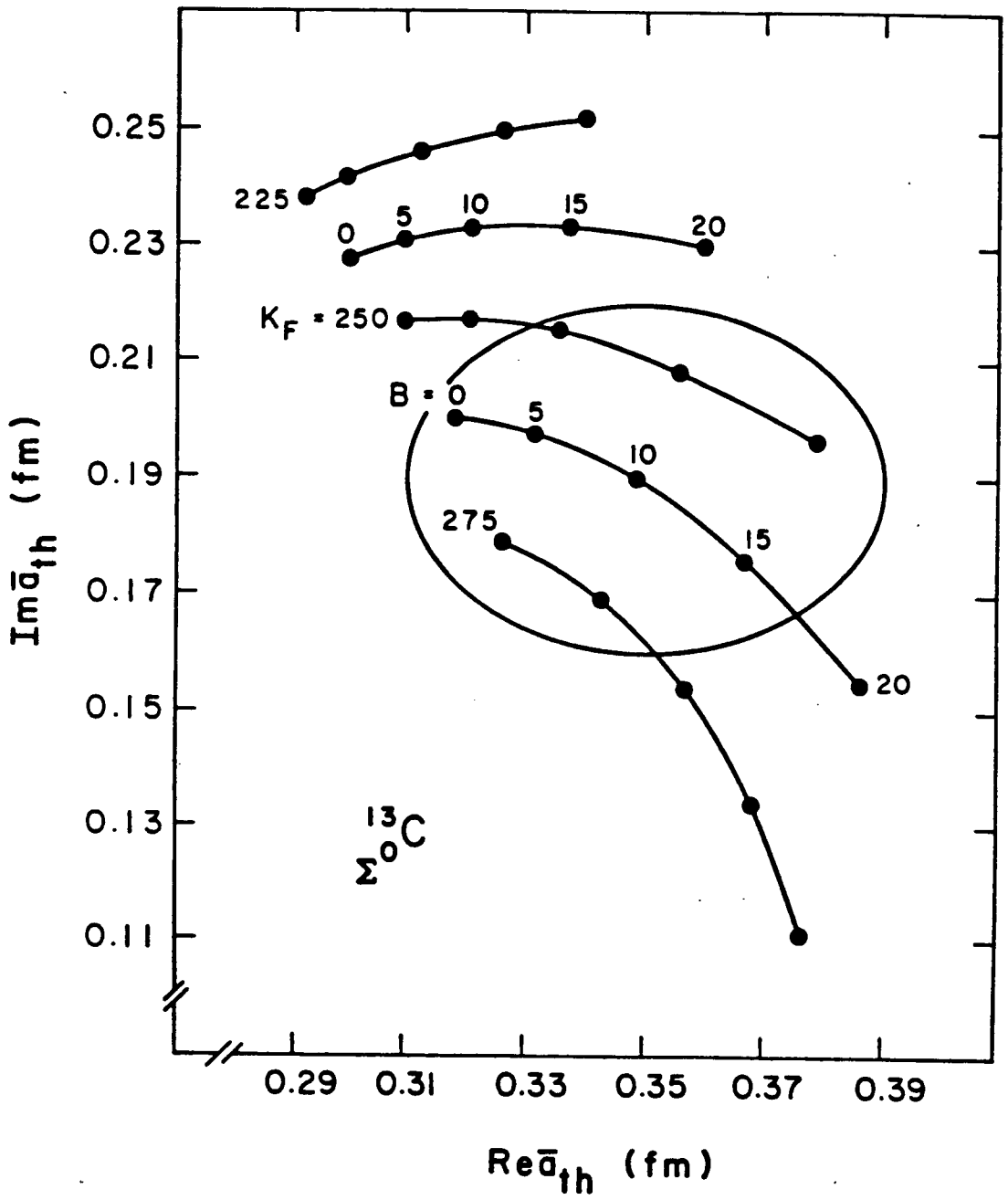

Fig. 7. Variation of the potential volume integral $\bar{a}_{th}$ with Fermi momentum (k_F in MeV/c) and nucleon binding energy (B in MeV) in $^{13}_{\Sigma^0}$C. The elliptical region is the range allowed by the analysis of Σ^- atoms [12]

However, it is worth noting that a decrease in k_F would lead to a larger value of $Im\bar{a}_{th}$. If the single particle potential was then scaled in some fashion to once again reproduce Batty's value of $Im\bar{a}_B$ smaller widths for s, and p-states than those reported here would result. In addition, with k_F reduced to 150 MeV/c and B increased to 0 MeV, which are probably more realistic in the atomic situation, $\bar{a}_{th}$ does not change dramatically, becoming 0.291+i0.252 fm. This is still comparable to the phenomenological value.

5.II. S-State Hypernuclei

In spite of the ambiguities outlined above we have been encouraged to proceed with the calculation of Σ nuclear states. For all the light hypernuclei considered in this work we have fixed the nucleon binding B at 10 MeV for simplicity. Because in s-state the Σ is largely confined to the nuclear volume, fairly high Fermi momenta have been chosen, ranging from 245 MeV/c in ${}^{5}_{\Sigma^0}$He to 260 MeV/c in ${}^{16}_{\Sigma^0}$O (or, average densities from 70-80% of nuclear matter). The self-consistent eigenvalues ϵ-iΓ/2 for s-state hypernuclei are presented in table V.

Several conclusions can be drawn from these results. Most importantly it is found that fairly narrow bound states

result when Pauli exclusion and nucleon binding are incorporated in a microscopic calculation. We also notice that for A<9 the model predicts that $\epsilon>0$. These are bound states though and not resonances. That is, they arise from an S-matrix pole in the second quadrant of the momentum plane.

Nucleus	κ_F (MeV/c)	B (MeV)	$\epsilon - i\Gamma/2$ (MeV)	Γ (MeV)
$\Sigma^0\,{}^{5}_{}He$	245	10	+2.49 - i0.88	1.75
$\Sigma^0\,{}^{7}_{}Li$	250	10	+0.81 - i0.99	1.98
$\Sigma^0\,{}^{9}_{}Be$	260	10	-0.46 - i1.95	3.89
$\Sigma^0\,{}^{12}_{}C$	260	10	-2.06 - i4.91	9.81
$\Sigma^0\,{}^{13}_{}C$	260	10	-2.59 - i5.31	10.62
$\Sigma^0\,{}^{16}_{}O$	260	10	-4.22 - i6.26	12.52

Table V. Is binding in light Σ^0 hypernuclei.

Although the earlier prediction of $\bar{a}$ was encouraging we also wish to test the sensitivity of these bound states (and the widths in particular) to small changes in the parameters. Again for $\Sigma^0\,{}^{13}_{}C$, the variation has been examined in detail. With values of B and k_F which approximately reproduce the extreme values permitted for $\bar{a}_B$ the binding has been calculated and these results are presented in

table VI. The real binding $|\epsilon|$ varies between 2 and 5 MeV, but Γ seem fairly insensitive, changing only from 9-11 MeV.

κ_F (MeV/c)	B (MeV)	$\bar{a}_{th}$ fm	$\epsilon - i\Gamma/2$ (MeV)	Γ (MeV)
250	22.5	0.39 + i0.19	-4.78 - i4.95	9.90
250	12.5	0.35 + i0.22	-2.22 - i5.63	11.26
260	10.0	0.35 + i0.19	-2.59 - i5.31	10.62
275	7.5	0.35 + i0.16	-3.00 - i4.65	9.30
275	-7.5	0.31 + i0.19	-2.00 - i4.84	9.68

Table VI. Variation of 1s binding in $^{13}_{\Sigma^0}C$ with κ_F and B.

Since Pauli exclusion and nucleon binding effects are major influences in producing these narrow states we have tried to isolate their contributions as much as possible. The binding has been calculated with, first, B fixed and k_F varied between 225-300 MeV/c and, second, k_F fixed and B varied from 0-30 MeV. These results are displayed in fig. 8. It can be seen that the inclusion of Pauli effects is essential to the correct description of the bound state, but, any reasonable choice of k_F leads to a small width.

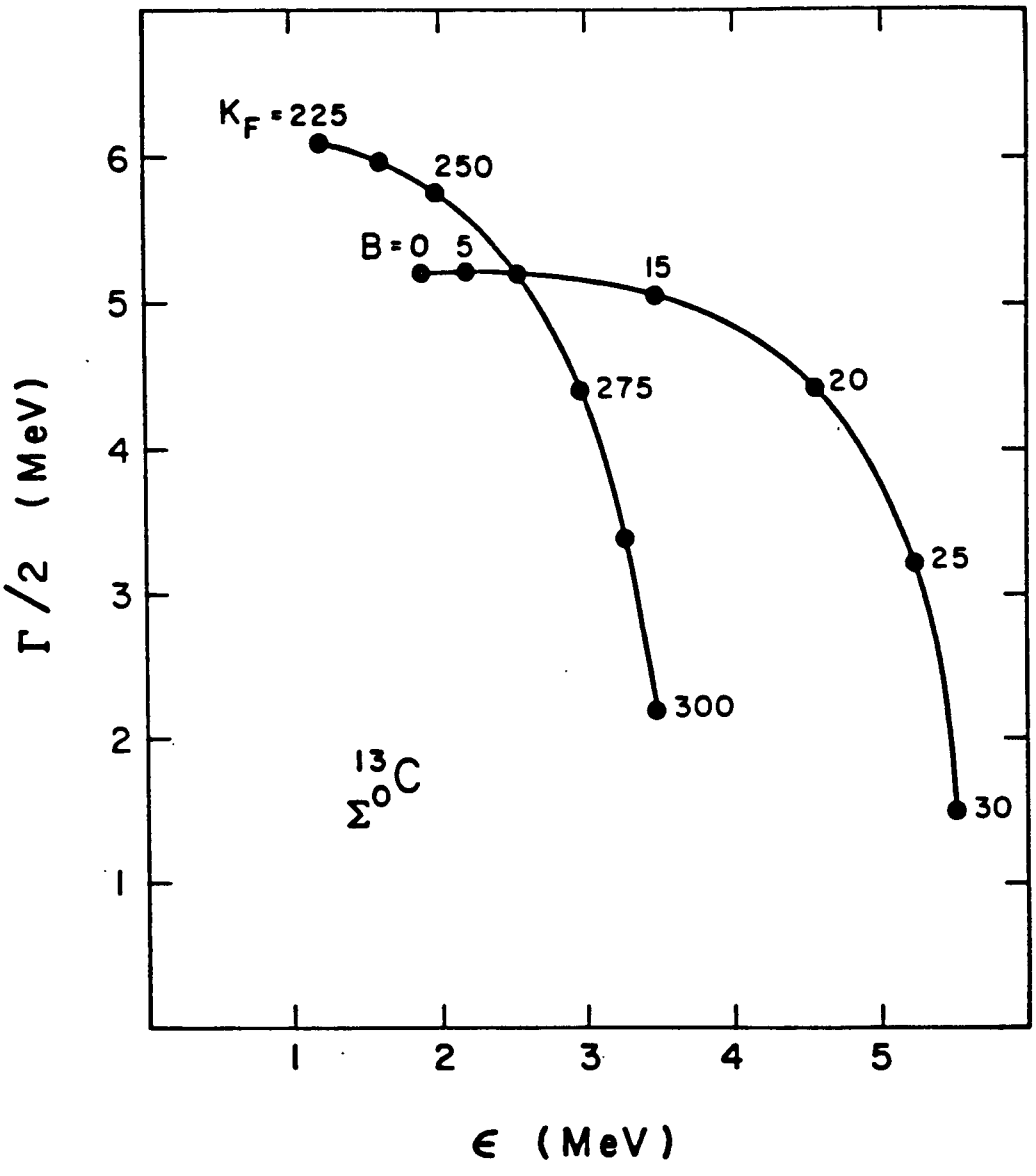

Fig. 8. Dependence of the s-state position ϵ and width Γ on Fermi momentum (k_F in MeV/c) and nucleon binding (B in MeV) in $^{13}_{\Sigma}C$.

The variation of Γ with large values of B is dramatic. The width is almost insensitive to changes in B from 0-20 MeV but decreases sharply for B>20 MeV.

This strong dependence of Γ on nucleon binding for large B should not be surprising. To take an extreme example, if the Σ and nucleon binding energies were greater than the Σ-Λ mass difference then the ΣN-ΛN conversion would never be energetically allowed and the decay width of the state would necessarily be zero. For more realistic cases it is expected, from phase space considerations alone, that the width must decrease rapidly for large reductions in the ΛN channel energy.

We have also examined the sensitivity of the ${}^{13}_{\Sigma^0}C$ state to the number of terms in the two-body form factor expansion. A priori one anticipates that the series will converge slowly. For example, consider the simple Taylor series expansion of the Yamaguchi form factor $v(k^2)$

$$v[(\underline{k}-\epsilon\underline{P})^2] = v(k^2+\epsilon^2P^2)\sum_{\ell=0}^{\infty}\epsilon^{\ell}[-2v(k^2+\epsilon^2P^2)\ \underline{P}\cdot\underline{k}]^{\ell} \qquad (135)$$

which is valid for all $\underline{k},\underline{P}$. An indicator of the importance of the $l>0$ terms is given by the coefficient ϵ. For a light particle ϵ^{ℓ} diminishes rapidly with l. For instance, for the pion ϵ is $\sim 1/8$ so that neglecting the angular dependence may be an excellent approximation in many cases. By

contrast, for the sigma $\epsilon > 1/2$ so that higher order terms are probably significant.

In table VII, we report the variation of the $^{13}_{\Sigma^0}C$ binding energy. Although the width may not be as sensitive as anticipated, three-, and four-figure accuracy requires three, and four terms respectively in the expansion. Certainly it is unjustified to ignore the angular dependence entirely.

No. of Terms	E+iΓ/2 (MeV)	Γ (MeV)	% change in Γ
1	-2.264 - i4.625	9.250	
			11.96
2	-2.585 - i5.253	10.506	
			0.96
3	-2.589 - i5.304	10.608	
			0.09
4	-2.587 - i5.309	10.618	

Table VII. Convergence of the 1s binding energy in $^{13}_{\Sigma^0}C$ with the number of terms in the two-body form-factor partial wave expansion.

The predictions for s-state seem fairly insensitive to moderate changes in the parameters of the model. However it is of interest to determine the sensitivity to the underlying model of the ΣN potentials. We have recalculated

the s-states using the model A parameters of Toker et al [28]. This model, although separable, differs qualitatively from ours. In their work they fit the $\Sigma^- p$ total cross-sections assuming them to be determined completely by the $^3S_1$ I=1/2 interaction, with no coupling to the ΛN $^3D_1$ channel.

The differences are clearly reflected in the results of the calculation, listed in table VIII. The real binding energies are similar in the two models, but with Toker's parameters the states are very narrow relative to ours. Although their two-body model is rather less absorptive than ours in the $^3S_1$ channel alone, the major source of this difference in widths is our inclusion of the ΛN $^3D_1$ and ^3P_J channels. These higher angular momentum states are not affected by Pauli suppression to the same degree as the S-waves, and in $^{13}_{\Sigma^0}C$ for example the P and D couplings are responsible for roughly 15 and 25% of the width respectively.

As mentioned earlier, our determination of ϵ is expected to be less reliable than of Γ, mainly because of the neglect of single-particle potentials in the energy variable of $\tau(\omega)$. Furthermore there is no statistically significant observation of an s-state hypernucleus.

Nevertheless the position and width calculated for the $^{12}_{\Sigma^0}C$ state coincides with a small bump in the spectrum of Bertini et al [3]. Also the weakly bound state in $^{9}_{\Sigma^0}Be$ is consistent with a shoulder in the data. Clearly much better experimental data are needed in these cases.

Nucleus	k_F (MeV/c)	B (MeV)	$\varepsilon - i\Gamma/2$ (MeV)	Γ (MeV)
$^{5}_{\Sigma^0}He$	245	10	+0.97 - i1.54	3.08
$^{7}_{\Sigma^0}Li$	250	10	-0.03 - i0.87	1.74
$^{9}_{\Sigma^0}Be$	260	10	-0.67 - i0.65	1.30
$^{12}_{\Sigma^0}C$	260	10	-3.31 - i1.42	2.85
$^{16}_{\Sigma^0}O$	260	10	-4.96 - i1.53	3.06

Table VIII. S-state binding energies in light Σ^0 hypernuclei as calculated with the model A parameters of Toker et al [28].

5.III. Separable Approximation of the Σ-Nucleus Potential

It is an interesting feature of the single-particle potential (80) that, despite the complexity of the expression, in practice it is separable. To see this, let us rewrite V_L as

$$V_L(k',k) = \int dP \sum_{\ell\ell'\ell''} \rho^{\ell}_{\ell\ell''}(k';k:P) \sum_{nm} v_n(k:P) v_m(k':P) C^{Lnm}_{\ell\ell'\ell''}(P) \qquad (136)$$

where $C(P)$ is a coefficient that depends on P but not on k

or k', and contains all the angular momenta summations as well. The density term ρ can be simplified in notation as well to

$$\rho^{\ell}_{\ell'\ell''}(k';k:P)=\sum_{m,m'=0}^{1} c^{\ell}_{\ell'\ell''}(P)\,k^{\ell+m}k'^{\ell'+m'}\,i_{\ell+m}(a^2kP)\,i_{\ell'+m'}(a^2k'P) \qquad (137)$$

with c(P) another P-dependent coefficient (which can be zero). In this form we notice that k and k' appear in separate functions in all terms of the integrand of eq.(136).

Strictly speaking, V_L is not separable because of the P integration but, in practice, the integral is always replaced by a finite sum over N discrete points P_i. The result is that V_L is approximated by a finite rank separable potential, and in this case the Lipmann-Schwinger equation can be solved algebraically.

In most instances it would simply not be practical to solve for T in this way since it would involve inverting a matrix of size $10^2 \times 10^2$, (or larger, depending on the number of quadrature points and terms in the expansions of the integrand). For the special case of a ^{4}He core though a number of simplifications become possible. All four nucleons are in s-state so that the ρ^{ℓ} term in eq.(136) is restricted to l=0. For the same reason we can expect that the two-body p-wave interactions are not as significant in $^5_{\Sigma}$He as in heavier nuclei. Finally, if the $\sum_n v_n$ can be

approximated by v_0 (and this will be tested), then the s-state potential becomes

$$V_0(k';k) = \sum_{i=1}^{N} \langle k'|g_i\rangle \lambda^{ii} \langle g_i|k\rangle \qquad (138)$$

with $$\langle k|g_i\rangle = e^{-a^2k^2/2} i_0(a^2 P_i k) v_0(k:P_i)$$

and $$\lambda^{ii} = 4\pi f_0 w_i P_i^2 e^{-a^2P_i^2} \sum_{SI} \frac{(2S+1)}{4} \frac{(2I+1)}{6} D^I_{0SS}[\omega(P^2)]$$

The T-matrix is solved, as in the two-body case, to be[6]

$$T(\omega) = |g\rangle[\lambda^{-1}(\omega) - \langle g|G_0(\omega)|g\rangle]^{-1}\langle g| \qquad (139)$$

with $|g\rangle$ the row matrix of $|g_i\rangle$, and $\lambda(\omega)$ the diagonal, energy dependent matrix of λ^{ii}. This equation can be reasonably solved by matrix inversion since the dimension of $\lambda^{-1} - \langle g|G|g\rangle$ is the same as the number of quadrature points.

We have solved the ${}^{5}_{\Sigma^0}$He T-matrix by this method and found that the binding energy is +2.72-0.76i MeV, as compared with the result with both S and P-wave ΣN interactions of +2.51-0.80i MeV, and the exact result with three form-factor terms as well of +2.49-0.88i MeV. The effect of including P-waves is mainly to increase the real binding of the state, whereas the width is more sensitive to the number of terms in the form-factor expansion. This is

---

[6] The term $\langle g|G|g\rangle$ must be multiplied by 3/4 because of the double-counting problem.

simply a reflection of the strong energy dependence in the ΣN t-matrix.

The approximation works reasonably well, and the simplicity of separable potentials for calculations suggests that this approach may be useful in systems where the interactions are smoother functions of energy than in the ΣN case.

5.IV. P-State Hypernuclei

Experimentally, the clearest evidence of narrow hypernuclear states comes, not from the ground states so far discussed, but rather from the recoillessly-produced 1p levels. To date, the positions and widths of these levels have not been fixed accurately but some indications are available. By comparing the Σ missing-mass spectrum with the corresponding well-known Λ spectrum, Brueckner et al.[4] have concluded that in ${}^{9}_{\Sigma^{0}}$Be the state is unbound by roughly 9 MeV and have placed an upper limit on the width of 8 MeV. They have also found a narrow p-level in ${}^{12}_{\Sigma^{0}}$C at 5 MeV excitation [3], and it has been suggested recently that in ${}^{6}_{\Sigma^{-}}$Li the width may be as small as 3 MeV [5]. It must be emphasized though that these are only indications. The data are not yet precise enough to pinpoint the positions to better than a few MeV accuracy.

Pauli exclusion and nucleon binding effects are not expected to influence the P-wave as much as in the ground state calculations. The centrifugal barrier obliges the Σ to interact primarily in the low density region of the valence nucleons so that, for consistency, both the Fermi momentum k_F and nucleon binding B should be reduced from their s-wave values. In all the light nuclei we consider, the nucleon binding has been raised to zero MeV and the Fermi momenta have been reduced substantially, ranging from 75 MeV/c in ${}^{5}_{\Sigma^0}$He to 175 MeV/c in ${}^{16}_{\Sigma^0}$O.

The method of solution is fairly straightforward. We have discussed at length the difficulties in calculating the S-matrix at complex momenta, and so use the Pade technique described in sect.4.IV. We search for poles in S by finding the conjugate zeros on the physical sheet. Anticipating the results somewhat, our attention is limited to the pole in the third momentum quadrant. The corresponding zero lies close to the physical axis and, as we have seen, the Pade method should then give reliable results.

The position of these poles are listed in table IX. The results are rich in information and several important observations can be made. First, it is noticed that for A>9 the model predicts the 1p level to be bound, which is evident from the position of the pole in the second

quadrant. That these states do in fact correspond to the resonance pole rather than the usual bound state pole is confirmed by following their motion for an increase in the Fermi momentum.

Increasing the Fermi momentum effectively decreases absorption by decreasing the coupling to the ΛN channel. Absorption depletes the Σ wavefunction at short distances, thereby acting as a short-range repulsion. By increasing k_F a bound state pole should then move towards the positive imaginary momentum axis, which is exactly the behaviour encountered already in s-state. A resonance pole, in light of our earlier discussion, will move in the opposite direction, crossing the negative real axis into the unphysical third quadrant.

Choosing ${}^{9}_{\Sigma^0}$Be as representative, we increase k_F from 125 to 200 MeV/c. It is found that the state becomes unbound, with the pole moving away to the third momentum quadrant at E =5.23+i2.19 MeV, clearly demonstrating these poles to be of the resonant variety.

The second feature we notice are the remarkably long lifetimes of these states, with $\Gamma \sim 4$ for ${}^{16}_{\Sigma^0}$O and as small as 0.5 for ${}^{9}_{\Sigma^0}$Be. This is truly paradoxical: it is the very fact that the potential is so strongly absorptive that the levels are narrow.

Nucleus	k_F (MeV/c)	B (MeV)	$E_p = \varepsilon - i\Gamma/2$ (MeV)	$E_p^{1/2} = \kappa + i\gamma$ $(MeV)^{1/2}$	Γ
${}^{5}_{\Sigma^o}He$	75	0	17.48 + i0.94	-4.18 - i0.112	-1.88
${}^{7}_{\Sigma^o}Li$	100	0	11.13 + i0.26	-3.34 - i0.039	-0.52
${}^{9}_{\Sigma^o}Be$	125	0	6.16 - i0.27	-2.48 + i0.054	0.54
${}^{12}_{\Sigma^o}C$	150	0	4.58 - i1.75	-2.18 + i0.402	3.50
${}^{16}_{\Sigma^o}O$	175	0	3.82 - i2.02	-2.02 + i0.501	4.04

Table IX. 1p binding energies in light Σ^o hypernuclei. States with $\gamma>0$ are quasi-bound

The case of ${}^{7}_{\Sigma^o}Li$ deserves special attention because, although the pole is very near to the real axis, the state is not quite bound. However, since the original choice of k_F and B was to some extent arbitrary, the question naturally arises whether for any reasonable choice of parameters the pole does cross the real axis to become a bound state. We find in fact that it does not. By reducing the Fermi momentum to zero and increasing the nucleon energy to +20 Mev (i.e B=-20 MeV) it is possible to decrease the width of the level to 0.06 MeV from 0.52 MeV, but the pole remains in the third quadrant.

Larger changes in k_F and B than the above would not be warranted on any physical grounds, but the results of the model calculation should not be construed of course as meaning that the ${}^{7}_{\Sigma^0}$Li p-state is necessarily unbound. Clearly a very small change in the overall strength of the coupling to the ΛN channel would be sufficient to produce binding in Li, without qualitatively affecting the p-state results for the other nuclei.

The elastic phase shifts δ, and absorption coefficients η, are also shown in fig. 9. For the A>9 nuclei we notice the π phase change between k=0 and ∞, confirming our interpretation of these as bound states. The deep minimum in the absorption coefficient is also clear near the position of the zero (or binding energy). By contrast, δ and η for the s-states are shown in fig. 10. For the heavier (A>9)nuclei the curves are seen to be nearly devoid of interesting structure, as expected for bound state poles at negative energies. The lighter He and Li curves, however, show dip near the (positive) bound state energies. Since in these cases the poles lie closer to the negative, real momentum axis than the imaginary axis, we know an S-matrix zero is very close to the positive, real axis.

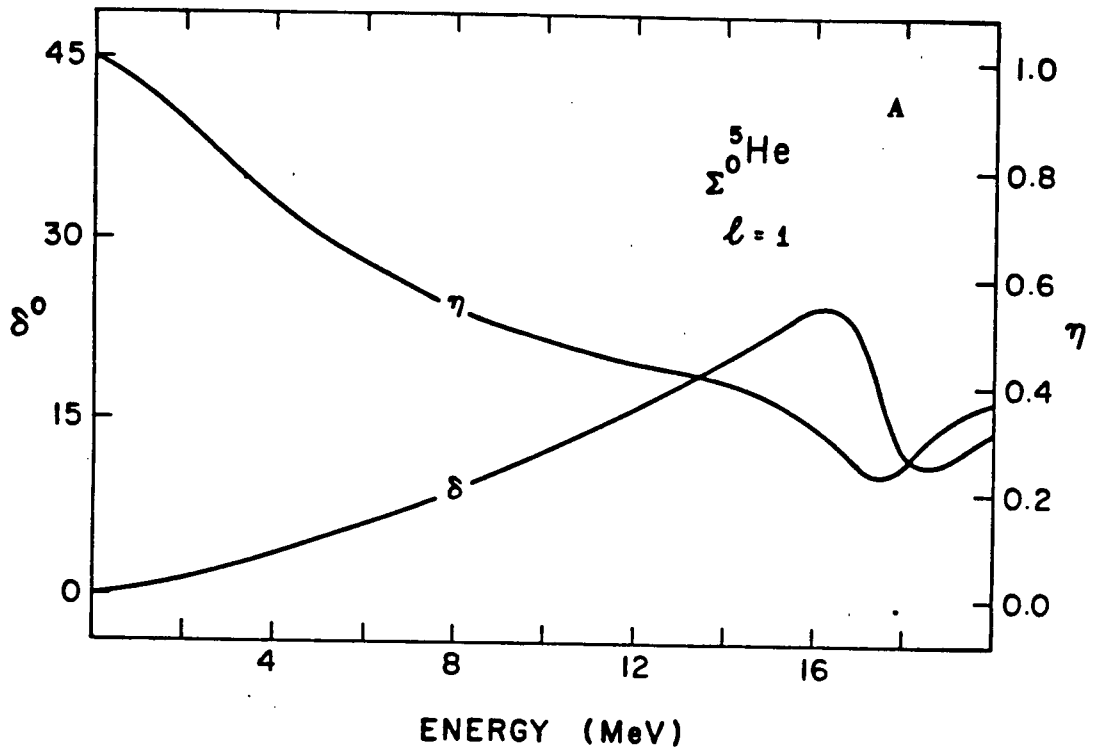

Fig. 9. P-wave phases δ and absorption coefficients η for low energy elastic Σ-nucleus scattering. For the light nuclei shown in a), and b) no bound states exist, as seen by the zero-degree phase shifts at zero energy. The 180° phase shifts for the nuclei with A>8, shown in c)->e), are evidence of bound states. These states are in the continuum, about where η is a minimum.

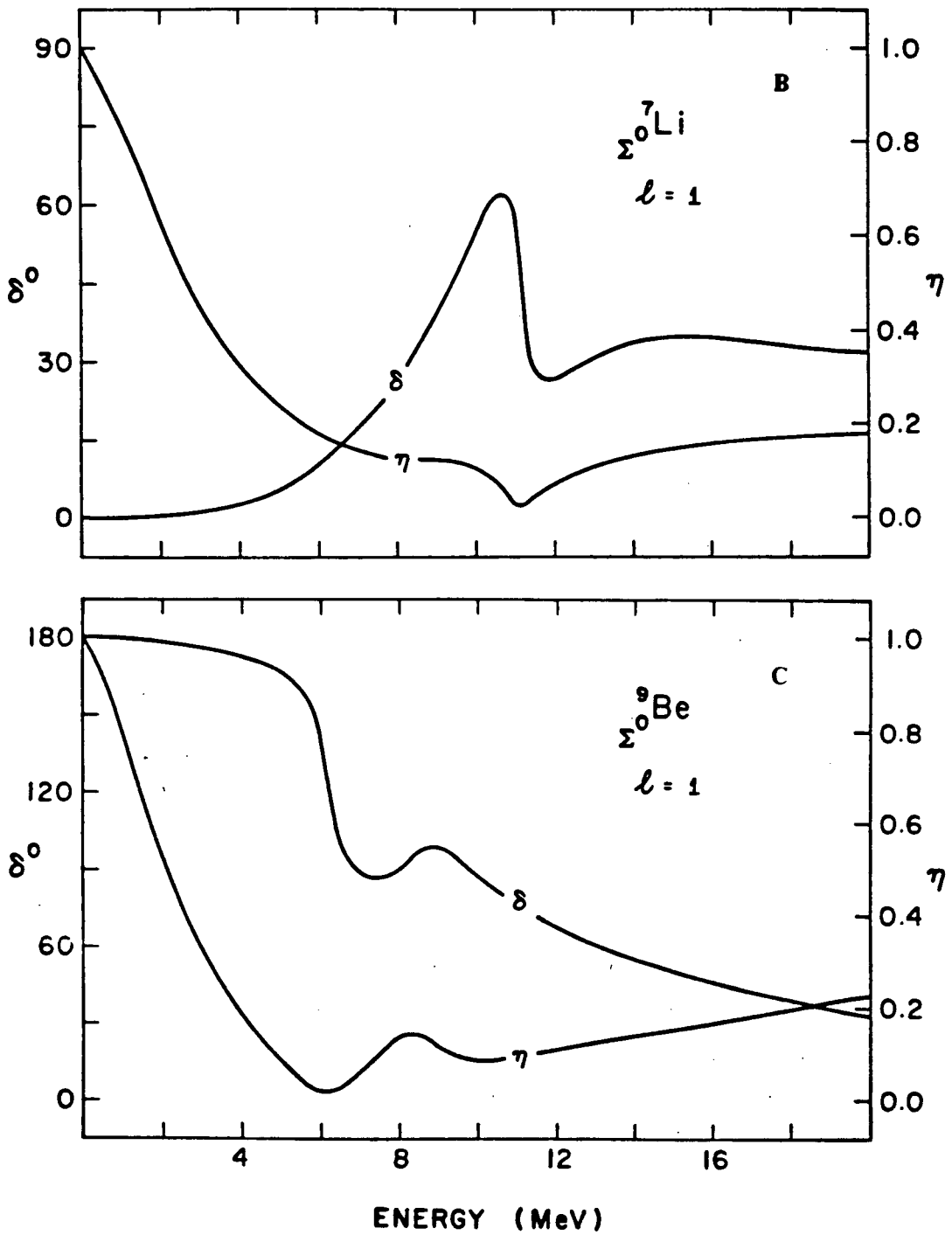
B
Σ^0 ^{7}Li
ℓ = 1
δ
η
90
60
30
0
δ°
1.0
0.8
0.6
0.4
0.2
0.0
η
C
Σ^0 ^{9}Be
ℓ = 1
δ
η
180
120
60
0
δ°
4
8
12
16
ENERGY (MeV)

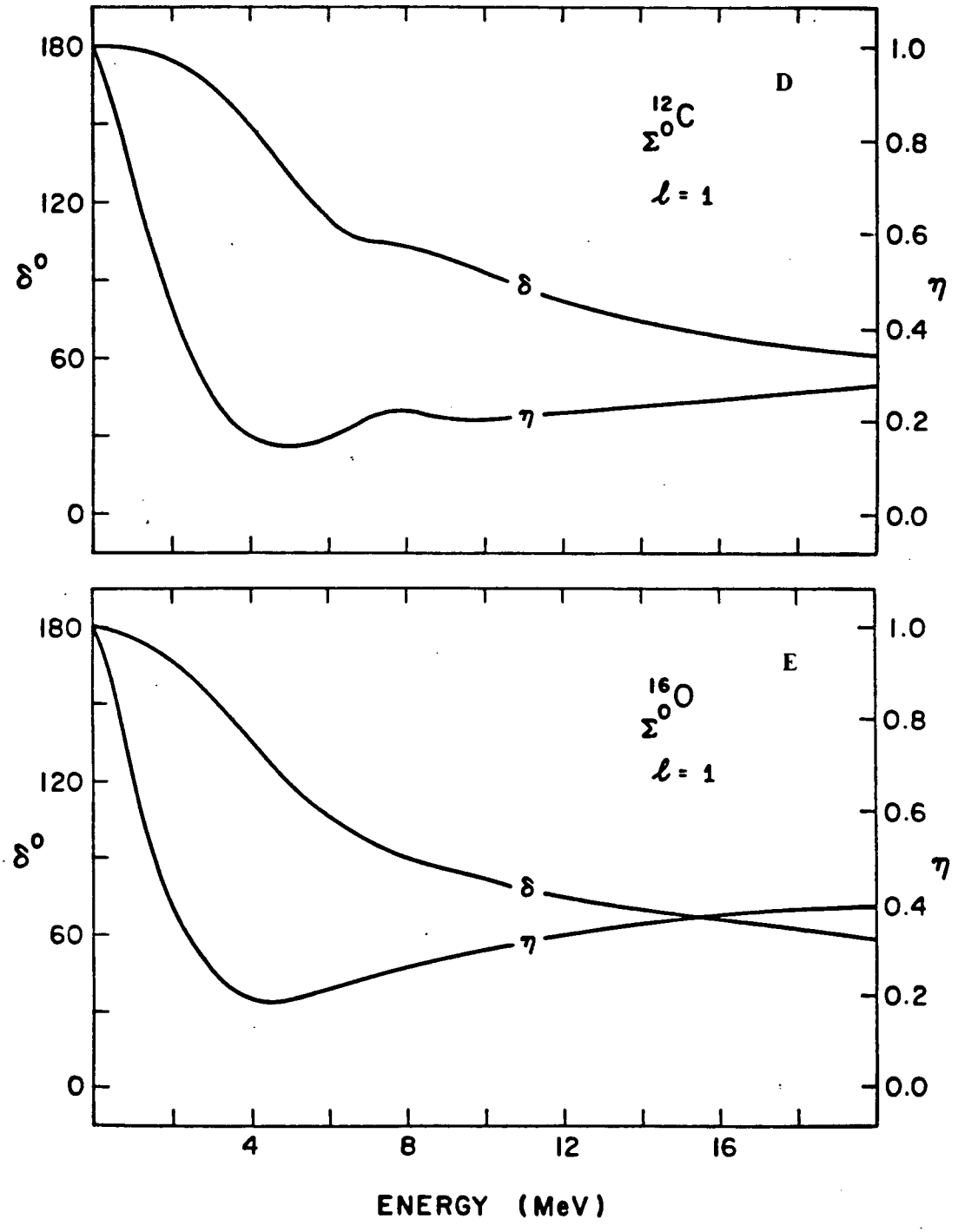
180
120
60
0
δ°
1.0
0.8
0.6
0.4
0.2
0.0
η
D
$^{12}_{\Sigma^0}C$
ℓ = 1
δ
η
E
$^{16}_{\Sigma^0}O$
ℓ = 1
4
8
12
16
ENERGY (MeV)

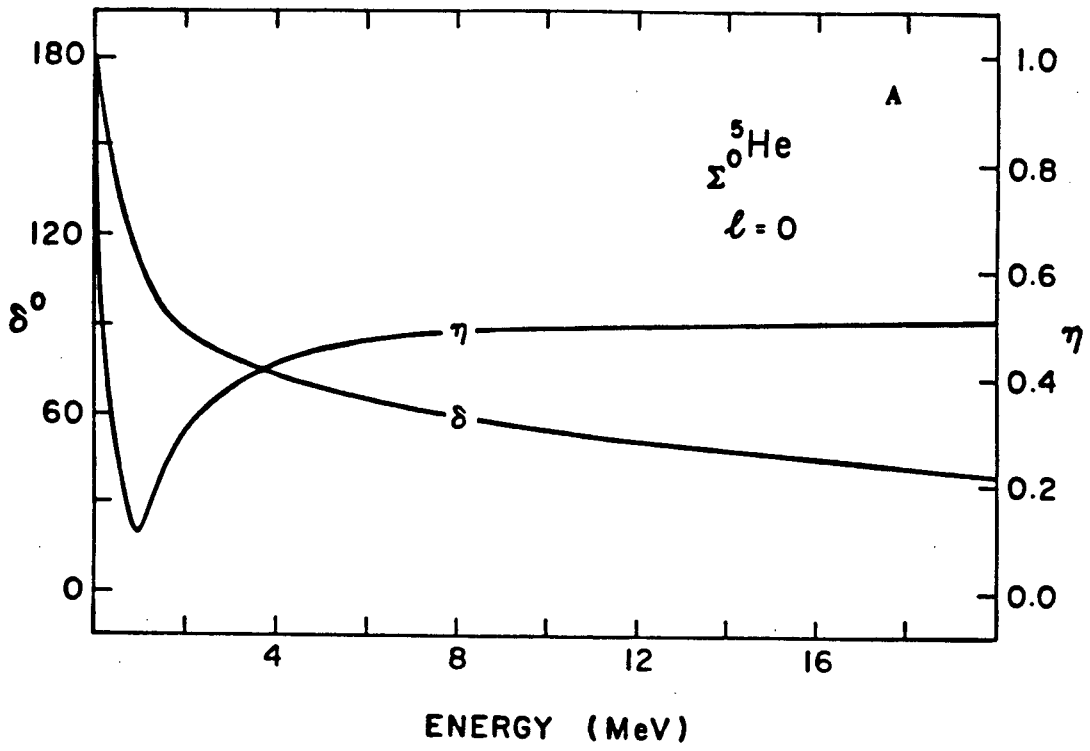

Fig. 10. S-wave phases δ and absorption coefficients η for low energy elastic Σ-nucleus scattering. For the light nuclei shown in a) and b) η has a dip near the bound state energies. For the heavier nuclei there is no interesting structure, as expected for negative binding energies.

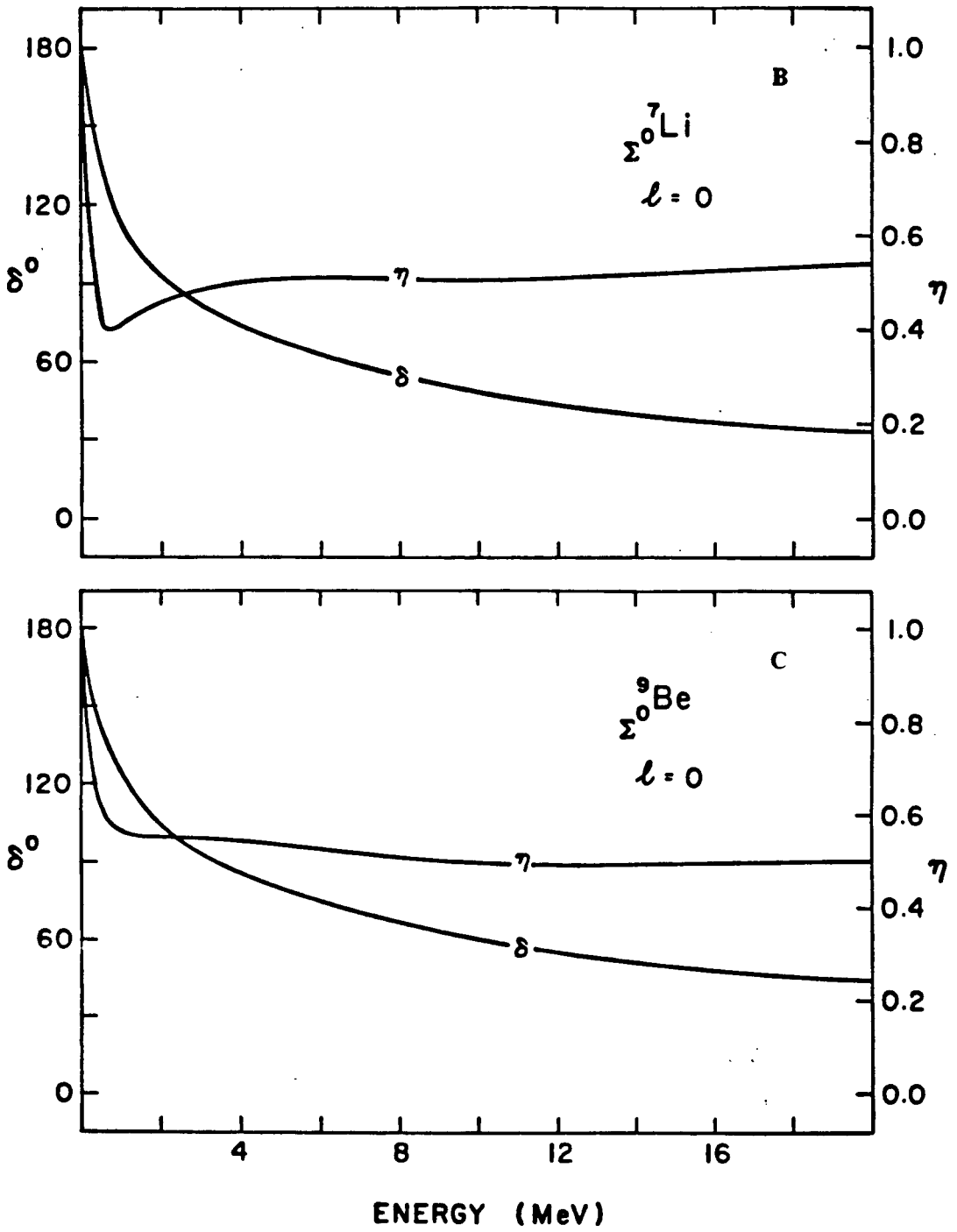
B
Σ^0 ^{7}Li
$\ell = 0$
C
Σ^0 ^{9}Be
$\ell = 0$
δ^0
η
180
120
60
0
1.0
0.8
0.6
0.4
0.2
0.0
4
8
12
16
ENERGY (MeV)

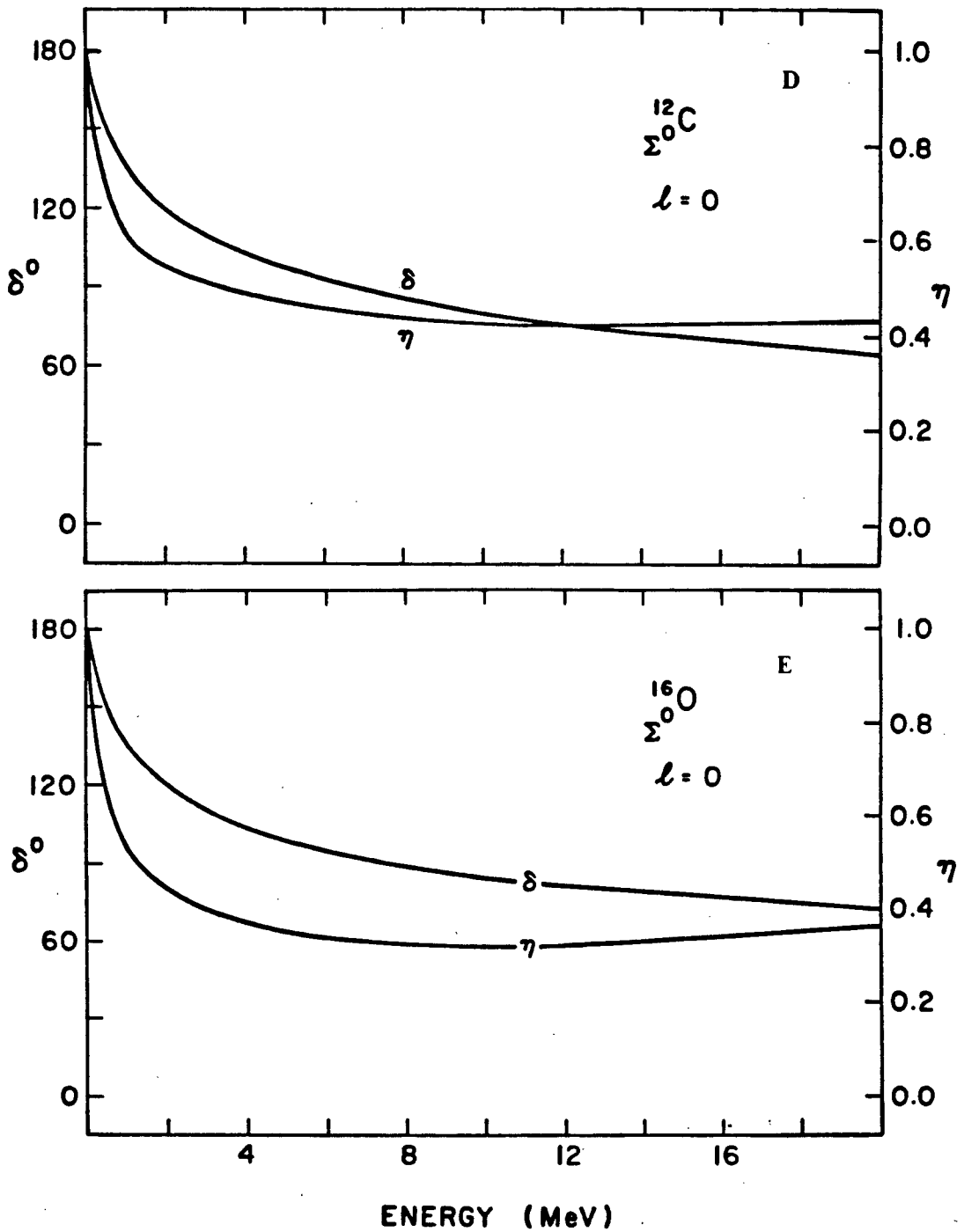
D
$^{12}_{\Sigma^0}$C
$\ell = 0$
δ
η
E
$^{16}_{\Sigma^0}$O
$\ell = 0$
δ
η
δ°
η
180
120
60
0
1.0
0.8
0.6
0.4
0.2
0.0
4
8
12
16
ENERGY (MeV)

Again, these states have been recalculated using the parameters of Toker *et al*, and these results are given in table X. The predictions are similar to those of our model but again there are some significant differences. First of all we remark that this model also predicts a $^{16}_{\Sigma^0}O$ bound state. In lighter nuclei the real component of the resonant energies are fairly close to our values, but it is important to appreciate that the bound states and narrower widths of our model arise from greater absorption, rather than greater attraction.

Nucleus	k_F (MeV/c)	B (MeV)	$E_p = \varepsilon - i\Gamma/2$ (MeV)	$E_p^{1/2} = \kappa + i\gamma$ $(MeV)^{1/2}$	Γ
$^{5}_{\Sigma^0}He$	75	0	9.01 + i18.7	-3.85 - i2.42	-37.4
$^{7}_{\Sigma^0}Li$	100	0	5.43 + i8.81	-2.81 - i1.57	-17.6
$^{9}_{\Sigma^0}Be$	125	0	3.14 + i3.70	-2.00 - i0.93	-7.40
$^{12}_{\Sigma^0}C$	150	0	2.94 + i1.40	-1.76 - i0.40	-2.80
$^{16}_{\Sigma^0}O$	175	0	1.20 - i0.34	-1.11 + i0.15	.68

Table X. Position of the 1p poles calculated with the model A parameters of Toker *et al* [28]. States with $\gamma>0$ are quasi-bound.

To complete this study, δ and η have been calculated for D-wave Σ-nucleus interactions. As can be seen in fig. 11, a dip is beginning to develop near 12 MeV excitation in $^{16}_{\Sigma^0}O$, but in general there is no indication of structure. These findings are in agreement with the phenomenological result of Gal et al [11] where, although their potential was more absorptive than ours, they found no bound D-states for nuclei lighter than silicon.

In brief summary then, we find that when nucleon binding and Pauli exclusion effects are included in a microscopic calculation narrow Σ s-states result. On the other hand we find that in p-wave, where these effects are small, the consequent strong nuclear absorption produces remarkably long-lived states in the continuum, in close agreement with experimental energies.

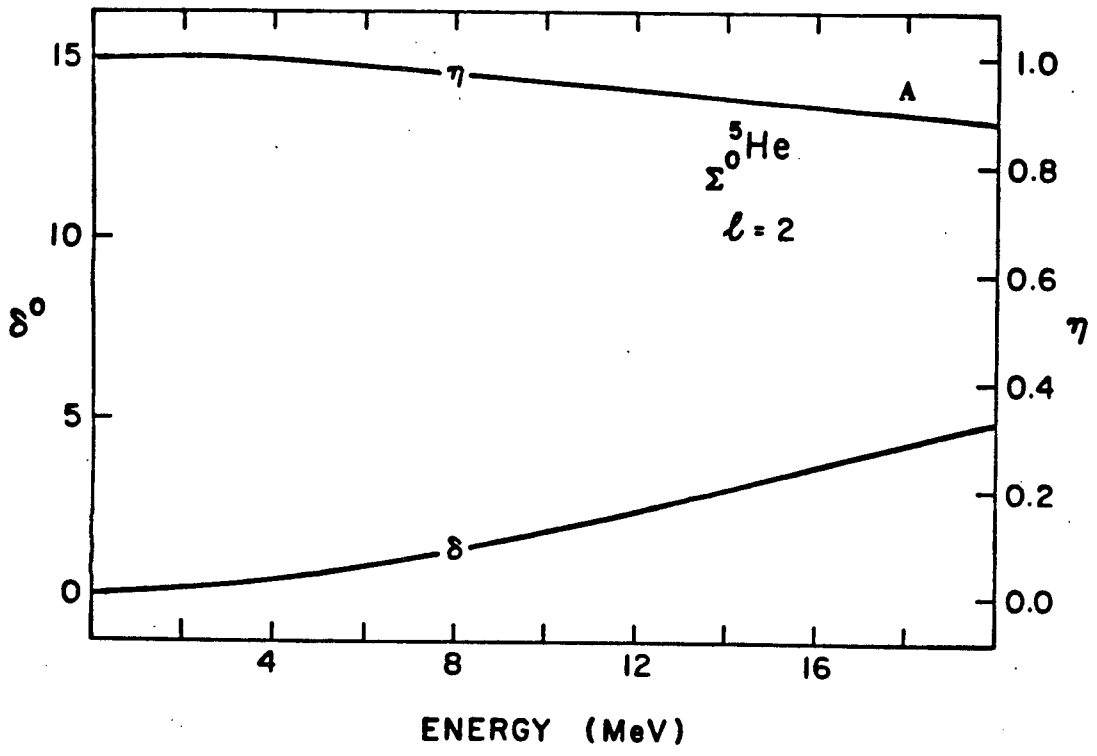

Fig. 11. D-wave phases δ and absorption coefficients η for low energy elastic Σ-nucleus scattering. Although a small dip in η is developing in $^{16}_{\Sigma}$O, the curves are generally devoid of structure.

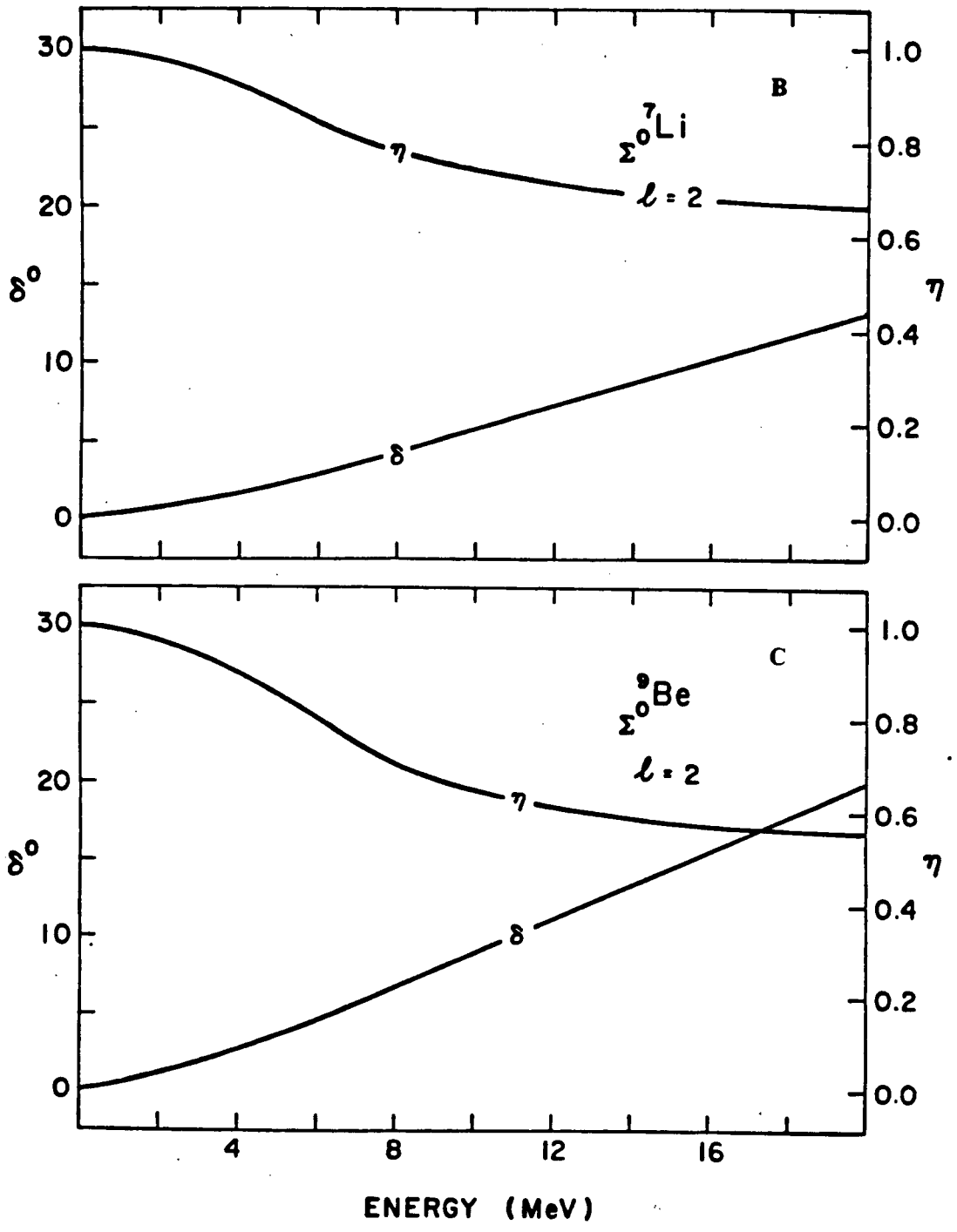
B
Σ^0 ^{7}Li
$\ell = 2$
η
δ
δ^0
30
20
10
0
1.0
0.8
0.6
0.4
0.2
0.0
C
Σ^0 ^{9}Be
$\ell = 2$
4
8
12
16
ENERGY (MeV)

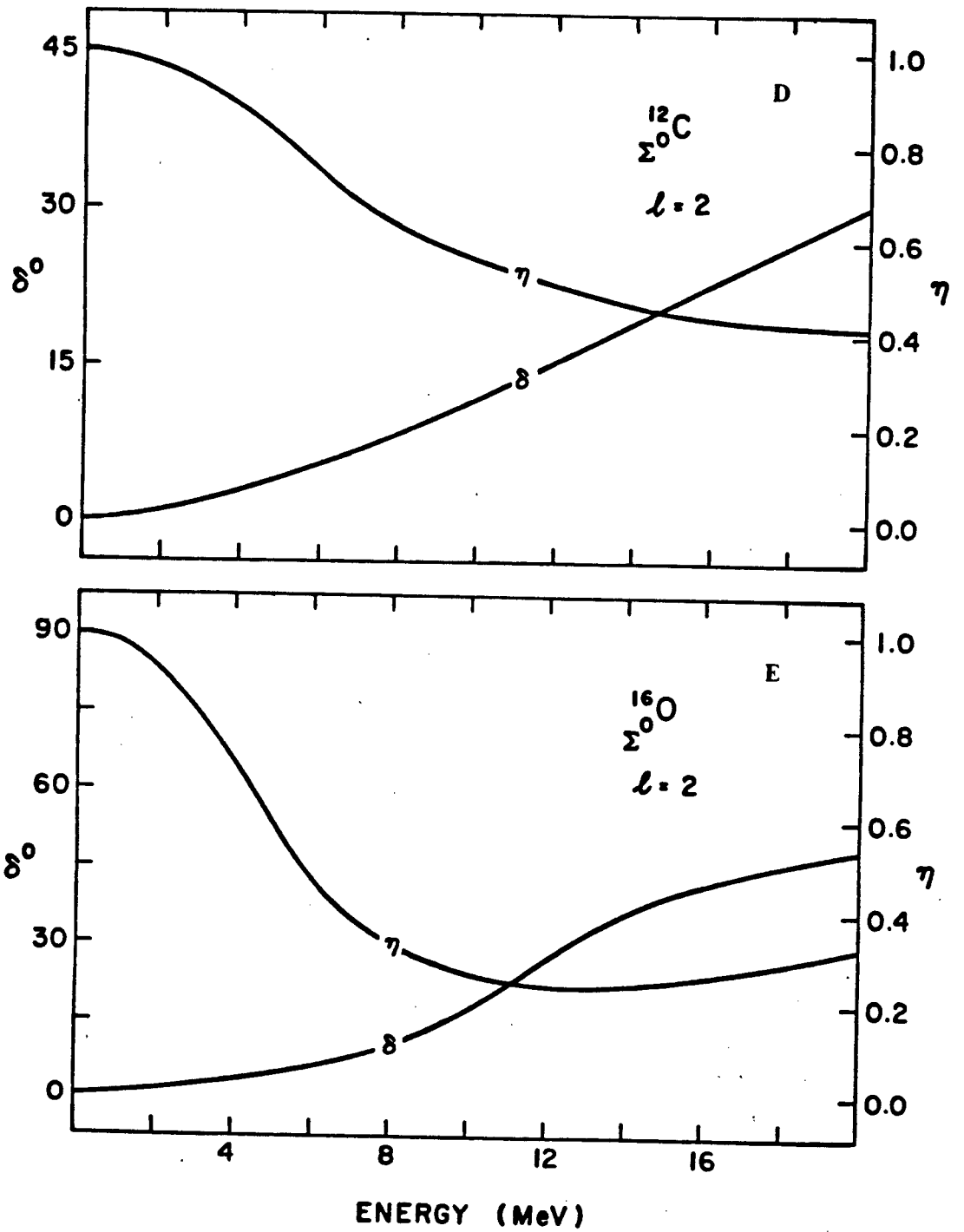
45
30
15
0
δ°
D
$^{12}_{\Sigma^0}C$
ℓ = 2
η
δ
1.0
0.8
0.6
0.4
0.2
0.0
η
90
60
30
0
δ°
E
$^{16}_{\Sigma^0}O$
ℓ = 2
η
δ
1.0
0.8
0.6
0.4
0.2
0.0
η
4
8
12
16
ENERGY (MeV)

CHAPTER 6 DISCUSSION AND CONCLUSIONS

Our aim in this work has been to calculate the widths of light Σ^0 hypernuclear states as accurately as possible. To this end we constructed a separable potential model to describe the ΣN scattering where it was found that, in addition the usual S-wave interactions, the $^3S_1(\Sigma N) \rightarrow {}^3D_1(\Lambda N)$ transition was essential to the description of the conversion reaction.

With these interactions as fundamental input, the Σ nucleus single particle potential was developed with careful attention to corrections arising from Pauli exclusion and nucleon binding effects. After making a minimum number of approximations we were able to evaluate analytically the angular integrals in the defining relation for this potential, and to show that in the appropriate limit it reduced to the phenomenological result obtained from the analysis of Σ^- atoms.

Most importantly, the self-consistent solutions of the momentum-space Schroedinger equation predicted narrow Σ states in both S and P waves, although the mechanisms responsible were quite different. In s-state, Pauli exclusion and nucleon binding effects produced long lived states with widths ranging from 1.8 MeV in ${}^{5}_{\Sigma^0}$He to 12.5 MeV

in $^{16}_{\Sigma^0}O$. In p-state by contrast, the Pauli principle had little influence on the potential and the resulting strong absorption produced narrow states in the Σ continuum with widths from 0.5 MeV in $^{9}_{\Sigma^0}Be$ to 4.0 MeV in $^{16}_{\Sigma^0}O$.

The mechanisms responsible for suppressing $\Sigma N \rightarrow \Lambda N$ conversion in s-states are well understood. In p-states though, the physical interpretation of strong absorption producing narrow widths is not at all clear. There is no denying that this runs contrary to one's prejudice that, with strong coupling to an open channel, a bound state will 'leak out' to the scattering state of equal energy and hence can not exist for any great length of time.

It is important that a picture of these states be developed and so let us first summarize their characteristics. Without a weak coupling hypothesis, long-lived states degenerate with the continuum can exist in the presence of an open channel. Such a state is unrelated to a bound state in the isolated channels and, indeed, would not exist as a normalizeable state in the absence of the strong coupling.

Gal, Toker, and Alexander [11] have tried to interpret this phenomena in a similar framework to resonances in (for example) e-He$^+$ scattering. In the latter system it is well known that a stable state of He with both electrons in the

n=2 level exists above the ionization energy for one electron. Consequently, in e-He^+ scattering a sharp resonance results for the incident energy (~27 eV) at which this state can be excited. Gal et al have pictured the narrow hypernuclear states as resonances in Λ-nucleus scattering. It is imagined that at some particular energy the Λ converts on a nucleon with the final state N kicked into an excited state and the Σ bound with negative binding energy.

The explanation is tempting because of its familiarity, and such states may well exist, but the model is quite wrong for the levels we are considering. First of all, their potential which produced these states was energy independent. It is not reasonable, therefore, to suggest that these states depend on the microscopic nucleon energy spectrum for their interpretation. Secondly, a resonance in the elastic cross section is expected with this picture. As we have seen though, in Σ-nucleus scattering an S-matrix zero, rather than a pole, is exhibited and the cross-section is completely smooth.

So the question remains as to the meaning of these states. To answer this we will consider the simplified example of the Σ and Λ channels coupled by a square-well potential matrix with elements $V_{YY'}$ and range R. In the

scattering formalism the outgoing waves are related to the incoming ones via the S-matrix as

$$\begin{pmatrix} \Psi_\Sigma^{OUT} \\ \Psi_\Lambda^{OUT} \end{pmatrix} = \begin{pmatrix} S_{\Sigma\Sigma} & S_{\Sigma\Lambda} \\ S_{\Lambda\Sigma} & S_{\Lambda\Lambda} \end{pmatrix} \begin{pmatrix} \Psi_\Sigma^{IN} \\ \Psi_\Lambda^{IN} \end{pmatrix} \tag{140}$$

in an obvious notation. A Σ bound state (of strictly infinite lifetime) corresponds to $S_{\Sigma\Lambda}\equiv 0$. In other words, the two channels are completely decoupled so that no net flux is lost from the Σ to Λ channels. It is straightforward to show [21] that this condition is satisfied for

$$K_\Sigma \cot K_\Sigma R = K_\Lambda \cot K_\Lambda R \tag{141}$$

where the $K_Y^2/2m$ are the channel eigenvalues. So we find that these states exist because of an interference effect, arising from a fine balance between the channel potentials. More generally, the above is related to Gal's result [11] that, for resonant or bound states above threshold, the width Γ (up to a normalization factor) is

$$\Gamma = \mathrm{Re}(k_\Sigma)|\Psi_\Sigma(R)|^2 + \mathrm{Re}(k_\Lambda)|\Psi_\Lambda(R)|^2 \tag{142}$$

where, again, R is the range of the potential, and $k_\Sigma^2/2m$, $k_\Lambda^2/2m$ are the channel eigenvalues. In this case the influence of the potentials is disguised in the wavefunctions, but it should be clear that with a pole on

sheet 2 (in the notation of Chapter 4) the real components of k_Σ, k_Λ are opposite in sign and cancellation occurs between the two terms of eq.(142), becoming complete as the pole moves across the real axis from sheet 4 to sheet 2.

In view of the two distinct causes of narrow widths in s and p-states it seems important that measurements of p-state Σ hypernuclei levels should first be extended to very light nuclei where they are predicted to be exceptionally long-lived. Secondly one would like reliable data for the s-states.

BIBLIOGRAPHY

1) C.J. Batty, Phys. Lett. 87B (1979) 324

2) A. Gal, Nukleonika 25 (1980) 447

3) R. Bertini et al, in Meson-Nuclear Physics, 1979 (Houston), ed. E.V. Hungerford (AIP, NY) p.703

4) W. Brueckner et al, in Proceedings of the Kaon Factory Workshop, 1979 (TRIUMF), ed. M.K. Craddock, p.136

5) H. Piekarz et al, Phys. Lett. 110B (1982) 428

6) R. Bertini et al, Phys. Lett. 90B (1980) 375

7) P.D. Barnes, invited talk at the 9th ICOHEPANS, Versailles (1981)

8) A. Gal, in Proceedings of the Second Kaon Factory Workshop, 1981 (TRIUMF), eds. R. Woloshyn and A. Strathdee, p.148

9) A. Gal and C.B. Dover, Phys. Rev. Lett. 44 (1980) 379

10) C.B. Dover and A. Gal, Phys. Lett. 110B (1982) 433

11) A. Gal, G. Toker and Y. Alexander, Ann. Phys. 137 (1981)

12) C.J. Batty et al, Phys. Lett. 74B (1978) 27

13) W. Stepien-Rudzka and S. Wycech, Nucl. Phys. A362 (1981)

14) R. Engelmann, H. Filthuth, V. Hepp and G. Zech, Phys. Lett. 21 (1966) 587

15) F. Eisele, H. Filthuth, W. Fohlisch, V. Hepp and G. Zech, Phys. Lett. 37B (1971) 204

16) A.W. Thomas, in Modern Three-Hadron Physics, 1977 (Springer-Verlag), ed. A.W. Thomas, p.12

17) C. Lovelace, in Strong Interactions and High Energy Physics, 1963 (Scottish Universities' Summer School), ed. R.G. Moorhouse, p.437, and
C. Lovelace, Phys. Rev. 135 5B (1964) B1225

18) M.M. Nagels, T.A. Rijken and J.J. DeSwart, Ann. Phys. 79 (1973) 338

19) M.M. Nagels, T.A. Rijken and J.J. DeSwart, Phys. Rev. D12 (1975) 744 ; D15 (1977)2547

20) M.M. Nagels, T.A. Rijken and J.J. DeSwart, Phys. Rev. D20 (1979) 1633

21) R.G. Newton, Scattering Theory of Waves and Particles, McGraw-Hill (1966)

22) M.L. Goldberger and K.M. Watson, Collision Theory, John Wiley and Sons (1964)

23) J.T. Londergan, K.W. McVoy and E.J. Moniz, Ann. Phys. 86 (1974) 147

24) H. van Haeringen and R. van Wageningen, Journal of Math. Phys. 16 (1975) 1441

25) H. van Haeringen, Nucl. Phys. A253 (1975) 355

26) O. Braun et al, Nucl. Phys. B124 (1977) 45

27) R. Dalitz, in Meson-Nuclear Physics, 1979 (Houston) ed. E.V. Hungerford (AIP,NY) p.621

28) G. Toker, A. Gal and J.M. Eisenberg, Nucl. Phys. A362 (1981) 405

29) J.A. Johnstone, ΣN Strong Interactions, (M.Sc. Thesis, unpublished) 1979

30) J. Dabrowski and J. Rozynek, Phys. Rev. C23 (1981) 1706

31) P.C. Tandy, E. Redish and D. Bolle, Phys. Rev. Lett. 35 (1975) 921

32) R,H. Landau and A.W. Thomas, Nucl. Phys. A302 (1978) 461

33) E. Lomon and M. McMillan, Ann. Phys. 23 (1963) 439

34) A.W. Thomas and R.H. Landau, Phys. Rep. 58 (1980) 121

35) R.C. Barrett and D.F. Jackson, Nuclear Sizes and Structure, Clarendon Press (1971)

36) M. Moshinsky, Nucl. Phys. 13 (1959) 104

37) M. Stingl and A.S. Rinat, Nucl. Phys. A154 (1970) 613

38) L. Fonda and R.G. Newton, Ann. Phys. 10 (1960) 490

39) K. Hartt, Phys. Rev. C22 (1980) 1377

40) G.A. Baker, Essentials of Pade Approximants, Academic Press (1975)

41) J.N. Massot, E. El-Baz and J. LaFoucriere, Rev. of Mod. Phys. 39 (1967) 288

APPENDIX I ANGULAR MOMENTUM GRAPHICS

The technique outlined below is a graphical method for calculating sums of 3J coefficients, adapted from the work of Massot, El-Baz, and LaFoucriere [41]. Only those results which are needed in the present work are given, and none of these are proven.

First, a Wigner 3J is defined by the picture

$$\begin{pmatrix} j_1 & j_2 & j_3 \\ m_1 & m_2 & -m_3 \end{pmatrix} \longrightarrow$$

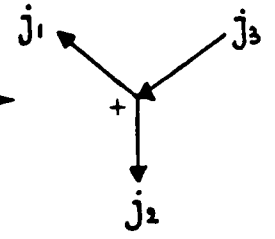

(AI.1)

The rules for constructing the picture are:

(1) The sign of the vertex is positive if the j's are read in an anti-clockwise direction, and negative if read clockwise.

(2) The arrows point outward from the vertex for positive m , and inward for negative m .

(3) Changing either the sign of the vertex or the arrow direction of all three lines gives a phase change of $(-)^{j_1+j_2+j_3}$. (The direction of one <u>free</u> line alone must not be changed.)

(4) The 3J represented by the diagram is invariant under rotations and geometric deformations.

To sum graphically over one m which is common to two 3J coefficients the corresponding free j line in each diagram are joined so that the arrows point in the same direction. For example,

$$\sum_{m_1} \begin{pmatrix} j_1 & j_2 & j_3 \\ m_1 & m_2 & m_3 \end{pmatrix} \begin{pmatrix} j_1 & j_4 & j_5 \\ m_1 & m_4 & m_5 \end{pmatrix} \qquad \text{(AI.2)}$$

$$= (-)^{j_4+j_5-m_4-m_5} \sum_{m_1} (-)^{j_1-m_1} \begin{pmatrix} j_1 & j_2 & j_3 \\ m_1 & m_2 & m_3 \end{pmatrix} \begin{pmatrix} j_1 & j_4 & j_5 \\ -m_1 & -m_4 & -m_5 \end{pmatrix}$$

and the sum is represented by

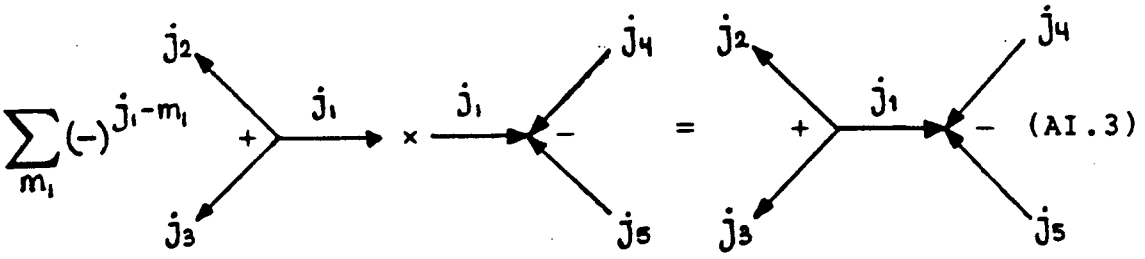

(AI.3)

The rules for summing over the projection m of j are that:

(5) A factor of $(-)^{j-m}$ must be present.

(6) Whenever two vertices are joined by a line j, the direction of that line may be reversed but this is accompanied by a phase change of $(-)^{2j}$.

(7) If there are three free lines, their loose ends may may be pinched together with the arrows pointing in the same direction. A 3J multiplies the diagram, represented by the three lines, with their arrows pointing in the original direction, and the opposite

sign at the vertex.

This last rule is demonstrated much more clearly by a picture

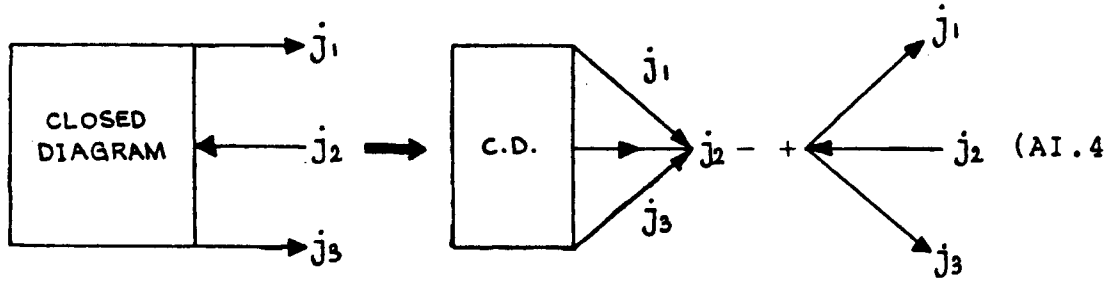

(AI.4)

This last rule also allows a large, closed diagram to be broken into smaller components as

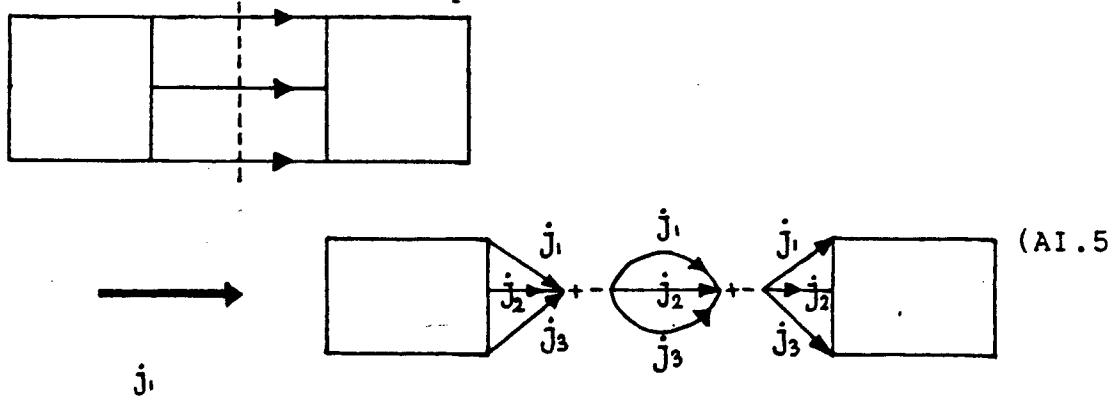

(AI.5)

with 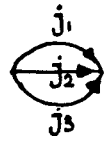 $= \sum_{m'} (-)^{\sum_i (j_i - m_i)} \begin{pmatrix} j_1 & j_2 & j_3 \\ m_1 & m_2 & m_3 \end{pmatrix} \begin{pmatrix} j_1 & j_2 & j_3 \\ -m_1 & -m_2 & -m_3 \end{pmatrix}$ (AI.6)

$= 1$ if j_1, j_2, j_3 obey the triangle inequality, and

$= 0$ otherwise.

For the purposes of this work, the only other results needed are the diagrams for 6J and 9J symbols. These are given by

$$\begin{Bmatrix} j_1 & j_2 & j_3 \\ \ell_1 & \ell_2 & \ell_3 \end{Bmatrix} =$$

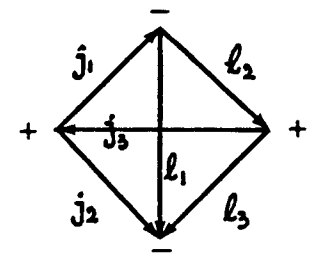

(AI.7)

and

$$\begin{Bmatrix} j_1 & j_2 & j_3 \\ \ell_1 & \ell_2 & \ell_3 \\ k_1 & k_2 & k_3 \end{Bmatrix} =$$

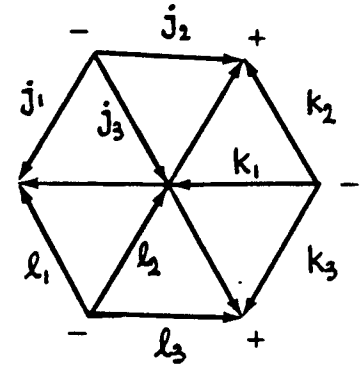

(AI.8)

As an example of the usefulness of this technique, equation (23) for the differential cross section will be derived. Concentrating on just the piece which involves $\sum_{\nu\nu'}$, we have

$$\sum_{\nu\nu'} \langle L0S\nu|J\nu\rangle\langle L''0S\nu|J'\nu\rangle\langle L'\nu-\nu'L''\nu'-\nu|10\rangle\langle L'\nu-\nu'S\nu'|J\nu\rangle \langle L''\nu-\nu'S\nu'|J'\nu\rangle(-)^{\nu-\nu'} \qquad \text{(AI.9)}$$

First, this is converted to 3J's as

$$\hat{J}^2\hat{J}'^2\hat{1}\,(-)^{L+L''-\nu-\nu'}\begin{pmatrix} S & J & L \\ \nu & -\nu & 0 \end{pmatrix}\begin{pmatrix} S & J' & L'' \\ \nu & -\nu & 0 \end{pmatrix}\begin{pmatrix} L' & L'' & L \\ \nu-\nu' & -\nu+\nu' & 0 \end{pmatrix} \begin{pmatrix} L' & S & J \\ \nu-\nu' & \nu'-\nu & \end{pmatrix}\begin{pmatrix} L'' & S & J' \\ \nu-\nu' & \nu'-\nu & \end{pmatrix} \qquad \text{(AI.10)}$$

This expression will be modified somewhat so that it resembles the 3J's of (AI.2) more closely for summation in

diagramatic form. We can introduce the dummy variables $M_J, M_J', M, M', M'', M'''$, and m. There will be no summation over M, M'', and m, and eventually their values will be set equal to zero, but for now non-zero values will allow us to assign directions and magnitudes to the arrows in the summation in a meaningful way. The (formal) summation over the other M's will not alter the result because their values are actually fixed by M, M'', and m. Also S, ν' will be relabelled as S', ν' for the moment to distinguish it from $S, '$.

The summation (AI. 9) can be expressed as

$$\hat{J}^2\hat{J}^{2\prime}\hat{l}\sum (-)^{J+J'}(-)^{J-M_J}(-)^{J'-M_J'}(-)^{S-\nu}(-)^{S'-\nu'}(-)^{L'-M'}(-)^{L'''-M'''} \begin{pmatrix} J & S & L \\ M_J & \nu & m \end{pmatrix}\begin{pmatrix} S & J' & L'' \\ -\nu & -M_J' & -M'' \end{pmatrix}\begin{pmatrix} L''' & L' & l \\ M''' & M' & m \end{pmatrix} \begin{pmatrix} L' & S' & J \\ -M' & -\nu' & -M_J \end{pmatrix}\begin{pmatrix} S' & L'' & J' \\ \nu' & -M'' & M_J' \end{pmatrix} \qquad \text{(AI.11)}$$

We have all the phases $(-)^{J-M}$ necessary to do this in diagrammatic form. In the following, the steps in manipulating the graphs will be shown with the overall phase of the sum indicated. Ignoring the $\hat{J}^2\hat{J}^{2\prime}\hat{l}$ term for now, the sum is represented by

(i)

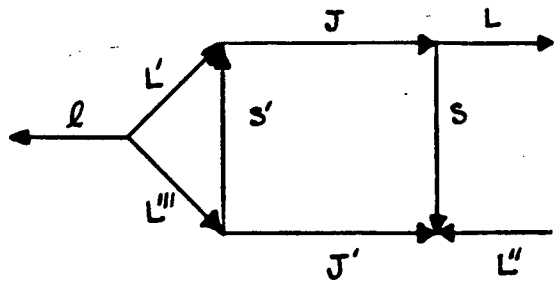

$(-)^{J+J'}$ (AI.12)

(ii)

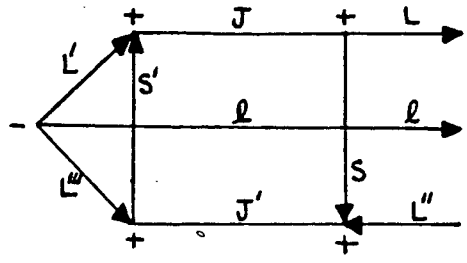

(-) $J+J'+L'+L'''+\ell$ (AI.13)

Rule 3: sign change of vertex

(iii)

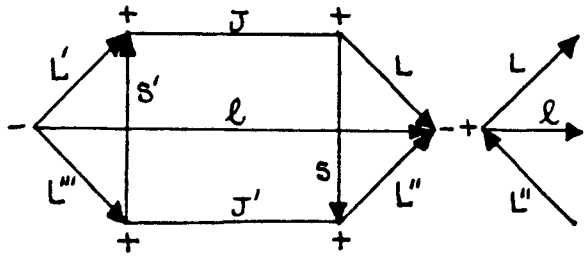

(-) $J+J'+L'+L'''+\ell$ (AI.14)

Rule 7: separation of a 3J and pinching the lines.

(iv)

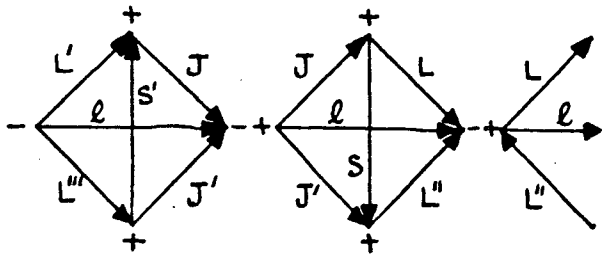

(-) $J+J'+L'+L'''+\ell$ (AI.15)

Rule 8: breaking of a larger diagram.

(v)

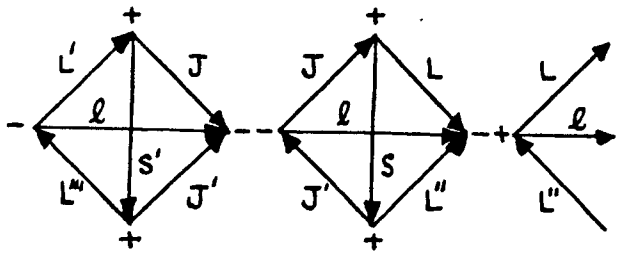

(-)$^{\ell}$ (AI.16)

Rule 4: change of the arrow directions

It is found by comparison with the picture of a 6J symbol that the whole expression has reduced to

$$\hat{J}^2\hat{J}^{2\prime}\hat{1}(-)^{L} \begin{Bmatrix} L'' & J' & S \\ 1 & L' & J \end{Bmatrix} \begin{Bmatrix} J' & L'' & S \\ 1 & J & L \end{Bmatrix} \begin{pmatrix} L & L'' & 1 \\ 0 & 0 & 0 \end{pmatrix} \qquad \text{(AI.17)}$$

Inserting this expression into eq.(21) gives eq.(23) for the differential cross-section.

APPENDIX II SOLUTION OF THE COUPLED-CHANNEL EQUATIONS

Following the procedure of Londergan *et al.* [23], we will outline the steps involved in solving for the coupled-channels t-matrix with rank-one separable potentials.

In general, for any potential operator v, and N coupled channels, the transition operator describing scattering from channel $|\alpha\rangle$ to the channel $|\beta\rangle$ is

$$t_{\beta\alpha} = v_{\beta\alpha} + \sum_{\gamma=1}^{N} v_{\beta\gamma} G_0^{\gamma} t_{\gamma\alpha} \qquad \text{(AII.1)}$$

where G_0^{γ} is the γ-channel Green's function defined by eq.(25). If the potentials are all rank-one separable, then $v_{\beta\alpha}$ can be written as $|v_\beta\rangle\lambda^{\beta\alpha}\langle v_\alpha|$ in Dirac notation. Here, $\lambda=-1(+1)$ for attractive (repulsive) interactions, and the strength of the potential has been absorbed into the form factors $|v\rangle$. In this case (AII. 1) can be solved algebraically.

Separating the $|\alpha\rangle\rightarrow|N\rangle$ transition from (AII.1) gives

$$t_{N\alpha} = |v_N\rangle\lambda^{N\alpha}\langle v_\alpha| + |v_N\rangle\sum_{\gamma=1}^{N-1}\lambda^{N\gamma}\langle v_\gamma|G_0^{\gamma} t_{\gamma\alpha} + |v_N\rangle\lambda^{NN}\langle v_N|G_0^{N} t_{N\alpha} \qquad \text{(AII.2)}$$

$$t_{N\alpha} = \left(|v_N\rangle\lambda^{N\alpha}\langle v_\alpha| + \frac{|v_N\rangle\sum_{\gamma=1}^{N-1}\lambda^{N\gamma}\langle v_\gamma|G_0^{\gamma} t_{\gamma\alpha}}{1-\lambda^{NN}\langle v_N|G_0^{N}|v_N\rangle}\right) \qquad \text{(AII.3)}$$

The result (AII.3) is then inserted into (AII.1) to eliminate the $|\alpha\rangle \rightarrow |N\rangle$ term from the summation. It is found that $t_{\beta\alpha}$ becomes

$$t_{\beta\alpha} = |v_\beta\rangle \lambda_N^{\beta\alpha}(E) \langle v_\alpha| + |v_\beta\rangle \sum_{\gamma=1}^{N-1} \lambda_N^{\beta\gamma}(E) \langle v_\gamma | G_0^\gamma \, t_{\gamma\alpha} \qquad \text{(AII.4)}$$

so that the t-matrix is now expressed in the form of N-1 coupled channels, with the rescaled coupling constants $\lambda_N^{\beta\gamma}(E)$ energy-dependent and defined as

$$\lambda_N^{\beta\gamma}(E)^{\circ} = \frac{\lambda^{\beta\gamma}}{1-\lambda^{NN}\langle v_N | G_0^N | v_N\rangle} \left[1 + \frac{\lambda^{\beta N}\lambda^{N\gamma} - \lambda^{NN}\lambda^{\beta\gamma}}{\lambda^{\beta\gamma}} \langle v_N | G_0^N | v_N\rangle\right] \qquad \text{(AII.5)}$$

By placing some rather weak restrictions on the coupling constants λ the second term in parentheses can be made to vanish.

$$\text{(i)} \quad \lambda^{ij}\lambda^{jk}\lambda^{ki} = \lambda^{ii} \,, \qquad \text{(AII.6)}$$

and

$$\text{(ii)} \quad \lambda^{ij} = \lambda^{ji}$$

The effect of these restrictions is to insist that the λ are identical for all interactions within a given set of coupled channels.

The N-1 channel can be removed from (AII.4) in an identical manner to the N-channel. This will result in redefined coupling constants again.

$$\lambda_{N-1}^{\beta\gamma}(E) = \lambda^{\beta\gamma}\left[1 - \lambda^{N-1\,N-1}\langle v_{N-1} | G_0^{N-1} | v_{N-1}\rangle - \lambda^{NN}\langle v_N | G_0^N | v_N\rangle\right]^{-1} \qquad \text{(AII.7)}$$

The remaining channels can all be removed in this way to leave the effective one-channel process:

$$t_{\beta\alpha} = |v_\beta\rangle\lambda^{\beta\alpha}(E)\langle v_\alpha| + |v_\beta\rangle\lambda^{\beta\beta}(E)\langle v |G_0^{\beta\beta} t_{\beta\alpha} \quad \text{(AII.8)}$$

with $$\lambda^{\beta\alpha}(E) = \lambda^{\beta\alpha}\left[1 - \sum_{\gamma=1}^{N-1} \lambda^{\gamma\gamma}\langle v_\gamma | G_0^\gamma | v_\gamma\rangle\right]^{-1} \quad \text{(AII.9)}$$

which has the solution

$$t_{\beta\alpha} = \frac{|v_\beta\rangle\lambda^{\beta\alpha}\langle v_\alpha|}{1 - \sum_{\gamma=1}^{N} \lambda^{\gamma\gamma}\langle v_\gamma | G_0^\gamma | v_\gamma\rangle} \quad \text{(AII.10)}$$

The summation over γ includes only the diagonal elements of all the coupled channels.

APPENDIX III PARTIAL WAVE EXPANSION OF $V_\Sigma(\underline{k}',\underline{k})$

In this section we will briefly outline the steps involved in solving for the single particle potential in the lth partial wave. The partial wave expansions of the nuclear wavefunction and the ΣN form factors follow simply enough from the recursion relations for the Legendre polynomials and so their forms will just be assumed here.

The single particle potential was defined in terms of the nuclear wavefunctions and reaction matrix τ as [eq.(74)]

$$V(\underline{k}',\underline{k}) = \int d\underline{P}\; F(\underline{P}-\underline{k}';\underline{P}-\underline{k})\tau(\underline{k}',\underline{P}-\underline{k}';\underline{k},\underline{P}-\underline{k}:\omega) \quad \text{(AIII.1)}$$

$$= \frac{1}{4\pi}\sum_{\ell=0}^{\infty}(2l+1)\; V_\ell(k':k)\; P_\ell(k\;k')$$

With the expansions of F and τ given by eqs.(75) and (77) the potential V_ℓ is

$$V_\ell(k':k) = \int d\underline{P}\sum_{\ell''\ell'''}\sum_{\ell'=0}^{1}\rho^{\ell'}_{\ell''\ell'''}\sum_{LSJ}\bar{D}_{LSJ}(\omega)\sum_{nm}v_n(k:P)v_m(k':P)\sum_{a,b=0}^{L}$$

$$\left\{\frac{\Gamma(2L+1)}{\Gamma(2a+2)\Gamma(2b+2)\Gamma[2(L+1-b)]\Gamma[2(L+1-a)]}\right\}^{1/2} \quad \text{(AIII.2)}$$

$$\sum_{\alpha\beta M}(-\epsilon P)^{a+b}k^{L-a}k'^{L'-b}\langle a\alpha L-aM-\alpha|LM\rangle\langle b\beta L-bM-\beta|LM\rangle$$

$$\frac{1}{4\pi}\int d\Omega_k\, d\Omega_{k'}\, d\Omega_P\,[P_\ell(\hat{k}\cdot\hat{k}')P_{\ell'}(\hat{k}\cdot\hat{k}')P_{\ell''}(\hat{k}\cdot\hat{P})P_{\ell'''}(\hat{k}:\hat{P})$$

$$P_n(\hat{k}\cdot\hat{P})P_m(\hat{k}:\hat{P})Y^{\alpha}_{a}(\hat{P})Y^{\beta*}_{b}(\hat{P})Y^{M-\alpha}_{L-a}(\hat{k})Y^{M-\beta*}_{L-b}(\hat{k}')]$$

Using the addition theorem for spherical harmonics the Legendre polynomials become

$$P_\ell P_{\ell'} P_{\ell''} P_{\ell'''} P_n P_m = \sum_{L'L''L'''} |\langle 101'0|L0\rangle|^2 |\langle n01''0|L''0\rangle|^2 |\langle m01'''0|L'''0\rangle|^2 P_{L'}(\hat{k}\cdot\hat{k}') P_{L''}(\hat{k}\cdot\hat{P}) P_{L'''}(\hat{k}'\cdot\hat{P}) \qquad \text{(AIII.3)}$$

$$\text{and } P_{L'} P_{L''} P_{L'''} = \hat{L}'^{-2}\hat{L}''^{-2}\hat{L}'''^{-2}(4\pi)^3 \sum_{M'M''M'''} Y_{L'}^{M'}(\hat{k}) Y_{L'}^{M'*}(\hat{k}') Y_{L''}^{M''}(\hat{k}) Y_{L''}^{M''*}(\hat{P}) Y_{L'''}^{M'''*}(\hat{P}) Y_{L'''}^{M'''}(\hat{k}') \qquad \text{(AIII.4)}$$

With the well-known result for the integral of three spherical harmonics that

$$(4\pi)^{1/2} \int d\Omega Y_{\ell_1}^{m_1}(\Omega) Y_{\ell_2}^{m_2}(\Omega) Y_{\ell_3}^{m_3}(\Omega) = \hat{l}_1 \hat{l}_2 \hat{l}_3 \begin{pmatrix} l_1 & l_2 & l_3 \\ 0 & 0 & 0 \end{pmatrix} \begin{pmatrix} l_1 & l_2 & l_3 \\ m_1 & m_2 & m_3 \end{pmatrix} \qquad \text{(AIII.5)}$$

the angular integrals of eq.(AIII.2) become

$$4\pi \sum_{L'L''L'''L^{IV}} \hat{L}'^2 \hat{L}''^2 \hat{L}'''^2 \hat{L}^{IV\,2} \hat{a}\hat{b}(\widehat{L-a})(\widehat{L-b}) \begin{pmatrix} l & l' & L' \\ 0 & 0 & 0 \end{pmatrix}^2 \qquad \text{(AIII.6)}$$

$$\begin{pmatrix} n & l'' & L'' \\ 0 & 0 & 0 \end{pmatrix}^2 \begin{pmatrix} m & l''' & L''' \\ 0 & 0 & 0 \end{pmatrix}^2 \begin{pmatrix} L' & L'' & L-a \\ 0 & 0 & 0 \end{pmatrix} \begin{pmatrix} L' & L''' & L-b \\ 0 & 0 & 0 \end{pmatrix}$$

$$\begin{pmatrix} b & L'' & L' \\ 0 & 0 & 0 \end{pmatrix} \begin{pmatrix} a & L''' & L' \\ 0 & 0 & 0 \end{pmatrix} \begin{pmatrix} L' & L'' & L-a \\ M' & M'' & M-\alpha \end{pmatrix} \begin{pmatrix} L' & L''' & L-b \\ M' & M''' & M-\beta \end{pmatrix}$$

$$\begin{pmatrix} L'' & b & L' \\ M'' & \beta & M' \end{pmatrix} \begin{pmatrix} L''' & a & L' \\ M''' & \alpha & M' \end{pmatrix}$$

When this result is combined with the rest of the expression in curly brackets of the last page, the sum over 'm' gives a term proportional to a 9J coefficient. In fact this is a particularly simple sum to do using the graphical technique described in appendix I. The columns can be interchanged with impunity inside any 3J without affecting the overall phase because the Σj's are restricted to even values. Diagrammatically, the summation is represented by

(AIII.7)

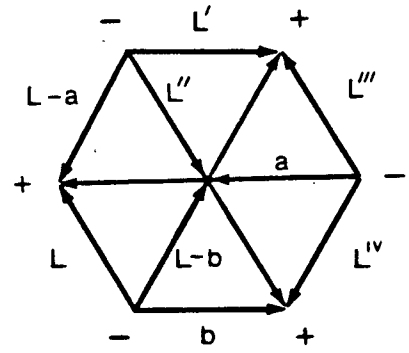

which, with the notation of appendix I, is just the 9J symbol:

$$\begin{Bmatrix} L\text{-}a & L' & L'' \\ L & L\text{-}b & b \\ a & L''' & L^{IV} \end{Bmatrix} \qquad \text{(AIII.8)}$$

Combining this result with the rest of the 3J symbols gives

the final result, eq.(80), for the potential in the lth partial wave.

With only S and P wave ΣN contributions the 9J is almost trivial because at least two of a,b,L-a,and L-b are always zero. The 9J then has the value:

(i) S-Wave; a,b,L,L-b,L-a = 0

$$\begin{Bmatrix} 0 & L' & L'' \\ 0 & 0 & 0 \\ 0 & L''' & L \end{Bmatrix} = \frac{1}{(2L'+1)} \delta_{L'L''L'''L^{iv}} \qquad \text{(AIII.9)}$$

(ii) P-Wave; (a) a,b=0;L,L-a,L-b=1

$$\begin{Bmatrix} 1 & L' & L'' \\ 1 & 1 & 0 \\ 0 & L''' & L \end{Bmatrix} = \frac{(-)^{1+L'+L''}}{3(2L''+1)} \delta_{L''L'''L^{iv}} \qquad \text{(AIII.10)}$$

(b) a,b=1;L-a,L-b=0

$$\begin{Bmatrix} 0 & L' & L'' \\ 1 & 0 & 1 \\ 1 & L''' & L \end{Bmatrix} = \frac{(-)^{1+L''+L^{iv}}}{3(2L'+1)} \delta_{L'L''L'''} \qquad \text{(AIII.11)}$$

(c) a,L-b=0;b,L-a=1

$$\begin{Bmatrix} 1 & L' & L'' \\ 1 & 0 & 1 \\ 0 & L''' & L \end{Bmatrix} = \frac{1}{3(2L'+1)} \delta_{L'L'''L^{iv}} \qquad \text{(AIII.12)}$$

(d) b,L-a=0;a,L-b=1

$$\begin{Bmatrix} 0 & L' & L'' \\ 1 & 1 & 0 \\ 1 & L''' & L \end{Bmatrix} = \frac{1}{3(2L'+1)} \delta_{L'L''L'''} \qquad \text{(AIII.13)}$$